LANDAU-ZENER TRANSITIONS IN NOISY ENVIRONMENTS AND IN MANY-BODY SYSTEMS

A Dissertation

by

DEQIANG SUN

Submitted to the Office of Graduate Studies of
Texas A&M University
in partial fulfillment of the requirements for the degree of

DOCTOR OF PHILOSOPHY

May 2009

Major Subject: Physics

LANDAU-ZENER TRANSITIONS IN NOISY ENVIRONMENTS AND IN MANY-BODY SYSTEMS

A Dissertation

by

DEQIANG SUN

Submitted to the Office of Graduate Studies of
Texas A&M University
in partial fulfillment of the requirements for the degree of

DOCTOR OF PHILOSOPHY

Approved by:

Chair of Committee,	Valery L. Pokrovsky
Committee Members,	Artem Abanov
	Wayne M. Saslow
	Stephen Fulling
Head of Department,	Edward Fry

May 2009

Major Subject: Physics

ABSTRACT

Landau-Zener Transitions in Noisy Environments and in Many-body Systems.

(May 2009)

Deqiang Sun, B.S., Nanjing University;

M.S., Texas A&M University

Chair of Advisory Committee: Dr. Valery L. Pokrovsky

This dissertation discusses the Landau-Zener (LZ) theory and its application in noisy environments and in many-body systems. The first project considers the effect of fast quantum noise on LZ transitions. There are two important time intervals separated by the characteristic LZ time. For each interval we derive and solve the evolution equation, and match the solutions at the boundaries to get a complete solution. Outside the LZ time interval, we derive the master equation, which differs from the classical equation by a quantum commutation term. Inside the LZ time interval, the mixed longitudinal-transverse noise correlation renormalizes the LZ gap and the system evolves according to the renormalized LZ gap. In the extreme quantum regime at zero temperature our theory gives a beautiful result which coincides with that of other authors. Our initial attempts to solve two experimental puzzles - an isotope effect and the quantized hysteresis curve of a single molecular magnet - are also discussed.

The second project considers an ultracold dilute Fermi gas in a magnetic field sweeping across the broad Feshbach resonance. The broad resonance condition allows us to use the single mode approximation and to neglect the energy dispersion of the fermions. We then propose the Global Spin Model Hamiltonian, whose ground state we solve exactly, which yields the static limit properties of the BEC-BCS crossover.

We also study the dynamics of the Global Spin Model by converting it to a LZ problem. The resulting molecular production from the initial fermions is described by a LZ-like formula with a strongly renormalized LZ gap that is independent of the initial fermion density. We predict that molecular production during a field-sweep strongly depends on the initial value of magnetic field. We predict that in the inverse process of molecular dissociation, immediately after the sweeping stops there appear Cooper pairs with parallel electronic spins and opposite momenta.

To My Parents: Sun Baoyun and Li Hongying

ACKNOWLEDGMENTS

First of all, my most sincere thanks go to my advisor Dr. Valery Pokrovsky, for teaching me the theories and methods necessary for this research, for guiding me through all the difficulties, and for supporting and encouraging me during all the processes in my research and my life. His knowledge, skills, and discipline have benefited me a lot and will continue to benefit me in the future.

I am indebted to my committee: Chair Dr. Valery Pokrovsky, members Dr. Artem Abanov, Dr. Wayne M. Saslow, and Dr. Stephen Fulling. They have provided, with kindness, their insight and suggestions, which are precious to me. Especially many thanks go to Dr. Artem Abanov, for amazingly generous financial support during the difficult times, for instruction, advice and direct collaboration in my research projects, and for encouragement and suggestions for my personal career development. I am honored that Dr. Wayne M. Saslow and Dr. Stephen Fulling joined my committee. They have discussed my progress with me many times and provided very helpful suggestions. I also want to express gratitude to Dr. Joseph B Natowitz for advice and help in the early stage of my study. Thanks to Dr. Konstantin Romanov for useful discussions.

And many thanks to all faculty and staff members in department of physics for your help. Especially I thank Dr. Teruki Kamon, Ms. Sandi Smith, Dr. Edward Fry, Dr. Lewis Ford, Ms. Minnette Bilbo and Ms.MaryAnn Batson.

Finally, I would like to express my eternal gratitude to my parents for their everlasting love and support.

TABLE OF CONTENTS

CHAPTER Page

LIST OF TABLES

LIST OF FIGURES

FIGURE Page

FIGURE Page

CHAPTER I

INTRODUCTION TO TWO-STATE SYSTEMS AND LANDAU-ZENER THEORY

A. Outline of this dissertation

The remaining sections of this chapter gives an introduction to Landau-Zener theory. First we discuss the Landau-Zener model in the time-dependent two-state systems. The static limit of LZ problem is then presented with great details. We also present the solution to the LZ equation by solving directly the Weber equation and by a semiclassical approach.

We apply the LZ theory to two systems which attracted attention recently. The first one is the single molecular magnet, and the second one is BCS-BEC crossover. In Chapter II we will discuss the part related to molecular magnets and in Chapter III we will discuss the BCS-BEC crossover.

Chapter II discusses the LZ theory in the noisy environment. The review and motivation of this problem is first given. We focus on the fast and quantum noise. We study the characteristic time for the noise itself, and for the interaction between the noise and the two-level system. Comparing with the characteristic LZ time, the evolution of the state is separated into two intervals, i.e., inside or outside $(-\tau_{LZ}, +\tau_{LZ})$. Inside this interval, we then derive the master equation by using a heuristic approach and solving a simplified microscopic Hamiltonian. Outside this interval we find that the evolution is equivalent to a LZ transition with a renormalized LZ gap due to the correlation between longitudinal and transverse noise. We also present an initial calculation on longitudinal-longitudinal correlation, which can be

---

This dissertation follows the style of Physical Review Letters.

neglected for weak noise though. The solution in each interval is studied and then matched at boundaries to give a complete picture of the evolution. The final state population and transition probability can reproduce previous results on fast classical noise, on pure LZ transitions, and on static limit. Especially our solution reproduces the same result obtained by other authors for the zero temperature situation. Our theory on the LZ transitions in a noisy environment is related to single molecular magnet. We discuss the application of our theory to the explanation of the isotope effect and the quantized hysteresis curve.

Chapter III discusses the untracold dilute fermi gas undergoing a broad Feshbach resonance. A short introduction is given to bosonic and fermionic fluidity and the connection between the two ends of superfluidity. The interaction of fermion atom with the magnetic field is explained. We focus on the broad Feshbach resonance which belongs to a strong coupling regime. We argue that the single mode approximation and neglection of fermion dispersion are appropriate under the broad Feshbach resonance condition. After the two approximations on the Hamiltonian, we propose the Global Spin Model and solve the static problem, which represents the static limit of the BEC-BCS crossover. For the dynamic problem, we convert it to a LZ problem and give a complete solution to this molecular production and dissociation problem. The solution represents a LZ-like formula with a strongly renormalized LZ gap that is independent of the initial fermion density. In both the static and dynamic situations, we estimated the cutoff momentum for the available states and slightly improved our previous estimate on this cutoff momentum to the current estimation. We conclude with our prediction that molecular production during a field-sweep strongly depends on the initial value of magnetic field, and that in the inverse process of molecular dissociation, immediately after the sweeping stops there appear Cooper pairs with parallel electronic spins and opposite momenta.

Finally Chapter IV gives the summary and conclusion on this research dissertation, and a brief outlook.

B. Quantum dynamics of two-state system

Two level quantum mechanical system plays an important role in physics fundamentals. The two-state problems are often encountered in quantum optics, magnetic resonance, atomic collisions and other areas of scientific research. The solutions of the time-dependent Schrodinger wave equation are hence important in quantum dynamics. The general time-dependent Schrodinger equation has the form

$$i\hbar\frac{d}{dt}\left|\Psi\right\rangle = H\left|\Psi\right\rangle. \tag{1.1}$$

Since it is a two level system, the matrix form is

$$i\hbar\frac{d}{dt}\begin{pmatrix} A_1 \\ A_2 \end{pmatrix} = \begin{pmatrix} H_{11} & H_{12} \\ H_{21} & H_{22} \end{pmatrix}\begin{pmatrix} A_1 \\ A_2 \end{pmatrix} \tag{1.2}$$

where A_1 and A_2 are, in the space spanned by basis $|\varphi_1\rangle$ and $|\varphi_2\rangle$, the complex components of the wavefunction $|\Psi\rangle$

$$\left|\Psi\right\rangle = A_1\left|\varphi_1\right\rangle + A_2\left|\varphi_2\right\rangle = \begin{pmatrix} A_1 \\ A_2 \end{pmatrix} \tag{1.3}$$

and H_{11},...,H_{22} are matrix elements of the Hamilonian operator H

$$H = \begin{pmatrix} H_{11} & H_{12} \\ H_{21} & H_{22} \end{pmatrix}. \tag{1.4}$$

In general all these components and matrix elements depend on t. The populations of each state are $|A_1(t)|^2$ and $|A_2(t)|^2$. Usually the initial condition is such that the

system is at ground state:

$$|A_2(-\infty)| = 1, |A_1(-\infty)| = 0 \tag{1.5}$$

For a realistic process, the matrix elements H_{ij} usually show a complicated dependence on time t through other physical parameters and that makes it difficult to obtain an exact solution for equation (1.2).

The simplest nontrivial case for which an exact solution for Eq. (1.2) can be found is when

$$H_{22} - H_{11} = 0.$$

Then this system has two stationary levels and couples to a time-dependent interaction, if H_{ij} is real $H_{ij} = H_{ji}$, which usually means the system involves in a strong-coupling or is close to a resonance. It can be easily calculated. By a phase transformation

$$A_i = a_i e^{[-i\int H_{ii}dt]}, \tag{1.6}$$

the time-dependent Schrodinger equation (1.2) becomes

$$\begin{aligned} i\dot{a_1} &= H_{12}a_2 e^{[-i\int(H_{22}-H_{11})dt]} = H_{12}a_2, \\ i\dot{a_2} &= H_{21}a_1 e^{[+i\int(H_{22}-H_{11})dt]} = H_{21}a_1. \end{aligned}$$

And by taking one more differentiation respecting to time t, we have a variable separated differential equation for each coefficient a_i:

$$\ddot{a_i} - \frac{\dot{H_{ij}}}{H_{ij}}\dot{a_i} + |H_{ij}|^2 a_i = 0,$$

where $H_{ij} = |H_{ij}|e^{i\nu}$ with ν defined as phase. For the special case of $\nu \approx 0$, or $H_{12} \approx H_{21}$, the solution that satisfies the initial condition (1.5) is a_1=cos$[\int H_{12}/\hbar dt]$, a_2=$-i$ sin$[\int H_{12}/\hbar dt]$. Together with the transformation (1.6), we can see that the diagonal matrix element provides only a phase shift to amplitude of each state and

this amplitude couples only to the time-dependent interaction. If the phase factor is not close to 0 and is not very large, this problem becomes much harder, though it is almost solved [1, 2, 3] in the case of a phase factor linear in time.

There exist various models for which an exact or approximate solution is studied and discovered [4, 5, 6, 7, 8, 9]. Here some important models with simple forms of H_{ij} are listed below in Table I.

Table I. Examples of some models of Hamiltonian for time-dependent two-state problem. All parameters are constant. Note that only the amplitude of H_{12} is explicitly written and the phase of H_{12} is implicitly included. This is also the assumption through all the following text. The reason is that in the Landau-Zener Model H_{12} always appear together with its complex conjugate as $H_{12}H_{21}^{\dagger}$ in the calculation of population.

Model	$H_{22} - H_{11}$	H_{12}	Refs.
Rosen-Zener	β	$\Delta sech(\gamma t)$	Rosen, Zener [10]
Landau-Zener	$\alpha(t - t_0)$	Δ	Landau, Zener [6, 7]
Demkov	β	$\Delta e^{-\gamma t}$	Demkov [9]
Nikitin	$\alpha e^{-\gamma t} + \beta$	Δ	Nikitin [8]
Exponential	$\alpha e^{-\gamma t} + \beta$	$\Delta e^{-\gamma t}$	George [5]

The model of considerable importance is the Landau-Zener model [6, 7], which provides an approximate solution to equation (1.2) under the assumption that

$$H_{22} - H_{11} = \alpha(t - t_0), H_{12} = \Delta, \text{where } \alpha \text{ and } \Delta \text{ are time-independent.} \qquad (1.7)$$

This theory is also sometimes referred as Landau-Zener-Stueckelberg theory [11] by other authors. For abbreviation purpose, we will call it LZ theory hereafter. As mentioned before, it has a broad range of application and has long been applied to

various problems since it's proposed. In the last decade, it was actively applied to the quantum molecular hysteresis of nanomagnets [12, 13, 14], to the charge transport properties of various kinds of nanodevices [15, 16, 17], and to the ultracold fermi gas [18, 19], and to the Qubit control [20, 21]. The LZ theory is one of basic dynamic problems of quantum mechanics.

Generally, this theory is useful for problems when the energy curves seem to cross. Although $H_{22} - H_{11} = \alpha(t - t_0)$ could incorporate complicated energy levels, realistic encounters are that both energy levels are approximately linear at least near crossing region.

If the Hamiltonian H is time-independent but depends on some physical parameter, and if the two unperturbed levels cross each other when this physical parameter changes, the perturbed levels will "repel" each other to avoid the crossing, as explained in section C. This is the static situation or the adiabatic limit of the dynamic situation. If this physical parameter becomes time-dependent and sweeps through the crossing point, the behavior of the system will be different depending on how fast the sweep is and how large the LZ gap is. As will be shown in section D, supposing the velocity this parameter is the only experiment controllable variable(which means the LZ gap is not varying), the fast sweeping drives the system evolves according to the unperturbed(or so called diabatic) curve, while the slow sweeping drives the system evolves according to the perturbed(or so called adiabatic) curve. Close to the crossing region, transitions between the two states are induced by the non-diagonal matrix element, which causes the level repulsion in adiabatic limit. The repulsion of levels is also called avoided crossing of levels. If the velocity of this physical parameter is not fast or slow, Landau-Zener model gives the asymptotic solution.

Assuming Δ can be neglected in the Landau-Zener model, i.e. $\Delta = 0$, and the

other condition $H_{22} - H_{11} = \alpha(t - t_0)$ is the same, we have a two level system with two levels crossing each other at time t_0. These two states(levels) are called diabatic states(levels), like curve E_1 and E_2 explained in section C. So, if the diabatic state is the ground state, i.e., the lower energy state, at time smaller than t_0, it occurs to be a higher energy state, at time larger than t_0. The particle placed into a diabatic state can follow it in time if $\Delta = 0$. But any perturbation will destroy this state and drive the system to the lower energy state if the transaction is allowed by the system symmetry. This means that the assumption of $\Delta = 0$ is not correct. As long as the diagonal terms have the relation similar to the first equation in LZ assumption (1.7), the non-diagonal elements must be considered. Specifically to molecular system, Von Neumann and Wigner in 1929 proved the non-crossing rule [22, 23], which states: Potential energy curves corresponding to electronic states of the same symmetry cannot cross, unless the crossing is an accidental event. The reason follows. Close to the crossing point the next order perturbation or approximation in the Hamiltonian, which is previously neglected, becomes important and the next order expansion destroys the crossing. In order for the crossing to take place, the constraints $H_{11} = H_{22}$ and $H_{12} = H_{21} = 0$ at the crossing point must be satisfied simultaneously, which is possible only if the number of parameters is more than one. If $H_{11}(R_0) = H_{22}(R_0)$ at crossing point where some parameter, say R, takes value R_0, then there is no reason to require $H_{12}(R_0) = 0$.This means the non-crossing rule is enforced for diatomic molecule since there is only one parameter, the internuclear separation. For polyatomic system, there are sufficient parameters available to achieve degeneracy, so the non-crossing rule is not enforced and states of different symmetry may cross. With more avoided crossings seen in polyatomic system, the non-crossing rule is extended in polyatomic system but to what extension is still arguable [24, 25, 26]. This topic will not be discussed here.

C. Static properties of two-state system

Now let us look at the situation that Hamiltonian is same as LZ Hamiltonian with time substituted by a time-independent parameter. Let us now assume

$$H_{22} - H_{11} = \eta(R - R_0), \Delta = H_{12} \neq 0, \text{where } \eta \text{ and } \Delta \text{ are time-independent.} \quad (1.8)$$

Hamiltonian is a linear function of some parameter R and the energy curves cross at value R_0. Δ in general is also a function of R. This is an exactly solvable static problem. For the close reference, the solution is reviewed here.

Suppose the two normalized orthogonal wave functions $|\varphi_1\rangle$ and $|\varphi_2\rangle$ are the eigenfunctions of Hamiltonian H, before the terms H_{12} and H_{21} are switched on. In reality, these functions need also be selected such that they are orthogonal to other states. The action of H_{12} and H_{21} (or Δ) is switched on when system is close to the crossing point. $|\varphi_1\rangle$ and $|\varphi_2\rangle$ can serve as basis. Denote them as $|1\rangle = \begin{pmatrix} 1 \\ 0 \end{pmatrix}$ and $|2\rangle = \begin{pmatrix} 0 \\ 1 \end{pmatrix}$. According to the Hermitian property, H_{11} and H_{22} are both real. Denote them by E_1 and E_2. $H_{11} = E_1 = \langle\varphi_1| H |\varphi_1\rangle$. $H_{22} = E_2 = \langle\varphi_2| H |\varphi_2\rangle$. Then Schrodinger equation is now

$$E \begin{pmatrix} C_1 \\ C_2 \end{pmatrix} = \begin{pmatrix} E_1 & H_{12} \\ H_{21} & E_2 \end{pmatrix} \begin{pmatrix} C_1 \\ C_2 \end{pmatrix}, \quad (1.9)$$

where C_1 and C_2 are the coefficients of eigenfunction of H expanded on $|\varphi_1\rangle$ and $|\varphi_2\rangle$.

In the view of perturbation theory, Hamiltonian H can be divided into two parts

$$H = H_0 + H', \quad (1.10)$$

where $H_0 = \begin{pmatrix} E_1 & 0 \\ 0 & E_2 \end{pmatrix}$ can be considered as the unperturbed term, and $H' = \begin{pmatrix} 0 & H_{12} \\ H_{21} & 0 \end{pmatrix}$ can be considered as the perturbation term. In other words, (E_1, E_2) and ($|\varphi_1\rangle$, $|\varphi_2\rangle$) are the eigenenergies and eigenstates of H_0. Let $\langle 1| H |2\rangle = |\Delta| e^{-i\gamma}$, or equivalently $|\Delta|$ and γ are defined as amplitude and phase of H_{12}.

Working in the representation of H_0 where $|1\rangle$ and $|2\rangle$ are basis, *without use of perturbation method*, we have the following exact solution, with the eigenvalues given by

$$E_\pm = \frac{1}{2}[(E_1 + E_2) \pm \sqrt{(E_1 - E_2)^2 + 4|\Delta|^2} = E_c \pm \sqrt{d^2 + |\Delta|^2}, \tag{1.11}$$

and the eigenstates given by

$$\left|\psi_-\right\rangle = \begin{pmatrix} \cos\frac{\theta}{2} \\ -\sin\frac{\theta}{2}e^{i\gamma} \end{pmatrix}; \text{ and } \left|\psi_+\right\rangle = \begin{pmatrix} \sin\frac{\theta}{2} \\ \cos\frac{\theta}{2}e^{i\gamma} \end{pmatrix}; \tag{1.12}$$

where $\left|\psi_\pm\right\rangle$ is the eigenstate corresponding to $E_\pm$ in the H_0 representation, and E_c, d and θ are defined such that

$$E_c = \frac{1}{2}(E_1 + E_2) = \frac{1}{2}(H_{11} + H_{22}), \tag{1.13}$$

$$d = \frac{1}{2}|(E_2 - E_1)| = \frac{1}{2}|(H_{11} + H_{22})|, \tag{1.14}$$

$$tan\theta = \frac{|\Delta|}{d}, \tag{1.15}$$

and $H_{12} = |\Delta| e^{i\gamma}$.

Again from perspective of perturbation theory, we can call E_1 and E_2 as "unperturbed levels", and call E_+ and E_- as "perturbed levels", though they are solved exactly without approximation.

When d/Δ is large, θ is small, $tan\theta \approx 0$ and we have

$$\begin{aligned} E_{\pm} &= E_c \pm d, \\ \left|\psi_{+,-}\right\rangle &= |2,1\rangle \mp \frac{1}{2}\theta\,|1,2\rangle\,. \end{aligned} \tag{1.16}$$

As it is seen from Eq. (1.16), if d is large, or equivalently the system is far from crossing point, the energy of perturbed states $E_{\pm}$ only slightly differs from that of unperturbed states $E_{1,2}$, and the perturbed states $\left|\psi_{\pm}\right\rangle$ are almost same as the unperturbed states $\left|\psi_{1,2}\right\rangle$. While at the crossing point, $d = 0$, Eqs. (1.11, 1.12) lead to the following result:

$$\begin{aligned} E_{\pm} &= E_c \pm |\Delta|\,, \\ \left|\psi_{\pm}\right\rangle &= \frac{1}{\sqrt{2}}(|1\rangle \mp |2\rangle). \end{aligned} \tag{1.17}$$

At the crossing point, the perturbed states energy $E_{\pm}$ deviates most from unperturbed states energy E_c and the adiabatic states $\left|\psi_{\pm}\right\rangle$ are half mixed from diabatic states $\left|\psi_{1,2}\right\rangle$. The maximum deviation between perturbed and unperturbed energies is $|\Delta|$, or the non-diagonal matrix element.

The minimum distance between the two perturbed energy levels E_+ and E_- are $2\,|\Delta|$. The perturbed state, say $\left|\psi_{-}\right\rangle$, evolves from almost completely $|\psi_2\rangle$ at the far left end, to half mixed by $|\psi_1\rangle$ and $|\psi_2\rangle$ at the crossing point, and ends again almost

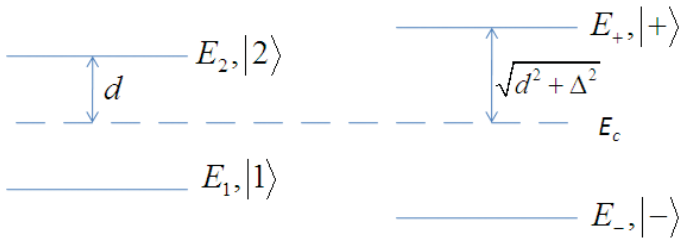

FIG. 1. If E_1 and E_2 are parallel levels, E_+ and E_- are just parallel shifts. Here the x-axes is the parameter R and the y-axes is the energy.

completely $|\psi_1\rangle$.

We can see that in order for $E_+(R_0) = E_-(R_0)$ to be valid, $\Delta(R_0) = 0$ must be also satisfied, besides $E_1(R_0) = E_2(R_0)$. These conditions may not be satisfied simultaneously. Crossing (of perturbed energy curves) is hence avoided except for accidental crossing.

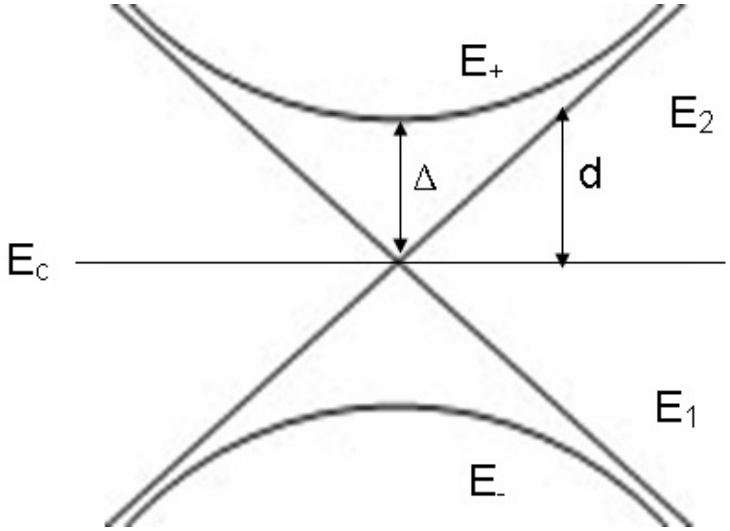

FIG. 2. If the "unperturbed levels" E_1 and E_2 cross each other at some parameter R_0, there will be level repulsion and avoided crossing, as seen by the "perturbed levels" E_+ and E_-. The meaning of x-y axis are same as previous figure. If the If the x-axis parameter becomes time-dependent, E_1 and E_2 are called diabatic levels, and E_+ and E_- are called adiabatic levels.

If the energy curves E_1 and E_2 are just parallel to each other, the new energy curve E_+ (or E_-) is just a parallel shift to the original one E_2(or E_1), as shown in Fig. 1. However, if the energy curves E_1 and E_2 cross each other when the parameter R is changed and passes R_0, the new energy curves E_+ and E_-, plotted according to the above equation (1.11), have an avoided crossing. This is illustrated in Fig. 2. In this figure the y-axis is the energy value and x-axis is some parameter according to which the energy would change, like magnetic field. In the discussion up to now,

the problem is still assumed time independent.

If the x-axis parameter becomes time-dependent, this picture can be considered as instantaneous static limit of the dynamic problem. In this time-dependent situation, the "unperturbed" terms are called "diabatic" terms and the "perturbed" terms are called "adiabatic" terms. For example, the two states $\left|\psi_+\right\rangle$ and $\left|\psi_-\right\rangle$ defined in Eq. (1.12) are called adiabatic states. Their corresponding energies, designated as E_+ and E_- in Fig. 2, are called adiabatic levels. The terms 'adiabatic levels' and 'diabatic levels' are associated with the Born-Opperheimer approximation, also known as adiabatic approximation, for calculation of diatomic molecule energy, for example. If the nuclei are moving slowly, which is assumed by the Born-Opperheimer approximation, then the energy follows the adiabatic curve.

D. Asymptotic solution of Landau-Zener problem

Now let us return to the Landau-Zener model (1.7), i.e. if R in the equation (1.8) becomes linearly dependent on time. The Hamiltonian is time-dependent and this problem can not be solved like in the previous static case. The operators at different times generally do not commute, and hence no general eigenvalues exist. However, Fig. 2, like each snapshot of the system at each time t, can still be used to illustrate the time dependent dynamic problem. For the time-dependent LZ Hamiltonian (1.7), the state is not $\left|\psi_+\right\rangle$ or $\left|\psi_-\right\rangle$, is not $|\psi_1\rangle$ or $|\psi_2\rangle$, but a superposition of $\left|\psi_+\right\rangle$ and $\left|\psi_-\right\rangle$, or a superposition of $|\psi_1\rangle$ and $|\psi_2\rangle$. We choose the last two states as basis because they are eigenvectors of the simple "unperturbed" Hamiltonian H_0. Following Rosen and Zener [6, 7], the Schrodinger equation (1.2) will be transformed to a simpler form. H_{11} and H_{22} are real functions of t. The transformation that

makes the diagonal elements vanish is

$$a_1 = A_1 e^{i\int^t H_{11}dt}; a_2 = A_2 e^{i\int^t H_{22}dt}. \tag{1.18}$$

Here we have set $\hbar = 1$. Note that a_1 and a_2 are now components of new wavefunction. The time dependent occupation probabilities for the two states are $|a_1|^2 = |A_1|^2$ and $|a_2|^2 = |A_2|^2$. The transformed Schrodinger equation is

$$i\frac{d}{dt}\begin{pmatrix} a_1 \\ a_2 \end{pmatrix} = \begin{pmatrix} 0 & H_{12}e^{-i\int^t (H_{22}-H_{11})dt} \\ H_{21}e^{i\int^t (H_{22}-H_{11})dt} & 0 \end{pmatrix}\begin{pmatrix} a_1 \\ a_2 \end{pmatrix} \tag{1.19}$$

Now a_1 and a_2 can be decoupled and each obeys the second order ordinary differential equation:

$$\ddot{a_1} + (i(H_{22} - H_{11}) - \frac{\dot{\Delta}}{\Delta})\dot{a_1} + |\Delta|^2 a_1 = 0 \tag{1.20}$$

This is the equation to be solved. At this point, it's necessary to apply the assumption (1.7) to proceed. Although Landau solved this problem by going to the complex plane of time t, we still follow the Zener way. By the substitution $H_{22} - H_{11} = \alpha(t - t_0)$, $\dot{\Delta} = 0$, $c_1 = a_1 e^{+i/2\int \alpha(t-t_0)dt}$, and $c_2 = a_2 e^{-i/2\int \alpha(t-t_0)dt}$, Eq. (1.20) for a_1 is reduced to a Weber equation and we also have a similar equation from a_2:

$$\begin{aligned} \ddot{c_1} + (\Delta^2 - i\alpha/2 + \alpha^2 t^2/4)c_1 = 0, \\ \ddot{c_2} + (\Delta^2 + i\alpha/2 + \alpha^2 t^2/4)c_2 = 0, \end{aligned} \tag{1.21}$$

where we have again come back to the assumption that Δ is just the amplitude. And

by the substitutions

$$n \equiv i\Delta^2/\alpha \equiv i\gamma_{LZ},$$
$$\tau \equiv \sqrt{\alpha}e^{-i\pi/4}t,$$

the Weber equation above for c_1 can be further reduced to the standard form

$$\ddot{c_1} + (n + 1/2 - \tau^2/4)c_1 = 0 \tag{1.22}$$

where $\ddot{c_1}$ means $d^2c_1/d\tau^2$. The standard form for c_2 can also be obtained by a similar substitution. The solution is called Weber function or parabolic cylinder function, which is expressed in terms of confluent hypergeometric functions. By choosing appropriate functions according to the initial condition (1.5), the superposition constants in the solution can be determined and the asymptotic value of $|c_1|^2$ is given by

$$|A_1(\infty)|^2 = |c_1(\infty)|^2 = 1 - e^{-2\pi\gamma_{LZ}}, \text{ where } \gamma_{LZ} = \Delta^2/\alpha. \tag{1.23}$$

It is also worthwhile to mention that the same asymptotic solution is obtained in lecture notes by Valery Pokrovsky [27] through a semiclassical approach. In the spirit of semiclassical approximation, the two independent solutions for Eq. (1.21) $\hbar^2\ddot{c} + p^2(\tau)c = 0$, are in the forms of

$$c_\pm = \frac{1}{\sqrt{p(\tau)}} e^{\pm i\int_{\tau_0}^{\tau} \frac{p(\tau)}{\hbar} d\tau} \tag{1.24}$$

where c denotes c_1 or c_2, $\tau \equiv \alpha t$, and $p^2(\tau) \equiv \gamma_{LZ} \pm i/2 + \tau^2/4$. At large $|\tau|$ the integration may be calculated by expanding $p(\tau)$ on a series of $1/\tau$. Take c_2 for example,

$$\begin{aligned} p(t) &= \sqrt{\tfrac{\tau^2}{4}(1 + \tfrac{\gamma_{LZ}+i/2}{\tau^2/4})} \\ p(t) &= \tfrac{\tau}{2}(1 + \tfrac{1}{2}\tfrac{\gamma_{LZ}+i/2}{\tau^2/4} + ...) \\ \textstyle\int^\tau p(\tau)d\tau &= \tfrac{\tau^2}{4} + (\tfrac{1}{2}i + \gamma_{LZ})\ln\tau + Const. \end{aligned} \tag{1.25}$$

At large $|\tau|$, the term $(1/\sqrt{p}) \times e^{+i*(\frac{1}{2}i\ln\tau)}$ is approximately zero, if the sign in the

exponent in Eq. (1.24) is +. In other worlds, the c_{2+} solution can be neglected. So

$$c_2 = \frac{1}{\sqrt{\tau/2}} e^{-i\tau^2/4 - i(\gamma_{LZ}+i/2)\ln\tau + Const.}, \tag{1.26}$$

when $\tau = e^{i\pi}$, the Const. is required to be $-\pi\gamma_{LZ}$ to meet the initial condition. So when t goes $+\infty$,

$$|c_2| = e^{-\pi\gamma_{LZ}}, \tag{1.27}$$

which is essentially same as Eq. (1.23). The probability in Eq. (1.23) $(1-e^{-2\pi\gamma_{LZ}})$ is the probability that the system remains in ground state (diabatic state $|1\rangle$ $(t=+\infty)$) if it is initially in ground state (diabatic state $|2\rangle$ $(t=-\infty)$). If γ is very large(or α is very small) then the system stays in the adiabatic state and if γ is very small(or α is very large) then the system has a transition from the lower adiabatic state to the higher adiabatic state. The expression $e^{-2\pi\gamma_{LZ}}$ gives the probability for the Landau-Zener transition from lower adiabatic state to higher adiabatic state. In one sentence, $(1-e^{-2\pi\gamma_{LZ}}$ is the population difference of the same *diabatic* state before and after t_0, while $e^{-2\pi\gamma_{LZ}}$ is the population difference of the same *adiabatic* state before and after t_0.

CHAPTER II

LANDAU-ZENER THEORY AND FAST QUANTUM NOISE

A. Review and motivation

The research on the Landau-Zener transitions in a noisy environment is motivated by the intensive development of quantum computing elements. New experimental realization of qubits [28] questioned again to what extent it is possible to minimize the decoherence, while simultaneously maintaining sufficiently strong coupling to the external signal. Molecular magnets display a substantial narrowing of the magnetic hysteresis curve at $T\ 1K$. This fact implies that the LZ process is strongly influenced by thermal noise in this range of temperature.

The theory of the LZ transition in a noisy environment has relatively long history. One of the first considerations was based on ideas of stochastic trajectories from Kasunoki [29]. In the pioneering work [30] Kayanuma calculated the transition amplitude in the presence of a fast transverse Gaussian classical noise with a specific (exponential) two-time correlation function*. This solution was simplified and extended to general shape of correlation function by V. Pokrovsky and N. Sinitsyn [31]. The same work considers a situation in which the transitions are produced by noise as well as by regular Hamiltonian. Pokrovsky and Scheidl [32] calculated the two-time correlation function of the transition probabilities for the LZ system subject to a fast classical transverse noise. Longitudinal noise was considered by Kayanuma [33], who proved that strong fast longitudinal noise enhances the nonadiabaticity, and the transition probability is given by a formula different from the LZ

*The definition of transverse and longitudinal noise and the definition of quantum noise will be introduced in next section.

formula, while slow longitudinal noise does not change the LZ transition probability. Gefen *et al.* [34] and Ao and Rammer [35] considered more wide range of parameters and found the situations in which the noise changes the transition probability. In the work [35] a rather detailed analysis of different limiting cases of temperature, coupling to the phonon bath, its spectral width and sweeping rate was presented. There occurred a controversy between the works [34] and [35]. Generally, there is no complete agreement between different authors on what happens in the adiabatic regime (very slow sweeping) in the presence of the longitudinal noise. Motivated by this disagreement Kayanuma and Nakayama performed a comprehensive analytical and numerical study of the LZ transition in the presence of longitudinal noise [36]. In particular they obtained a formula for the case of strong decoherence which is valid in both low-temperature and high-temperature limits. In all these works the quantum nature of the longitudinal noise was taken in account.

Despite of significant progress a complete theory of the LZ transition in noisy environment still does not exist. Theoretical works considered either quantum longitudinal noise with transitions originated from the regular transition matrix element or the classical transverse noise. Quite recently Wubs *et al.* [37] have found an elegant exact formula for the transition probability of the two-state system interacting with the phonon bath at zero temperature *. The noise had both longitudinal and transverse components. Their correlation and quantum nature were substantial. No limitations to the noise strength and spectral width were assumed. However, the limitation of zero temperature (phonon bath is in the ground state) does not allow

*The result for survival probability obtained [37] is a consequence of the theorem proposed by Brandobler and Elser [38] as a hypothesis and proved rigorously by Dobrescu and Sinitsyn [39]. Wubs *et al.* have found the same method independently, but a little later. Important steps toward the proof of the Brandobler-Elser hypothesis were made by A.V. Shytov [40], N.A. Sinitsyn [41] and M.V. Volkov and V.N. Ostrovsky [42, 43].

to extend these results to more realistic situations.

The purpose of this chapter is to present a theoretical description of the LZ system subject to a *fast quantum* noise which has both transverse and longitudinal components. It is not yet a complete theory, since it does not cover slow and intermediate noise, but in its range of applicability it allows to understand clearly all relevant physical regimes and phenomena. We will show that, due to the fastness of the noise, the LZ transition in the presence of the longitudinal noise and the transitions due to the transverse noise are separated in time, whereas the correlation between the transverse and longitudinal noise leads to a renormalization of the regular transition matrix element in the LZ Hamiltonian. For a moderately strong transverse noise we derive master equations governing the population of the two states and study their solution. If the transverse noise is strong and also fast, the two-state system falls into adiabatic regime. The population of levels comes to the equilibrium with the spin bath if the bath is in the state of thermal equilibrium. We argue that a very strong noise is classical and adiabatic. In this situation, as it was shown in [31], the populations of the two levels are equal.

The plan of the remaining of this chapter is as follows. In section B we introduce the Hamiltonian and characterize the noise. In section C we present simple heuristic arguments resulting in master equations. In section D we derive the master equations starting from microscopic Hamiltonian for the case of the transverse noise only and zero LZ transition matrix element. In section E we derive the renormalization of the regular transition matrix element due to correlation of longitudinal and transverse noise. In section F we analyze the influence of the longitudinal noise. In section G we find the solution of master equation and study it. In section H we match the solution of the master equation with the solution of the LZ problem without transverse noise. Section I contains the discussion and conclusion, where we compare our theory with

that by Wubs *et al.* [37], and we briefly analyze possible applications of our theory to molecular magnets.

B. Statement of the problem

We consider a two-state system interacting with a noisy environment. The latter is a large system (bath) with a stationary density matrix. We neglect the influence of the LZ transitions onto the state of the bath. For a definiteness we will speak about the phonon bath, though it can include other Boson excitations like spin waves, excitons, photons. Then the total Hamiltonian of the system can be represented as follows:

$$H = H_2 + H_b + H_{int} \tag{2.1}$$

The term H_2 in equation (2.1) is the Hamiltonian that represents the two-state system, as discussed in Eq. (1.4):

$$H_2 = -\frac{\Omega(t)}{2}\sigma_z + \Delta\sigma_x, \tag{2.2}$$

where σ_x and σ_z are Pauli matrices, $\sigma_z = \begin{pmatrix} 1 & 0 \\ 0 & -1 \end{pmatrix}$, $\sigma_x = \begin{pmatrix} 0 & 1 \\ 1 & 0 \end{pmatrix}$, and $\Omega(t)$ is the time-dependent frequency or the energy difference between the so-called diabatic levels, $\Omega(t) \equiv E_2 - E_1$, Δ is the non-diagonal matrix element. The two state Hamiltonian H_2 in Eq. (2.2) is slightly different than that in Eq. (1.4), but if we substitute the transformation $a_i = A_i e^{-i\int^t E_c dt}$ to the Eq. (1.1) we will have the equivalent Hamiltonian H_2. If t would be not time but some other parameter of the Hamiltonian, then non-zero Δ provides repulsion of the adiabatic levels (the Wigner-Neumann theorem on avoided levels crossing). For brevity we will call further the regular transition matrix element Δ the LZ gap. Usually the linear approximation for

the frequency $\Omega(t) = \dot{\Omega}t$ proposed by Landau and Zener is acceptable, but sometimes it is necessary to go beyond this approximation. Namely, in real experiment the sweeping of $\Omega(t)$ stops at some finite value, which can be not large in the frequency scale of the problem. Therefore we will keep notation $\Omega(t)$ throughout this article.

The term H_b in equation (2.1) is the phonon bath Hamiltonian:

$$H_b = \sum_{\mathbf{q}} \omega_{\mathbf{q}} b_{\mathbf{q}}^{\dagger} b_{\mathbf{q}}, \tag{2.3}$$

where $\omega_{\mathbf{q}}$ are the phonon frequencies and $\mathbf{q}$ are their momenta, $b_{\mathbf{q}}$ and $b_{\mathbf{q}}^{\dagger}$ are the operators of the phonon annihilation and creation, satisfying the standard quantum commutation relations $[b_{\mathbf{q}}, b_{\mathbf{q}'}] = 0, [b_{\mathbf{q}}^{\dagger}, b_{\mathbf{q}'}^{\dagger}] = 0, [b_{\mathbf{q}}, b_{\mathbf{q}'}^{\dagger}] = \delta_{\mathbf{q},\mathbf{q}'}$.

The Hamiltonian for interaction between two-state system and phonons reads:

$$H_{int} = u_{\parallel}\sigma_z + u_{\perp}\sigma_x, \tag{2.4}$$

where $u_{\parallel}$ and $u_{\perp}$ are the transverse noise and longitudinal noise operators. The transverse noises couple to the two-state system by making the system transit from one state to another while the longitudinal noises couple to the two-state system by making the energy curve deviate from its original path. The Hermitian operators $u_{\parallel}$ and $u_{\perp}$ responsible for the longitudinal and transverse noise depend linearly on the phonon operators. Each of them is a sum of two Hermitian conjugated operators containing either phonon annihilation or creation operators only:

$$u_{\alpha} = \eta_{\alpha} + \eta_{\alpha}^{\dagger};\ \eta_{\alpha} = \frac{1}{\sqrt{V}} \sum_{\mathbf{q}} g_{\alpha}(\mathbf{q})\, b_{\mathbf{q}};\ \alpha = \parallel, \perp \tag{2.5}$$

where $g_{\alpha}(\mathbf{q})$ are complex coupling amplitudes and V is the volume of the system supporting phonons. The quantum character of the noise manifests itself in non-commutativity of operators η_{α} and $\eta_{\alpha}^{\dagger}$. The problem consists in calculation of tran-

sition and surviving probabilities for the two-state system at a fixed noise density matrix. In the absence of the noise, the transition amplitudes, calculated from solving the Weber equation, constitute the LZ transition matrix belonging to the SU(2) group and depending on the dimensionless LZ parameter $\gamma_{LZ} = \Delta^2/\dot{\Omega}$:

$$T_{LZ} = \begin{pmatrix} \alpha & \beta \\ -\beta^* & \alpha^* \end{pmatrix} \tag{2.6}$$

$$\alpha = e^{-\pi\gamma_{LZ}};\ \beta = -\frac{\sqrt{2\pi}\exp\left(-\frac{\pi\gamma_{LZ}}{2} + i\frac{\pi}{4}\right)}{\sqrt{\gamma_{LZ}}\Gamma\left(-i\gamma_{LZ}\right)}$$

If γ_{LZ} is small, the system with the probability close to 1 remains in initial diabatic state; if γ_{LZ} is large the system with probability close to 1 proceeds along the adiabatic state, i.e. changes the initial diabatic state to the alternative one. So the Landau-Zener transition is preferred when γ_{LZ} is large. From the Fig. 3, we can see that the characteristic time for the system to transit from one state to the other is estimated at $\Delta/\dot{\Omega}$, due to smaller energy barrier in the region $|t-t_0| < \tau_{LZ}$. If $\gamma_L Z$ is small and $\Delta/\dot{\Omega}$ is too small, we estimate it at a larger value $\dot{\Omega}^{-1/2} = (\Delta/\dot{\Omega})/\sqrt{\gamma_{LZ}}$. So the characteristic time necessary for the LZ transition is $\tau_{LZ} = \max\left(\Delta/\dot{\Omega}, \dot{\Omega}^{-1/2}\right)$.

Since the noise is Gaussian, the influence of the noise onto the two-state system is completely described by the noise correlation functions:

$$\left\langle \eta_\alpha(t)\,\eta_\beta^\dagger(t')\right\rangle = \frac{1}{V}\sum_{\mathbf{q}} g_a(\mathbf{q})\,g_\beta^*(\mathbf{q})\,(n_{\mathbf{q}}+1)\,e^{i\omega_{\mathbf{q}}(t'-t)} \tag{2.7}$$

$$\left\langle \eta_\alpha^\dagger(t)\,\eta_\beta(t')\right\rangle = \frac{1}{V}\sum_{\mathbf{q}} g_a(\mathbf{q})\,g_\beta^*(\mathbf{q})\,n_{\mathbf{q}}e^{i\omega_{\mathbf{q}}(t-t')} \tag{2.8}$$

Here $n_{\mathbf{q}} = \left\langle b_{\mathbf{q}}^\dagger b_{\mathbf{q}}\right\rangle$ are the average phonon occupation numbers and $\langle ...\rangle$ means averaging over the phonon bath ensemble, not necessarily in thermal equilibrium. The

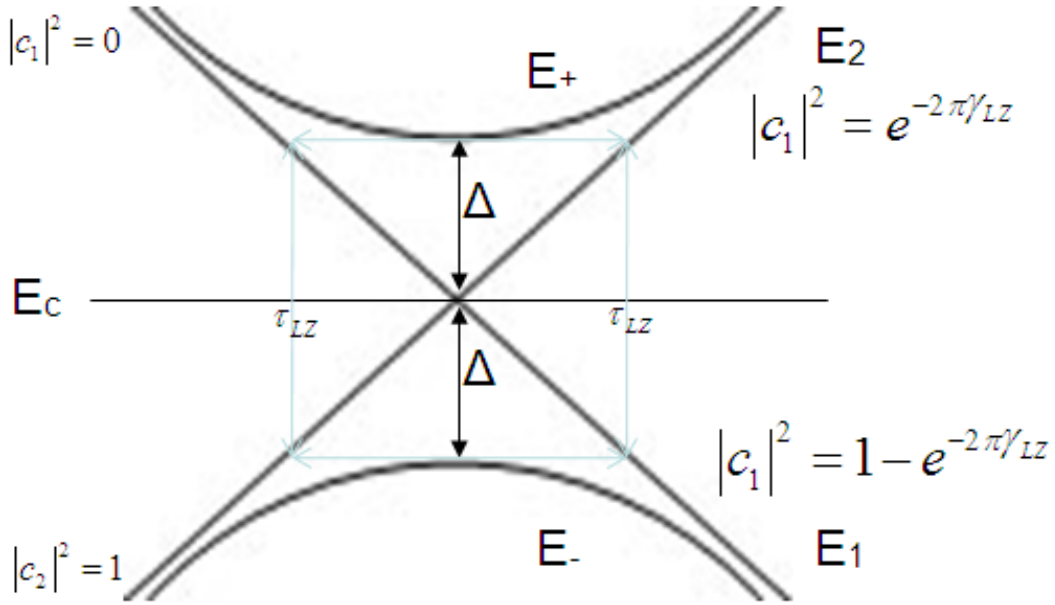

FIG. 3. Illustration of initial condition and asymptotic situation, and illustration of LZ time. The final state population depends on the LZ parameter.

Fourier-components of the correlation functions (2.7, 2.8) read:

$$\left\langle \eta_\alpha \eta_\beta^\dagger \right\rangle_\omega = \frac{2\pi}{V} \sum_{\mathbf{q}} g_a(\mathbf{q}) g_\beta^*(\mathbf{q}) (n_{\mathbf{q}} + 1) \delta(\omega - \omega_{\mathbf{q}}) \tag{2.9}$$

$$\left\langle \eta_\alpha^\dagger \eta_\beta \right\rangle_\omega = \frac{2\pi}{V} \sum_{\mathbf{q}} g_a(\mathbf{q}) g_\beta^*(\mathbf{q}) n_{\mathbf{q}} \delta(\omega + \omega_{\mathbf{q}}) \tag{2.10}$$

Note that one of the two correlators contains only positive, whereas the second one contains only negative frequencies. If the noise is in equilibrium at temperature T, the Fourier-transforms of correlation functions obey a simple relation ($\omega > 0$):

$$\frac{\left\langle \eta_\alpha \eta_\beta^\dagger \right\rangle_\omega}{\left\langle \eta_\alpha^\dagger \eta_\beta \right\rangle_{-\omega}} = e^{\frac{\omega}{T}} \tag{2.11}$$

Let us denote ω_g the range of frequencies in which the coupling coefficients $g_\alpha(\mathbf{q})$ do not vanish. If the occupation numbers $n_{\mathbf{q}}$ are of the same order of magnitude for all states within this region of frequencies, then ω_g determines the spectral width of

the noise $\Delta\omega$. In some cases, for example at low temperature $T \ll \omega_g$, there appears a second, smaller scale of frequency (T). The noise correlation time is $\tau_n = 1/\Delta\omega$. It is different for the two correlation functions $\left\langle \eta_\alpha(t)\,\eta_\beta^\dagger(t')\right\rangle$ and $\left\langle \eta_\alpha^\dagger(t)\,\eta_\beta(t')\right\rangle$ at low temperature and it is equal to ω_g^{-1} for both at high temperature. By definition the noise is fast if $\Delta\omega \gg \Delta$, or $\tau_n \ll \Delta^{-1}$. Noise starts to produce transition if $\Delta\omega \geq \Omega(t)$. This condition is equivalently $t \leq 1/\dot{\Omega}\tau_n \equiv \tau_{acc}$, where we define the accumulation time τ_{acc} as the time interval smaller than which noise produces transitions. The accumulation time τ_{acc} must be much larger than correlation time τ_n in order for noise to produce any transition. From $\tau_{acc} \gg \tau_n$ and combined with $\tau_n \ll \Delta^{-1}$, we have $\tau_n \ll \min\left(\dot{\Omega}^{-1/2}, \Delta^{-1}\right)$, or $\Delta\omega \gg \max\left(\dot{\Omega}^{1/2}, \Delta\right)$. We can also see that $\tau_{acc} \ll \tau_{LZ}$ by the definition of fast quantum noise. This inequality makes possible the time separation of the evolution of the system.

Besides its spectral characteristics the noise is characterized by its strength. The most natural measure of the noise strength is the average square of its amplitude:

$$\begin{aligned}\left\langle u_\alpha^2(t)\right\rangle &= \left\langle \eta_\alpha(t)\,\eta_\alpha^\dagger(t)\right\rangle + \left\langle \eta_\alpha^\dagger(t)\,\eta_\alpha(t)\right\rangle \\ &= \frac{1}{V}\sum_{\mathbf{q}} |g_a(\mathbf{q})|^2 (2n_{\mathbf{q}}+1)\end{aligned} \tag{2.12}$$

The noise is weak if $\langle u_\alpha^2(t)\rangle \ll \dot{\Omega}$. Weak noise can be accounted as a small perturbation to the LZ result. We call the noise moderately strong if it obeys the inequalities: $\dot{\Omega} \leq \langle u_\alpha^2(t)\rangle \ll \tau_n^{-2}$. Though for moderately strong noise the perturbation theory is generally invalid at accumulation time scale determined in the next section, we will show that it works during sufficiently small intervals of time still longer than τ_n. Most of our results relate to the weak and moderate noise, i.e. for the noise obeying the condition $\langle u_\alpha^2(t)\rangle \ll \tau_n^{-2}$, which we will call not strong. The noise is called strong if $\langle u_\alpha^2(t)\rangle \geq \tau_n^{-2}$. Note, that generally $\dot{\Omega}$ depends on time, so that the noise may be

Table II. Definitions of time scales.

τ_n	τ_{LZ}	τ_{acc}	$\tau_{r\alpha}$
$\tau_n = 1/\Delta\omega$	$\tau_{LZ} = \max(\Delta/\dot{\Omega}, \dot{\Omega}^{-1/2})$	$\tau_{acc} = \left(\dot{\Omega}\tau_n\right)^{-1}$	$\tau_{r\alpha} = \left(\langle u_\alpha^2(t)\rangle \tau_n\right)^{-1}$

Table III. Definitions of fastness and strength of quantum noise.

fast	weak	moderate	strong
$\tau_n \ll \min(\dot{\Omega}^{-1/2}, \Delta^{-1})$	$\langle u_\alpha^2(t)\rangle \ll \dot{\Omega}$	$\dot{\Omega} \leq \langle u_\alpha^2(t)\rangle \ll \tau_n^{-2}$	$\langle u_\alpha^2(t)\rangle \geq \tau_n^{-2}$

weak or moderate during one time interval and strong during another one. Another time scale, which we call the relaxation time $\tau_{r\alpha} = \left(\langle u_\alpha^2(t)\rangle \tau_n\right)^{-1}$ (see [36], where it is called phase relaxation time), is defined by the condition that the probability of finding the system in state 1 or 2 changes significantly. When the noise is strong, the relaxation time becomes less than the noise correlation time τ_n. The definitions of different time scales and their connection to the parameters of the problem are collected in the Table II and Table III. It is convenient to introduce dimensionless coupling function $\lambda_{\alpha\mathbf{q}} = |g_\alpha(\mathbf{q})| / (\omega_g a^3)$, where a is the lattice constant, $\alpha = \|, \perp$. In condensed matter systems the values $\lambda_{\alpha\mathbf{q}}$ never become large. Migdal [44] argued that large coupling constants would lead to the lattice instability and reconstruction. Though his arguments related directly to the electron-phonon coupling, his idea is very general. If $\lambda_{\alpha\mathbf{q}}$ are not large, a large value of $\langle u_\alpha^2(t)\rangle \tau_n^2$ can be reached only if phonon occupation numbers $n_\mathbf{q}$ become large. In the equilibrium case it means that the temperature must be large. Very strong noise is classical, irrespective of its specific density matrix. An analogue of the LZ parameter for the noise reads $\gamma_{n\alpha} = \langle u_\alpha^2(t)\rangle / \dot{\Omega}$ [31]. If it is small, the noise brings only a small perturbation to

the LZ picture; if it is large, the occupation numbers of the two-state system follow adiabatically the instantaneous value of frequency. We will return to this point later.

C. Heuristic approach

In the previous section we argued that the LZ gap and longitudinal noise become ineffective for transitions beyond the LZ time interval $(-\tau_{LZ}, \tau_{LZ})$. We show later in this section that the transverse noise produces transitions during much longer time interval $(-\tau_{acc}, \tau_{acc})$. Therefore, for $|t| \gg \tau_{LZ}$ it is necessary to solve a simplified problem with $\Delta = 0$ and $u_{\|} = 0$, so that all transitions are only due to the transverse noise. In this section we develop a heuristic approach to this simplified problem.

Since $\tau_n \ll \dot{\Omega}^{-1/2}$, the instantaneous frequency of the two-state system does not change during correlation time of the noise and it can be considered as a constant. Thus, it is possible to calculate the instantaneous rate of transition probability using the standard quantum mechanical technique for transitions between stationary energy levels.

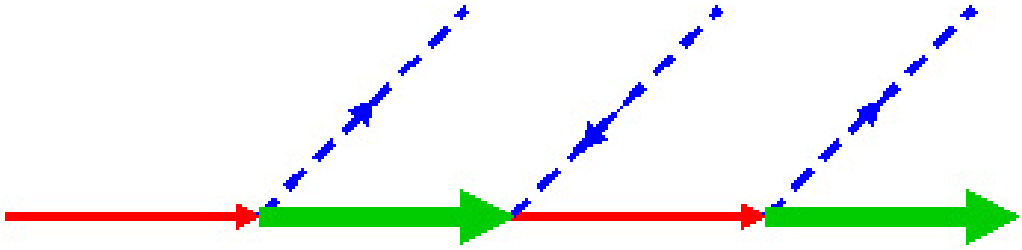

FIG. 4. Feynman graph for a 3-phonon process. Thin solid lines correspond to the state 1; thick solid lines correspond to the state 2; dashed blue lines correspond to phonons.

If the noise is not strong, the transition probability can be calculated in the first Born approximation. Indeed, according to the Fermi golden rule the rate of

transition probability per unit time before the level crossing reads:

$$p_{1\to 2}\left(t\right)=2\pi\left\langle \eta_{\perp}^{\dagger}\eta_{\perp}\right\rangle _{\Omega(t)} \tag{2.13}$$

In the framework of the considered model the next after single-phonon is three-phonon transition shown in Fig. 4. Its contribution to the transition probability reads:

$$p_{1\to 2}^{(3)}\left(t\right)=2\pi\times\left\langle \int\frac{d\omega_{1}d\omega_{2}}{\left(2\pi\right)^{2}}\frac{\eta_{\omega_{1}}^{\dagger}\eta_{\omega_{2}}^{\dagger}\eta_{\Omega(t)-\omega_{1}-\omega_{2}}^{\dagger}}{\omega_{1}\omega_{2}}+\text{herm. conj.}\right\rangle \tag{2.14}$$

The 3-phonon contribution can be neglected if the noise is moderately strong. In the same approximation it is possible to neglect the correction to the transition frequency due to the interaction with the phonon bath. Thus, the occupation numbers of the diabatic states $N_{1,2}$ at negative time obey following master equation:

$$\dot{N}_{1}=2\pi\left(-\left\langle \eta_{\perp}^{\dagger}\eta_{\perp}\right\rangle _{|-\Omega(t)|}N_{1}+\left\langle \eta_{\perp}\eta_{\perp}^{\dagger}\right\rangle _{|\Omega(t)|}N_{2}\right) \tag{2.15}$$

which must be complemented by conservation law $N_1+N_2=1$. For positive time equation (2.15) must be modified as follows:

$$\dot{N}_{1}=2\pi\left(-\left\langle \eta_{\perp}\eta_{\perp}^{\dagger}\right\rangle _{|\Omega(t)|}N_{1}+\left\langle \eta_{\perp}^{\dagger}\eta_{\perp}\right\rangle _{|-\Omega(t)|}N_{2}\right) \tag{2.16}$$

The noise produces transitions as long as its spectral width exceeds the instantaneous frequency $|\Omega\left(t\right)|$. The accumulation time estimated from this requirement is $\tau_{acc}=\left(\dot{\Omega}t_{n}\right)^{-1}$ [31]. Since the noise is assumed to be fast the accumulation time τ_{acc} is much longer than the noise correlation time τ_n. In real experiment the sweeping of frequency may stop or saturate before the accumulation time is reached. The master equations enable one calculating the occupation numbers at any time rather than asymptotically at $t\to\infty$. The accumulation time is also much longer than the LZ

time τ_{LZ}. Therefore, it is possible to neglect the action of the noise during the LZ time interval $(-\tau_{LZ},\tau_{LZ})$ and neglect the LZ gap Δ beyond this time interval. It means that the action of the fast transverse noise and of the LZ gap are separated in time as it was earlier shown for classical noise [31]. The solution of the LZ problem without transverse noise and the noise transition problem with zero LZ gap Δ should be matched at some intermediate time. It will be done in Section H.

The action of the fast longitudinal noise is very different from that of the transverse one. The longitudinal noise does not produce transitions in the absence of the LZ gap. Therefore, its action is effectively limited to the LZ time interval. In the next section we demonstrate that the fast longitudinal noise must be sufficiently strong to produce a substantial change in the LZ transition probability. Namely it must satisfy an inequality $\left\langle u_{\parallel}^{2}\right\rangle \gtrsim \dot{\Omega}/\left(\Delta\tau_{n}\right) \gg \dot{\Omega}$. An analogous criterion for the transverse noise is much more liberal: $\langle u_{\perp}^{2}\rangle \gtrsim \dot{\Omega}$. For a comprehensive analysis of the longitudinal noise action we refer the reader to the cited articles [36, 35, 34]. Beyond the LZ time interval the classical longitudinal noise modulates the transverse noise by a factor $\exp\left(-i\int_{t_0}^{t}u_{\parallel}d\tau\right)$. Correlation functions $\left\langle \eta_{\perp}\left(t\right)\eta_{\perp}^{\dagger}\left(t'\right)\right\rangle$ must be substituted by $\left\langle \eta_{\perp}\left(t\right)\eta_{\perp}^{\dagger}\left(t'\right)\exp\left(-i\int_{t'}^{t}u_{\parallel}d\tau\right)\right\rangle$. Neglecting the correlation between longitudinal and transverse noise and employing the Gaussian statistics of the noise, one can express the latter correlator as follows:

$$\begin{aligned}\left\langle \eta_{\perp}\left(t\right)\eta_{\perp}^{\dagger}\left(t'\right)\exp\left(-i\int_{t'}^{t}u_{\parallel}d\tau\right)\right\rangle &= \left\langle \eta_{\perp}\left(t\right)\eta_{\perp}^{\dagger}\left(t'\right)\right\rangle \\ &\times\exp\left[-\frac{1}{2}\int_{t'}^{t}\int_{t'}^{t}dt_{1}dt_{2}\left\langle u_{\parallel}\left(t_{1}\right)u_{\parallel}\left(t_{2}\right)\right\rangle\right]\end{aligned} \tag{2.17}$$

The transverse noise correlator decays rapidly when the modulus of difference $|t-t'|$ exceeds τ_n. Therefore, the value in the exponent in the right-hand side of

equation (2.17) can be estimated as $\left\langle u_{\parallel}^{2}\right\rangle \tau_{n}^{2} \ll 1$. This estimates shows that the longitudinal noise can be neglected beyond the LZ time interval. In the next section we consider this question in more details.

Though physical arguments of this section leading to the master equation sound convincing, we used an implicit assumption that the quantum coherence is negligibly small. In the next section we derive the master equation rigorously starting from the microscopic Hamiltonian. This derivation shows that, though quantum coherence is substantial at small time intervals less than τ_n, it does not play any role at larger time scale.

D. Derivation of master equations

In this section as in the previous one we consider time interval beyond Landau-Zener interval $(-\tau_{LZ}, \tau_{LZ})$ and neglect the LZ gap Δ and longitudinal noise. Our goal is to find the dependence of the occupation numbers N_α $(\alpha = 1, 2)$ on time. The same problem can be formulated as calculation of the average value of projectors $P_\alpha = |\alpha\rangle \langle\alpha| = \frac{1}{2}(1 \pm \sigma_z)$ [33, 35]. We consider the case $\Delta = 0$, $u_{\parallel} = 0$. The calculation will be performed in the interaction representation with the diagonal time-dependent unperturbed Hamiltonian $H_0 = -\frac{\Omega(t)}{2}\sigma_z + H_b = -\frac{\Omega(t)}{2}(|1\rangle\langle 1| - |2\rangle\langle 2|) + H_b$ and the interaction Hamiltonian $V = u_\perp \sigma_x = u_\perp (|1\rangle\langle 2| + |2\rangle\langle 1|)$. Being transformed to the interaction representation, the interaction Hamiltonian depends on time as follows:

$$V_I(t) = e^{iH_0 t} V e^{-iH_0 t} = u_\perp(t)\left(|1\rangle\langle 2|\, e^{-i\int_{t_0}^{t}\Omega(\tau)d\tau} + |2\rangle\langle 1|\, e^{i\int_{t_0}^{t}\Omega(\tau)d\tau}\right), \qquad (2.18)$$

where

$$u_\perp(t) = e^{iH_b(t-t_0)} u_\perp(t_0)\, e^{-iH_b(t-t_0)} \qquad (2.19)$$

In terms of the evolution operator in the interaction representation

$$U_I(t,t_0) \equiv T[e^{-i\int_{t_0}^{t} V_I(\tau)d\tau}], \tag{2.20}$$

the time-dependent occupation numbers can be expressed as

$$N_\alpha(t) = \mathrm{Tr}\left[\rho_0 U_I^{-1}(t,t_0)\, P_\alpha U_I(t,t_0)\right] \tag{2.21}$$

where ρ_0 is the initial density matrix which is the direct product of two independent density matrices $\rho_0 = \rho_2\rho_b$, where the first factor is the density matrix of the two-state system and the second one is that of the bath.

The expression (2.21) is a Keldysh contour ordered average from $-\infty$ to 0 and then to $-\infty$ again. The detailed calculation is explained in Appendix A. For now, the calculation on these averages is done by employing a simplified version of the Keldysh-Schwinger technique [45, 46] used already for a similar purpose in [33, 35, 36]. Each of the two evolution operators is presented as a series of time ordered integrals. A general term of such an expansion contains a product of two multiple time integrals. With each time variable t_k a vertex $V_I(t_k)$ is associated. The product of vertices is ordered in chronological time order in $U_I(t,t_0)$ and in anti-chronological time order in $U_I^{-1}(t,t_0)$. All operators of $V_I(t_k)$ belonging to $U_I^{-1}(t,t_0)$ are located on the left ("later") than corresponding operators belonging to $U_I(t,t_0)$.

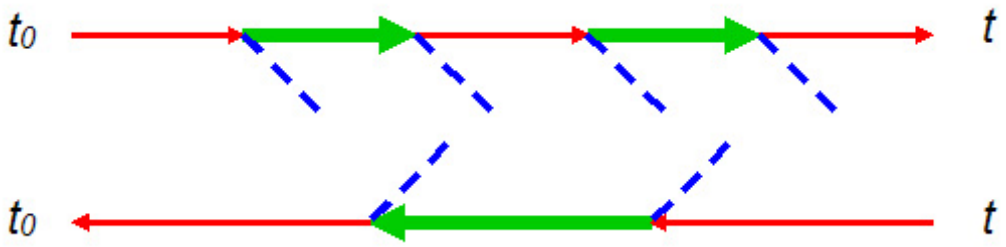

FIG. 5. An example of a term in the perturbation theory. Points correspond to vertexes $V_I(t_j)$.

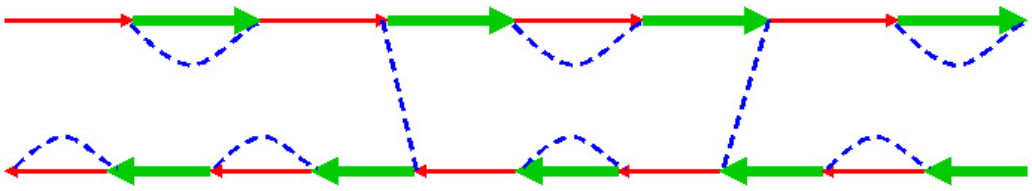

FIG. 6. A typical graph without phonon line crossings dominantly contributing to the survival and transition probability.

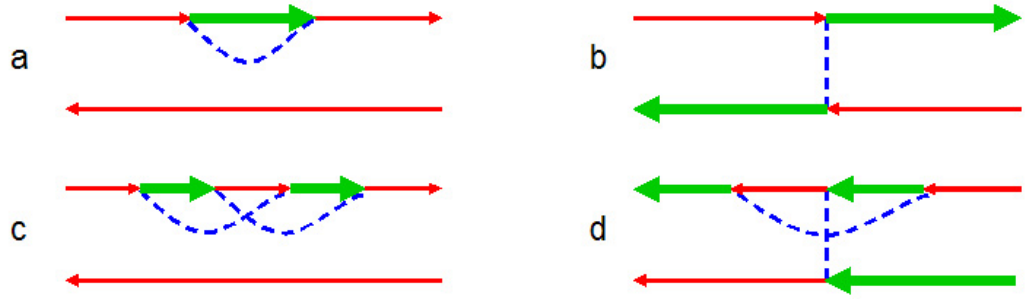

FIG. 7. Elementary graphs. a) b) without phonon line crossing; c) d) with phonon line crossing.

A particular contribution is graphically depicted in Fig. 5 before the averaging over phonon bath is performed. It consists of two lines both starting at t_0 and ending at t. The upper line symbolizes $U_I(t,t_0)$ and the lower one symbolizes $U_I^{-1}(t,t_0)$. Each solid line represents either the propagator of the state 1 (thin (red) line) or that of the state 2 (thick(green) line). The dashed line represent a phonon absorption or emission. Vertices on these lines correspond to the operators $V_I(t_k)$. Each vertex contains one phonon operator $u(t_k)$ and changes the state of the two-state system.

The presence of the projection operator P_α in equation (2.21) implies that the state closest to the final time t on both lines must be $|\alpha\rangle$. Applying the Wick's rule for phonons, one should form all possible pairing of (phonon) noise lines*. Different

*The Wick pairing ensures that the numbers of the state alternations on the upper and the lower lines are either both even or both odd. Therefore, the occupation numbers depend only on diagonal matrix elements of the initial density matrix.

contributions can be represented by Feynman graphs such as shown in Fig. 6. These propagators have the form:

$$G_{1,2}(t,t') = \exp\left(\pm\frac{i}{2}\int_{t'}^{t}\Omega(\tau)\,d\tau\right) \tag{2.22}$$

By introducing these propagators we absorb the phase factors from the vertex (2.18). The dashed (blue) lines represent the correlation functions of the transverse noise $D(t,t') = \langle T(u_\perp(t)\,u_\perp(t'))\rangle$. Each vertex carries the factor i at the upper line and $-i$ at the lower line. Integration over all time arguments must be performed in chronological order at the upper line and in anti-chronological ordering at the lower line. In the case of fast not strong noise the main contribution to the occupation numbers comes from the graphs without crossing or overlapping of the phonon lines. An example of a graph without overlapping is shown in Fig. 6. In comparison with elementary graphs without phonon line overlapping or crossing (Fig. 7a,b) the contributions of the graphs containing overlapping or crossing (Fig. 7c,d,) have additional small factors of the order of $\langle u_\perp^2\rangle\,\tau_n^2$ and can be neglected if the transverse noise is moderately strong. Indeed the time interval between the ends of each phonon lines is about τ_n.

It's difficult to calculate Eq. (2.21) directly according to Fig. 6. We consider a set of graphs representing difference of the number of particles N_α at time t and $t+\Delta t$. If we can calculate the differential difference, we can derive an dynamic equation for the state evolution. Δt must satisfy the strong inequality $\tau_n \ll \Delta t \ll (\langle u_\perp^2\rangle\,\tau_n)^{-1}$. First, there are graphs with phonon lines connecting the interval $(t, t+\Delta t)$ with the interval (t_0, t). Their contribution can be neglected since it is relatively proportional to a small ratio $\tau_n/\Delta t$. The contribution of k non-overlapping or intersecting noise lines inside the interval $(t, t+\Delta t)$ is proportional to $(\langle u_\perp^2\rangle\,\tau_n\Delta t)^k \ll 1$. Therefore,

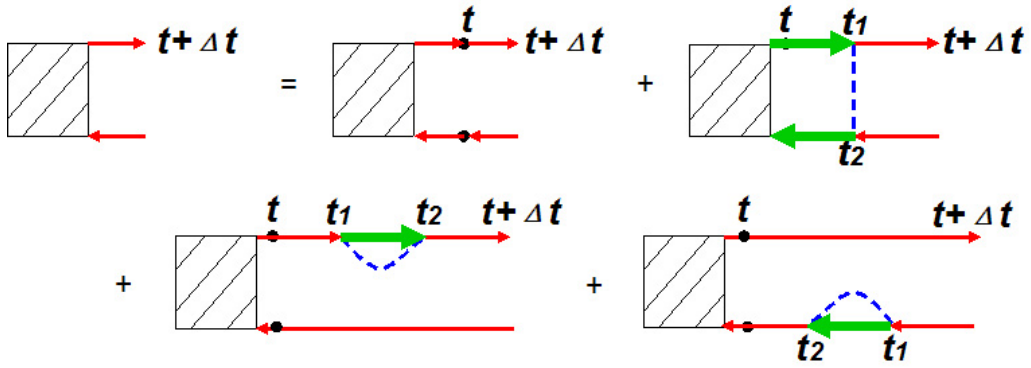

FIG. 8. Graphic equation connecting $N_\alpha\,(t+\Delta t)$ and $N_\alpha\,(t)$ containing 0 or 1 phonon line.

the dominant contribution to the set comes from graphs containing exactly zero or one line inside the interval $(t, t+\Delta t)$. Note the coarse-grain description: the master equation is invalid at time scale τ_n and shorter. The graphical equation connecting $N_\alpha(t+\Delta t)$ with $N_\alpha(t)$ is shown in Fig. 8, where the graph with a box and two red thin lines at the left side of sign = denotes the number of particles occupying state 1 at time= $t+\Delta t$, and the four graphs at the right side of sign = denotes the four possible (upto first order approximation) evolutions from t to $t+\Delta t$. There is no line in the first graph, meaning that $N_\alpha(t)$ did not change during this time interval. This is the zeroth order of expansion of $N_\alpha(t+\Delta t)$. The other there graphs, represented by (Γ_1,Π_1, Π_2), correspond to evolution with one phonon line connecting ((+,-),(+,+),(-,-)) branches. So according to Fig. 9 we have the equation

$$N_\alpha\,(t+\Delta t) = N_\alpha\,(t) + \Gamma_1 + \Pi_1 + \Pi_2 \tag{2.23}$$

To find their analytical expression, we calculate the contribution of the 3 elementary subgraphs for $\alpha = 1$ shown in Fig. 9.

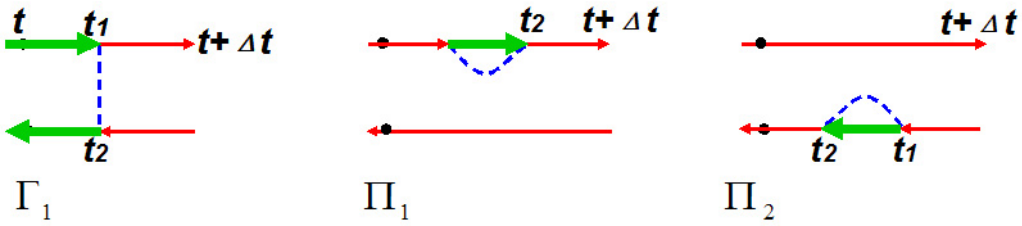

FIG. 9. Three elementary graphs with one phonon line in the interval $t, t+\Delta t$.

They read:

$$\begin{aligned}\Gamma_1 &= \int_t^{t+\Delta t} dt_1 \int_t^{t+\Delta t} dt_2 \left\langle u_\perp(t_1)\, u_\perp(t_2)\right\rangle e^{-i\int_{t_2}^{t_1}\Omega(\tau)d\tau} \\ &\approx 2\pi \left\langle u_\perp u_\perp\right\rangle_{-\Omega(t)} \Delta t\end{aligned} \tag{2.24}$$

$$\begin{aligned}\Pi_1 &= -\int_t^{t+\Delta t} dt_1 \int_{t_1}^{t+\Delta t} dt_2 \left\langle u_\perp(t_1)\, u_\perp(t_2)\right\rangle e^{+i\int_{t_2}^{t_1}\Omega(\tau)d\tau} \\ &\approx -\Delta t \int_{-\infty}^{0} \left\langle u_\perp(\tau)\, u_\perp(0)\right\rangle e^{+i\Omega(t)\tau} d\tau\end{aligned} \tag{2.25}$$

$$\begin{aligned}\Pi_2 &= -\int_t^{t+\Delta t} dt_1 \int_{t}^{t_1} dt_2 \left\langle u_\perp(t_1)\, u_\perp(t_2)\right\rangle e^{+i\int_{t_2}^{t_1}\Omega(\tau)d\tau} \\ &\approx -\Delta t \int_{0}^{\infty} \left\langle u_\perp(\tau)\, u_\perp(0)\right\rangle e^{+i\Omega(t)\tau} d\tau\end{aligned} \tag{2.26}$$

where the short notation for the Fourier transform is introduced

$$\left\langle u_\perp(t_1) u_\perp(t_2)\right\rangle_{-\Omega(t)} \equiv \int_{-\infty}^{\infty} e^{i\Omega t} \left\langle u_\perp(t) u_\perp(0)\right\rangle dt. \tag{2.27}$$

In this calculation we used the fastness of the noise $\left(\tau_n \ll \Delta t,\ \tau_n \ll \sqrt{\dot{\Omega}}\right)$ to substitute the integral in the exponent by $\Omega(t)(t_1 - t_2)$ and to extend the integration

over the difference $t_1 - t_2$ to infinite limits. The graph 6a connects $N_1(t + \Delta t)$ to $N_2(t)$, two others graphs connect $N_1(t + \Delta t)$ to $N_1(t)$. Different signs in the contributions (2.24) and (2.25, 2.26) are associated with the fact that the vertex at the upper line contains a factor $-i$, whereas it acquires the factor $+i$ at the lower line. The contributions from the last two graphs together are

$$\Pi_1 + \Pi_2 = -\langle u_\perp(t_1) u_\perp(t_2) \rangle_{\Omega(t)} \Delta t. \tag{2.28}$$

Collecting all contributions together, we arrive at the following differential equation for N_1 when Δt approaches zero

$$\frac{dN_1}{dt} = N_2 \langle u_\perp u_\perp \rangle_{-\Omega} - N_1 \langle u_\perp u_\perp \rangle_{\Omega}, \tag{2.29}$$

and a similar equation for N_2

$$\frac{dN_2}{dt} = N_1 \langle u_\perp u_\perp \rangle_{\Omega} - N_2 \langle u_\perp u_\perp \rangle_{-\Omega}. \tag{2.30}$$

According to the definition of u operator, we can further calculate the Fourier transform Eq. (A.12) as following

$$\begin{aligned} \left\langle \eta_\perp \eta_\perp^\dagger \right\rangle_{-\Omega} &= \theta(-\Omega) \int \frac{d^3q}{(2\pi)^2} \delta(|\Omega - \omega_q|) |g_q|^2 (n_q + 1) = \theta(-\Omega) \left\langle \eta_\perp \eta_\perp^\dagger \right\rangle_{|\Omega|}, \\ \left\langle \eta_\perp^\dagger \eta_\perp \right\rangle_{\Omega} &= \theta(\Omega) \int \frac{d^3q}{(2\pi)^2} \delta(|\Omega - \omega_q|) |g_q|^2 n_q = \theta(\Omega) \left\langle \eta_\perp^\dagger \eta_\perp \right\rangle_{|-\Omega|}, \end{aligned} \tag{2.31}$$

where $\theta(x)$ is the step function which is 1 at positive arguments and 0 at negative arguments.

By the fact that $N_1 + N_2 = 1$ and imposing the new variable $s_z = \frac{N_1 - N_2}{2} = N_1 - \frac{1}{2} = \frac{1}{2} - N_2$ the master equation look simpler:

$$\frac{ds_z}{dt} = 2\pi(-s_z \times \left[\left\langle \eta\eta^\dagger \right\rangle_{|\Omega|} + \left\langle \eta^\dagger \eta \right\rangle_{-|\Omega|} \right] - \frac{1}{2} \mathrm{sign}\Omega \times \left[\left\langle \eta\eta^\dagger \right\rangle_{|\Omega|} - \left\langle \eta^\dagger \eta \right\rangle_{-|\Omega|} \right])_{\Omega = \Omega(t)} \tag{2.32}$$

Master equation (2.32) can be treated as application of the Fermi Golden Rule to the transition between the two levels separated by an instantaneous frequency $\Omega(t)$. The Fermi Golden Rule or the first Born approximation at a fixed moment of time can be applied since the frequency variation during the noise correlation is small and the perturbation caused by the noise in the corresponding stationary problem is weak. The perturbation theory is valid if $\sqrt{\langle u_\perp^2 \rangle} \ll |\Omega(t)|$. Within the accumulation time interval the instantaneous frequency is of the same order of magnitude as the spectral width of the noise: $|\Omega(t)| \sim \tau_n^{-1}$. The same inequality ensures that the frequency exceeds the width of the levels and the change of frequency due to the interaction with the noise.

Thus, we have proved by microscopic calculation that the quantum coherence is negligible for the time evolution of the occupation numbers. Now the question about the influence of the longitudinal noise onto the master equation is in order. First we demonstrate that correlations of the type $\langle u_\parallel(t)\, u_\parallel(t') \rangle$ do not change the master equation. Indeed, let us consider the influence of the longitudinal noise onto the difference between $N_\alpha(t + \Delta t)$ and $N_\alpha(t)$. In analogy with the case of the transverse noise, the contribution of one longitudinal phonon line inside the interval $(t, t + \Delta t)$ must be taken in account. This contribution does not depend on preceding evolution of the system just because it contains only propagators whose time arguments are confined by the interval $(t, t + \Delta t)$. Therefore, it is the same as it would be in the absence of the transverse noise. Since the longitudinal noise does not produce transitions in the absence of the transverse noise, the total contribution of 3 graphs of Fig. 9 for longitudinal noise is zero. Direct calculation confirms this statement.

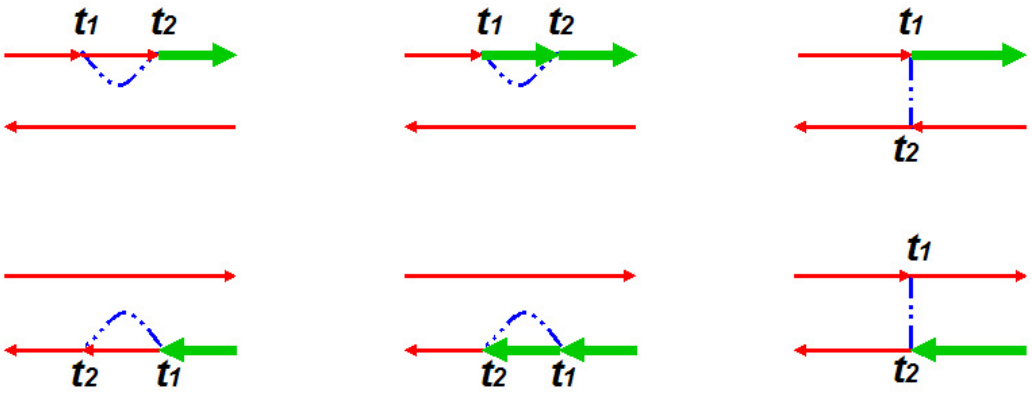

FIG. 10. Graphs containing mixed noise correlator (dash-dot line) and responsible for the LZ gap renormalization.

E. Renormalization of the LZ gap

The problem of mixed correlations between transverse and longitudinal noise is more subtle. The line of mixed correlation starts at one state, to say 1, and ends at another one (2) as shown in Fig. 10. The self-energy part associated with the graphs of Fig. 10 reads:

$$\Pi_{mix} = |1\rangle\langle 2| \, e^{-i\int_{t_0}^{t}\Omega(\tau)d\tau} \times [\int_{-\infty}^{0} \left\langle u_{\parallel}(t') \, u_{\perp}(0)\right\rangle dt' - \int_{0}^{\infty} \left\langle u_{\perp}(t') \, u_{\parallel}(0)\right\rangle dt'] + \text{H.C.} \tag{2.33}$$

This operator has the same form as the operator $\Delta\sigma_x$ in the interaction representation. Thus, at a time scale much longer than τ_n, the mixed correlation renormalizes the LZ gap to a value

$$\tilde{\Delta} = \Delta + i\int_{0}^{\infty} \left\langle \left[u_{\perp}(t'), u_{\parallel}(0)\right]\right\rangle dt' \tag{2.34}$$

For the transformation of the integrals in equation (2.33) into integral in equation (2.34) we employed the time-translation invariance: $\left\langle u_{\parallel}(-t) \, u_{\perp}(0)\right\rangle = \left\langle u_{\parallel}(0) \, u_{\perp}(t)\right\rangle$.

Thus, the statement that one can neglect the action of the transverse noise within the LZ time interval is not completely correct: it is legitimate to neglect transverse-transverse correlations, but the mixed correlations can significantly change the LZ gap up to turning it into zero and changing its sign.

The commutator entering equation (2.34) does not depend on the phonon occupation numbers, i.e. on temperature. It is instructive to express the renormalization of the LZ gap in terms of the phonon model (Section B, equations (2.5, 2.7, 2.8)):

$$\tilde{\Delta} - \Delta = -\frac{1}{V} \sum_{\mathbf{q}} \frac{g_{\parallel}(\mathbf{q})\, g_{\perp}(\mathbf{q})}{\omega_{\mathbf{q}}} \tag{2.35}$$

F. Longitudinal noise

Next we consider the action of the purely longitudinal noise within the LZ time interval. For this problem the transverse noise will be ignored. We start with the classical longitudinal noise to have an idea when it produces substantial changes. The noise is classical if the phonon occupation numbers are large (high temperature), but the noise still may be weak or moderate if the coupling functions $\lambda_{\alpha}(\mathbf{q})$ are small enough. If the noise is classical, the proper diagonal Hamiltonian is $H_0 = \left(-\frac{\Omega(t)}{2} + u_{\parallel}\right)\sigma_z + H_b$, whereas the non-diagonal part is $V = \Delta\sigma_x$. In the interaction representation the non-diagonal part acquires the following form:

$$V_I(t) = \Delta\left(|1\rangle\langle 2|\, e^{i\int_{t_0}^{t}\left(\Omega - 2u_{\parallel}\right)d\tau} + \text{herm. conj.}\right) \tag{2.36}$$

Calculation of the transition probability is very similar to that considered above (see equation (2.21) and Fig. 5), but the vertexes correspond to $V_I(t)$ given by (2.36) (we will call them $\Delta-$vertexes) and instead of connecting pairs of noise amplitudes it is necessary to calculate average of a product $\prod_j \exp\left[\pm 2i\int_{t_0}^{t_j} u_{\parallel}(\tau_j)\, d\tau_j\right]$. Number

of the signs $-$ in the exponent is equal to the number of signs $+$. Therefore, the dependence on the initial moment of time t_0 vanishes. The Gaussian statistics allows to calculate the average of the product:

$$\left\langle \prod_j \exp\left[\pm 2i \int_{t_0}^{t_j} u_\parallel(\tau_j)\, d\tau_j\right]\right\rangle$$
$$= \exp[-2^{2k-1} \int_{t_0}^{t_1} d\tau_1 ... \int_{t_0}^{t_{2k}} d\tau_{2k} \sum_C \left(\pm \left\langle u_\parallel(j_1) u_\parallel(j_2)\right\rangle \left\langle u_\parallel(j_3) u_\parallel(j_4)\right\rangle + ...\right)] \tag{2.37}$$

where summation is performed over all possible divisions of arguments τ_j into pairs. Each correlator vanishes if the modulus of corresponding time difference $|\tau - \tau'|$ exceeds τ_n. The substantial range of integration over remaining variable $(\tau + \tau')/2$ is about $\tau_{LZ} = \Delta/\dot{\Omega}$. Therefore the order of magnitude of the number obtained in the exponent (2.37) after integration is $\sim \left(\left\langle u_\parallel^2 \right\rangle \tau_n \tau_{LZ}\right)^k$. This value must be of the order or larger than 1 to ensure a significant change of the transition probability by the longitudinal noise. This requirement is equivalent to the inequality $\left\langle u_\parallel^2 \right\rangle \gtrsim \dot{\Omega}/(\Delta\tau_n) \gg \dot{\Omega}$. For the transverse noise the analogues criterion is much softer [31]: $\langle u_\perp^2 \rangle \gtrsim \dot{\Omega}$.

The quantum longitudinal noise does not commute with itself at different moments of time. Therefore, it must be included into the non-diagonal Hamiltonian. Then, besides of $\Delta-$vertexes one should consider the noise vertexes. Thus, the graphs contain triangular vertices symbolizing a transition between states 1 and 2 and each containing factor Δ, the two-state propagators $G(t, t')$ defined by equation (2.22) and dotted lines symbolizing the correlators of the longitudinal noise $D_\parallel(t, t') = \left\langle T u_\parallel(t)\, u_\parallel(t')\right\rangle$ which are connected to the two-state propagators by the vertices carrying factors $\pm i$. We obtain the same estimate considering the contribution of an elementary graph with one noise line. However, for the fast longitudinal

noise it is possible to find not only an estimate, but also a system of integral equations for the transition amplitudes. These equations are linear, but they are numerous and their kernel contains a complex combination of parabolic cylinder functions. Their analysis is now in progress. Therefore, their derivation is transferred to the AppendixB.

G. Solution of the master equation and noise diagnostic

The master equation (2.32) allows an explicit solution:

$$\begin{aligned} s_z(t) =& s_z(t_0)\exp\left(-\int_{t_0}^{t} f(\tau)\,d\tau\right)+\int_{t_0}^{t} g(t')\exp\left(-\int_{t'}^{t} f(\tau)\,d\tau\right)dt', \\ &\text{where } f(t)=2\pi\left(\left\langle\eta\eta^{\dagger}\right\rangle_{|\Omega(t)|}+\left\langle\eta^{\dagger}\eta\right\rangle_{-|\Omega(t)|}\right), \\ &\text{and } g(t)=-\pi\mathrm{sign}\Omega(t)\left(\left\langle\eta\eta^{\dagger}\right\rangle_{|\Omega(t)|}-\left\langle\eta^{\dagger}\eta\right\rangle_{-|\Omega(t)|}\right). \end{aligned} \tag{2.38}$$

For classical noise $g(t)=0$, and equation (2.38) reproduces the result obtained in the reference [31]. At zero temperature $\left\langle\eta^{\dagger}\eta\right\rangle_{-|\Omega(t)|}=0$ and $g(t)=-\frac{1}{2}\mathrm{sign}\Omega(t)\,f(t)$. In these two cases the measurement of occupation numbers or $s_z(t)$ gives direct information on spectral power of noise. In classical case we find $4\pi\left\langle\eta\eta^{\dagger}\right\rangle_{|\Omega(t)|}=-\frac{d}{dt}\ln|s_z|$; in purely quantum case ($T=0$) the relationship is slightly more complicated: $2\pi\left\langle\eta\eta^{\dagger}\right\rangle_{|\Omega(t)|}=-\frac{d}{dt}\ln\left|s_z+\frac{\mathrm{sign}\Omega(t)}{2}\right|$. In general case it is possible to find both spectral functions $f(t)$ and $g(t)$ by performing two series of measurements with different initial states. Thus, the two-state system is an ideal noise analyzer.

Next we consider regimes of very fast and very slow (adiabatic) frequency sweeping. In the regime of fast sweeping $\left\langle\eta\eta^{\dagger}\right\rangle\ll\dot{\Omega}$ the perturbation theory for equation (2.38) is valid. Indeed the integral $\int_{t_0}^{t} f(\tau)\,d\tau$ can be rewritten in terms of spectral

power as follows:

$$\int_{t_0}^{t} f(\tau)\, d\tau = 2\pi\dot{\Omega}^{-1} \int_{\Omega(t_0)}^{\Omega(t)} \left(\left\langle \eta\eta^{\dagger} \right\rangle_{|\omega|} + \left\langle \eta^{\dagger}\eta \right\rangle_{-|\omega|} \right) d\omega \tag{2.39}$$

The integral in the r.-h. side of equation (2.39) reaches its maximum value, equal to the average square fluctuation $\left\langle \eta\eta^{\dagger} + \eta^{\dagger}\eta \right\rangle$ at $\Omega(t_0) = -\infty$ and $\Omega(t) = +\infty$. If the condition of fast sweeping is satisfied, the exponent in equation (2.38) can be expanded into a series over small noise parameter $\gamma_n = \left\langle \eta\eta^{\dagger} + \eta^{\dagger}\eta \right\rangle / \dot{\Omega}$. The variation $\Delta s_z(t) = s_z(t) - s_z(t_0)$ is small at any time. In the leading approximation it reads:

$$\begin{aligned} \Delta s_z(t) = -2\pi\dot{\Omega}^{-1} \int_{\Omega(t_0)}^{\Omega(t)} & [\left\langle \eta\eta^{\dagger} \right\rangle_{|\omega|} (s_z(t_0) + \frac{\mathrm{sign}\omega}{2}) \\ & + \left\langle \eta^{\dagger}\eta \right\rangle_{-|\omega|} (s_z(t_0) - \frac{\mathrm{sign}\omega}{2})] d\omega \end{aligned} \tag{2.40}$$

In the opposite regime of slow (adiabatic) sweeping the noise parameter γ_n is large. In this case the exponents in equation (2.38) vary very rapidly allowing asymptotic calculation of s_z. However, in adiabatic regime it is simpler to start directly with the master equation (2.32). Neglecting the time derivative in it, we find the adiabatic solution:

$$s_z(t) = \frac{g(t)}{f(t)} = -\frac{\mathrm{sign}\Omega(t)}{2} \frac{\left\langle \eta\eta^{\dagger} \right\rangle_{|\Omega(t)|} - \left\langle \eta^{\dagger}\eta \right\rangle_{-|\Omega(t)|}}{\left\langle \eta\eta^{\dagger} \right\rangle_{|\Omega(t)|} + \left\langle \eta^{\dagger}\eta \right\rangle_{-|\Omega(t)|}} \tag{2.41}$$

If the photon bath is in equilibrium with temperature T, equation (2.41) implies $s_z(t) = -\tanh\frac{\Omega(t)}{2T}$. As it could be expected, at slow sweeping the two-state system adiabatically accepts the equilibrium population with the temperature of the bath. This conclusion shows that in the case of the quantum noise one must be more careful with the asymptotic behavior of the time-dependent frequency than in genuine LZ problem or even in the analogues problem with the classical noise. In the latter

problems the linear approximation for $\Omega(t) = \dot{\Omega}t$ was satisfactory. However, this approximation may be invalid for the quantum noise if the sweeping stops before the frequency $\Omega(t)$ reaches the spectral width of the noise . In the opposite case the value $s_z(t)$ saturates after $t = \tau_{acc}$. In classical adiabatic case $s_z(t)$ becomes zero after a short time $\tau_{tr} = \left(\left\langle|\eta_\perp|^2\right\rangle \tau_n\right)^{-1}$. A similar time scale for the longitudinal noise was introduced by Kayanuma and Nakayama [36].

At the edge of the adiabatic regime $\gamma_n \sim 1$ the fast noise is still moderately strong, i.e. $\sqrt{\langle\eta\eta^\dagger\rangle} \ll \tau_n^{-1}$. It means that, when the noise becomes strong $\sqrt{\langle\eta\eta^\dagger\rangle} \gtrsim \tau_n^{-1}$, the system is already in deeply adiabatic regime. If the phonon bath is in equilibrium, the two-state system also is in equilibrium with the noise. This equilibrium state is established in a time-independent, but strongly non-linear system. The interaction of the two-level system characterized by the time-independent frequency Ω with the strong noise renormalizes the frequency and creates a finite width for each level. The situation becomes simpler in the limit of very strong noise $\sqrt{\langle\eta\eta^\dagger\rangle} \gg \tau_n^{-1} \gtrsim \Omega$. In this case the initial energy difference Ω between levels can be neglected. The two states become equivalent and their occupation numbers are equal (1/2), i.e. $s_z = 0$. The same result can be obtained from the fact that, as we already argued, the very strong noise must be classical. Equation (2.41) can be considered as an interpolation between weak and very strong noise. Therefore, it gives a reasonable description of intermediate regime.

H. Transitions in the presence of the LZ gap and noise

As we demonstrated earlier, for the fast moderately strong noise, the effective time of the LZ transition due to the regular LZ gap $\tau_{LZ} = \Delta/\dot{\Omega}$ is much less than the accumulation time $\tau_{acc} = \left(\dot{\Omega}\tau_n\right)^{-1}$. Therefore it is possible to ignore the transverse

noise within the LZ time interval $|t| \lesssim \tau_{LZ}$ and to ignore the LZ gap Δ beyond this interval. In this section we match the LZ solution modified by longitudinal noise inside the LZ interval with the solution of the problem with the transverse noise and $\Delta = 0$ (see Section G) beyond this interval. For this purpose we choose a time scale t_1 such that $\tau_{LZ} \ll t_1 \ll \tau_{acc}$ and first consider the solution (2.38) of master equation in the interval $(-\infty, -t_1)$ then use LZ solution with longitudinal noise ignoring transverse noise in the interval $(-t_1, t_1)$ and again use the solution of the master equation in the interval $(t_1, +\infty)$. The next step is to put $t_1 = 0$ for the solution of master equation and to put $t_1 = \infty$ for the solution of the LZ equations with longitudinal noise.Limiting values of the solutions at intervals left from $\pm t_1$ serve as initial values for solutions at intervals right from them. First we consider the interval $(-\infty, -t_1)$. For simplification we accept in the solution (2.38) $t_0 = -\infty$. Since $t_1 \ll \tau_{acc}$ it can be replaced by 0 in the solution (2.38) with high precision $\sim t_1/\tau_{acc}$. Thus, at the left edge of the interval $(-t_1, t_1)$ we find:

$$\begin{aligned} s_z(-t_1) \simeq s_z^{(-)} = \exp\left(-\int_{-\infty}^{0} f(\tau)\, d\tau\right) s_z(-\infty) \\ + \int_{-\infty}^{0} g(t') \exp\left(-\int_{t'}^{0} f(\tau)\, d\tau\right) dt' \end{aligned} \tag{2.42}$$

This value can be treated as an initial condition $s_z^{(-)}$ at $t = -\infty$ for the LZ problem with the longitudinal noise. If the solution of this problem is known, the value $s_z^{(+)}$ at $t = +\infty$ can be calculated. The information necessary to make this calculation effective is the knowledge of two numbers if there is no coherence in the initial system. The density matrix $\rho^{(+)}$ at $t = +\infty$ is obviously a linear function of the initial density matrix $\rho^{(-)}$. There exists a linear 4×4 matrix Λ performing this transformation:

$$\rho_{\alpha\beta}^{(+)} = \Lambda_{\alpha\beta,\mu\nu} \rho_{\mu\nu}^{(-)} \tag{2.43}$$

The requirement that $\mathrm{Tr}\rho^{(+)} = 1$ if $\mathrm{Tr}\rho^{(-)} = 1$ implies the following equation: $\Lambda_{\alpha\alpha,\mu\nu} = \delta_{\mu\nu}$. If $\rho_{12}^{(-)} = \rho_{21}^{(-)} = 0$, the equation (2.43) results in following relationship between $s_z^{(+)}$ and $s_z^{(-)}$:

$$s_z^{(+)} = (\Lambda_1 + \Lambda_2)\, s_z^{(-)} + (\Lambda_1 - \Lambda_2)\,, \tag{2.44}$$

where we introduced abbreviations Λ_1 and Λ_2 for $\Lambda_{11,11}$ and $\Lambda_{22,22}$, respectively. If the longitudinal noise is absent or sufficiently weak, the LZ values for Λ_α are:

$$\Lambda_1 = \Lambda_2 = \exp\left(-2\pi\gamma_{LZ}\right) - \frac{1}{2} \tag{2.45}$$

If $\left\langle u_\parallel^2 \right\rangle \ll \dot{\Omega}/\left(\Delta\tau_n\right)$, the longitudinal noise is weak enough to neglect the longitudinal-longitudinal correlations. Still the correlation of the longitudinal and transverse noise can significantly change the effective LZ gap (see equation (2.34)) . The values $\Lambda_{1,2}$ for some specific situations in which the longitudinal noise is substantial can be extracted from the cited works [35, 36].

The value $s_z^{(+)}$ from equation (2.45) serves in turn as initial condition at $t = +0$ for the master equation. Its solution (2.38) at $t = +\infty$ leads to the final result:

$$\begin{aligned} s_z(+\infty) = (\Lambda_1 + \Lambda_2)e^{-2\pi\gamma_\perp} s_z(-\infty) + (\Lambda_1 - \Lambda_2)e^{-\pi\gamma_\perp} \frac{\pi}{\dot{\Omega}} \times \int_0^\infty [(\left\langle \eta\eta^\dagger \right\rangle_\Omega - \left\langle \eta^\dagger\eta \right\rangle_{-\Omega}) \\ \times e^{-\frac{2\pi}{\dot{\Omega}}\int_\Omega^\infty (\left\langle \eta\eta^\dagger \right\rangle_\omega + \left\langle \eta^\dagger\eta \right\rangle_{-\omega})d\omega} [(\Lambda_1 + \Lambda_2)e^{-\frac{4\pi}{\dot{\Omega}}\int_0^\Omega (\left\langle \eta\eta^\dagger \right\rangle_\omega + \left\langle \eta^\dagger\eta \right\rangle_{-\omega})d\omega} - 1]]d\Omega \end{aligned} \tag{2.46}$$

Here $\gamma_\perp = \left\langle u_\perp^2 \right\rangle / \dot{\Omega}$. We remind that the occupation numbers are related to s_z as $N_{1,2} = 1/2 \pm s_z$. Below we write the survival probability for the case when the longitudinal-longitudinal correlations can be neglected $\left\langle u_\parallel^2 \right\rangle / \dot{\Omega} \ll \left(\Delta\tau_n\right)^{-1}$. In this case $s_z\left(-\infty\right) = 1/2$, the values $\Lambda_{1,2}$ are determined by equation (2.45) and from

equation (2.46) we find:

$$P_{1\to 1} = \frac{1}{2}\left[1 + e^{-2\pi\gamma_\perp}\left(2e^{-2\pi\gamma_{LZ}} - 1\right)\right] + \frac{\pi}{\dot{\Omega}} \times \int_0^\infty (\langle \eta\eta^\dagger \rangle_\Omega - \langle \eta^\dagger\eta \rangle_{-\Omega}) \\ \times e^{-\frac{2\pi}{\dot{\Omega}}\int_\Omega^\infty (\langle \eta\eta^\dagger \rangle_\omega + \langle \eta^\dagger\eta \rangle_{-\omega})d\omega}[(2e^{-2\gamma_{LZ}} - 1)e^{-\frac{4\pi}{\dot{\Omega}}\int_0^\Omega (\langle \eta\eta^\dagger \rangle_\omega + \langle \eta^\dagger\eta \rangle_{-\omega})d\omega} - 1]d\Omega \tag{2.47}$$

To take in account the correlation between the longitudinal and transverse noise one should replace the LZ gap Δ in the expression for $\gamma_{LZ} = \Delta^2/\dot{\Omega}$ by the renormalized value from equations (2.34, 2.35).

I. Discussion, applications to molecular magnet

In the case of weak transverse noise or very fast sweeping $\gamma_\perp \ll 1$ equations (2.46, 2.47) turn into the result (2.44) and the LZ survival probability, respectively. In the opposite case of the strong transverse noise or slow sweeping $\gamma_\perp \gg 1$ the occupation numbers accept their stationary values at fixed instantaneous frequency independently on the value of LZ parameter γ_{LZ}. The classical noise corresponds to large phonon occupation numbers $n_{\mathbf{q}}$. In this case the operators η and $\eta^\dagger$ commute; all terms containing commutators $\langle \eta\eta^\dagger \rangle_\Omega - \langle \eta^\dagger\eta \rangle_{-\Omega}$ can be neglected. Then theory reproduces the result for classical fast noise [31]. It is instructive to compare equation (2.47) with the exact survival probability for $T = 0$ obtained in the recent article by Wubs *et al.* [37]. At zero temperature the average value $\langle \eta^\dagger(t)\,\eta(t') \rangle$ as well as its Fourier transform turns into zero. This fact allows to calculate the integrals in equation (2.47). More physically visible way of obtaining the same result is to keep in mind that there is no live phonon at $T = 0$ and only spontaneous emission of phonons is possible. Therefore, if initially only the lower state was populated, the phonon cannot be emitted before the levels crossing. This consideration immediately

gives $s_z^{(-)} = s_z(-\infty) = \frac{1}{2}$ and $s_z^{(+)} = \frac{1}{2}(2e^{-2\gamma_{LZ}} - 1)$. Employing general equation (2.38), we find the value $s_z(+\infty) = \frac{1}{2}[2\exp(-2\pi(\gamma_{LZ} + \gamma_\perp)) - 1]$ and the survival probability:

$$\begin{aligned} P_{1\to 1} &= \exp(-2\pi(\gamma_{LZ} + \gamma_\perp)) \\ &= \exp[-\frac{2\pi}{\dot{\Omega}}((\Delta - \frac{1}{V}\sum_{\mathbf{q}} \frac{g_\parallel(\mathbf{q})\, g_\perp(\mathbf{q})}{\omega_{\mathbf{q}}})^2 + \left\langle \eta_\perp(0)\, \eta_\perp^\dagger(0) \right\rangle)] \end{aligned} \tag{2.48}$$

This result with precision of notations coincides with the exact result by Wubs *et al.* [37], equations (6-8), obtained without any limitations to the strength of noise and ratios of characteristic time scales. Surprisingly the multiphonon processes as well as the longitudinal-longitudinal noise correlations do not contribute at all to the survival and transition probabilities even at very high noise intensity. At zero temperature such a high noise level can be reached only by enhancement of the coupling amplitudes. Though large coupling amplitudes are physically implausible, as a mathematical model they are absolutely legitimate. The fact that these high-intensity processes do not play role in the transitions supports our speculations that the master equation range of validity may be broader than it follows from our derivation.

Our theory is relevant to molecular magnets, first of all because the condition of the noise fastness is perfectly satisfied in the experiment. Indeed, the highest magnetic field rate used in the experiments with Fe_8 and Mn_{12} was 10^3 Gs/s [12, 47]. This rate corresponds to $\dot{\Omega} = 10^{10}\mathrm{s}^{-2}$. The lowest temperature used in the cited measurements was about 0.05K. The dimensionless ratio of the value $\sqrt{\dot{\Omega}}$ to the smaller of the noise spectral widths is $\hbar\sqrt{\dot{\Omega}}/T \sim 10^{-5}$.

Here is a brief introduction to molecular magnet. A molecule magnet is an intermediate size molecule containing a ferromagnetic core confined in organic ligands.

They show slow relaxation of the magnetization originated purely from molecule itself. It means first of all a hard magnet, which shows hysteresis loop when being magnetized in a magnetic field. It is also a magnet purely from single molecule whose usually extremely weak interaction with neighboring molecules is not necessary for the magnetism to occur. The single molecule magnets are usually consisting of a small number of transition metal ions connected by simple bridges like O^{2-} or OH^{-} or other and then surrounded by various ligands. The most prominent examples are Mn12 [48] and Fe8 [49]. Mn12 and Fe8 are abbreviations for [Mn12O12(CH3COO)16(H2O)4]

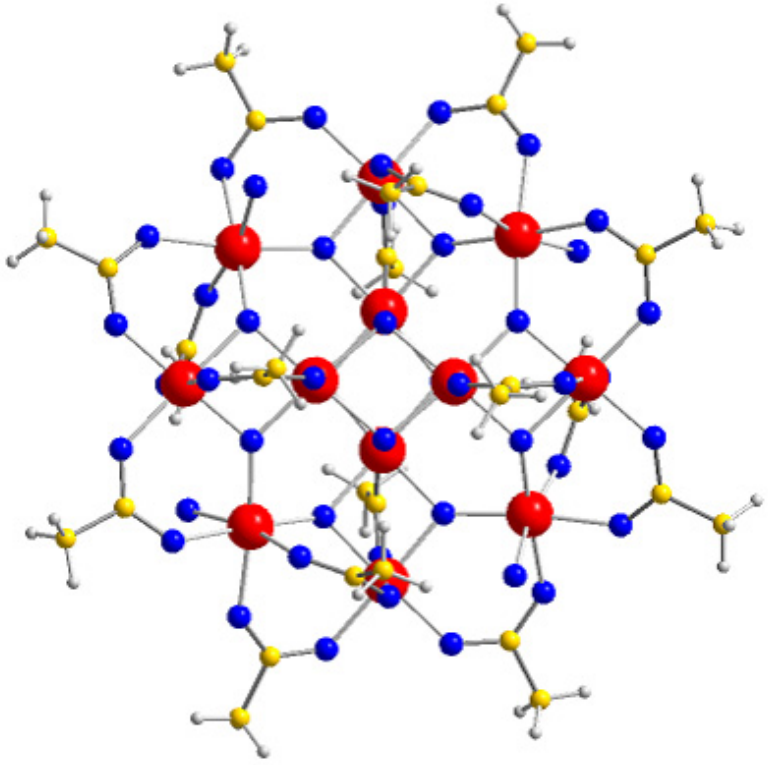

FIG. 11. Mn12 molecule. Red ions are Mn(Mn^{3+} or Mn^{4+}), blue ones are O. Ligands are surrounding. The total spin $S = 10$ and ground state $S_z = \pm 10$.

.2CH3COOH.4H2O and [(C6H15N3)6 Fe8O2(OH)12] .Br7H2O.Br.H2O, respectively. The Mn12 molecule consists of 12 manganese ions, four Mn(IV) ions (s=3/2) in a

central tetrahedron surrounded by eight Mn(III) ions (s=2), bound by oxide and acetate ions. Both Mn12 and Fe8 have a spin ground state of S = 10 (indicating $8 \times 2 - 4 \times (3/2)$), and an Ising-type magneto-crystalline anisotropy, which stables the spin states $M = \pm 10$ and generates an energy barrier for the reversal of the magnetization of about 67 K for Mn12 and 25 K for Fe8. As shown in Fig. 11, for the magnetic core of Mn12, the magnetic atoms in the molecule are sufficiently close to each other intermediated by Oxygen bridges, and have a rather strong exchange interaction. On the other hand, the distance between centers of different molecules are about 15 A°. Centers of different molecules are well separated by the ligands of the molecules. Therefore, the intermolecular interactions are utterly negligible and magnetic molecules can be considered as being independent.

The curve of magnetization vs the field, recorded at a temperature of 2 Kelvin, is very remarkable (see Fig. 12).It shows that the molecular crystal of Mn12 behaves like a traditional hard magnet, with strong remnant magnetism and a strong coercive field. At the same time it is like a quantum system. Since starting from temperature about $0.5K$ the hysteresis loop does not change more width with the temperature decreasing. At certain values of the magnetic field, the curve shows regularly spaced steps which are the signature of the magnetic quantum tunneling effect, which was discovered in 1995 [47].

After Mn12, new classes of magnetic molecules were synthesized, including the class of spin rings and the class of giant Keplerate molecules and chain or planar structure of these molecules [50, 51, 52, 53, 54, 55, 56]. For molecules Fe8 which possess a high ground state spin and well separated higher lying levels the following single-spin Hamiltonian

$$H = -DS_z^2 + E(S_x^2 - S_y^2) - g\mu_B S \cdot H \tag{2.49}$$

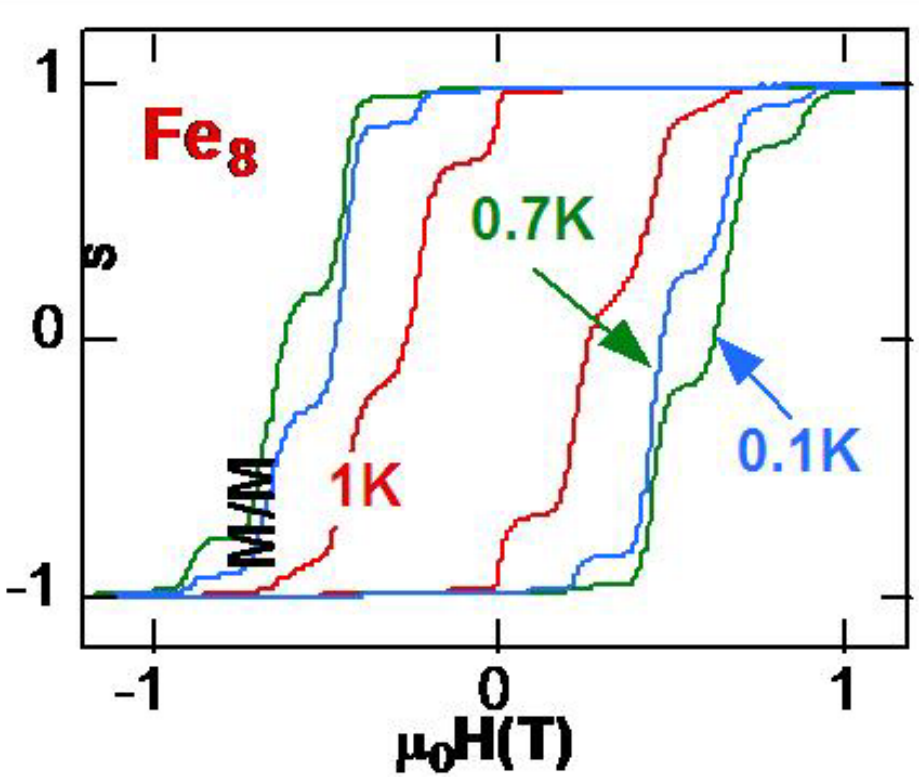

FIG. 12. There are steps at regular intervals of magnetic field in the hysteresis loop of a macroscopic sample of oriented Mn12Ac crystals. This phenomenon became later known as Quantum Tunneling effect.

is appropriate, see e.g. Ref. [57]. For Mn12, due to the tetragonal structure, the forth powers S_x^4 and S_x^4 are important. Here, S_x, S_y, and S_z are the three components of the spin operator, D and E are the anisotropy constants, and the last term of the Hamiltonian describes the Zeeman energy associated with an applied field H . This Hamiltonian accepts the hard, the medium, and the easy axis of magnetization for the x, y and z direction, respectively. D and E are anisotropy constants, $D > E$, both positive. The last term is the Zeeman energy. H is the external magnetic field.

If there are only terms containing S_z, i.e. $E = H_x = H_y = 0$, the system has an energy spectrum labeled with the values of spin projections $S_z = M$, $M \in [-s, s]$. Terms containing S_x or S_x^2 usually lifts degeneracy(if there is one) and introduces

transitions for $m - m' = 1$ or 2.

For S=10, at H =0, the states $M = \pm 10$ have the lowest energy. Although terms $E(S_x^2 - S_y^2)$ mix the two states, the level splitting is very small($(E/D)^1 0$) and therefore the levels can still be labeled by M approximately. When a field is applied along easy axis, $H = -DS_z^2 + E(S_x^2 - S_y^2) - g\mu_B S_z H_z$, the energy of the states with $M < 0$ increase while that for states with $M > 0$ decrease. Therefore, different energy levels cross at certain fields(Fig. 13). The crossing is avoided due to transverse terms S_x^2, S_y^2, S_x, S_y. The energy gap, the so-called tunnel splitting $\Delta_{M,M'}$ can also be tuned by an applied field in the xy-plane via the $S_x H_x$ and $S_y H_y$ Zeeman terms. Interestingly the gap shows a oscillating dependence on field in the H_x direction (hard anisotropy direction), due to the Berry's phase [14].

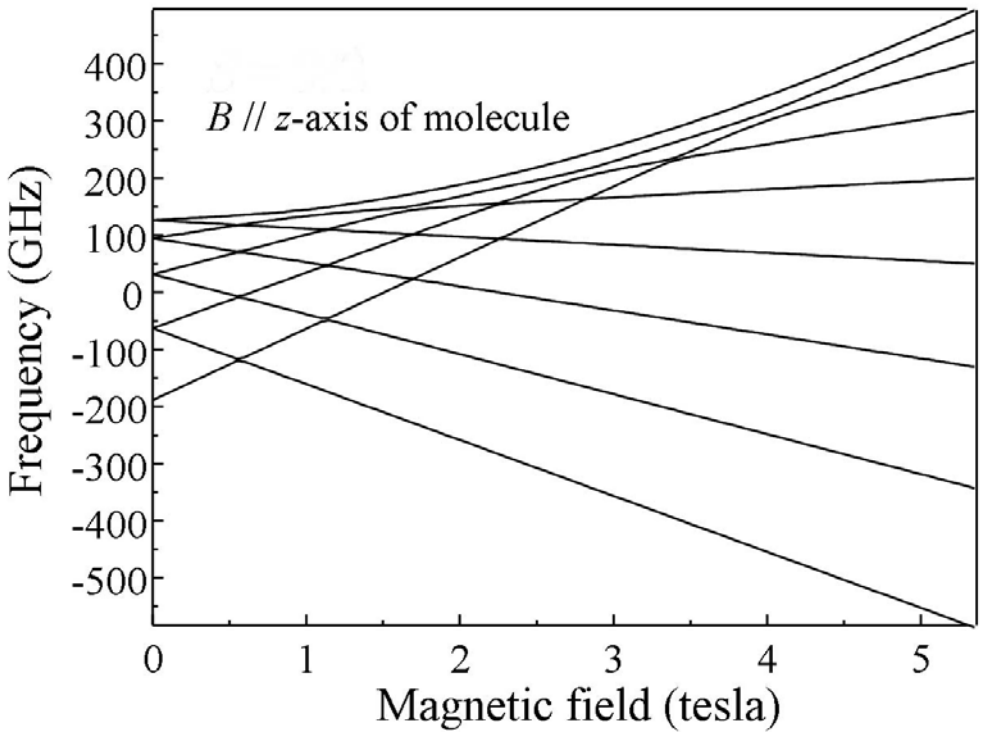

FIG. 13. Sketch of part of a spectrum of high spin molecule in magnetic field. As magnetic field changes, there are crossings of energy levels.

The renormalization of the gap due to the correlation between longitudinal and transverse noise (see section E) allows resolving at least qualitatively two puzzles which appeared in experimental studies of nanomagnets.

The first of them relates to the selection rules at transitions. At zero field Hamiltonian $H = -DS_z^2 + ES_x^2$. Such a Hamiltonian has non-degenerate spectrum, but at large S the lowest energy levels characterized with a dominant projection of spin $\pm M$ are only slightly split. Being placed into the time-dependent magnetic field these states change their energy and cross each other. The LZ transitions at such crossings are due to the term bS_x^2 in the Hamiltonian. Therefore, only transitions by ± 2 in M are allowed by theory in contradiction with the experiment. The renormalization of the gap lifts this contradiction because the spin-phonon interaction introduces terms like $u_{xz}S_xS_z$. They result in non-zero renormalized gap between the states with different parities of M and zero initial gap.

The second puzzle is the isotopic variation of the LZ gap Δ. Wernsdorfer *et al.* [14] have found a significant effect at isotopic substitution of Fe_{58} by Fe_{57} and H by D in the molecule Fe_8, as in Fig. 14. The isotopic dependence looks puzzling if the origin of the gap is electronic spin-orbit interaction, but it is quite natural in the gap renormalization due to phonons.

In principle our theory can explain the temperature dependence of the hysteresis curve in molecular magnets. The molecular hysteresis curve displays clearly pronounced steps at definite, temperature independent values of the magnetic field [12, 47, 58]. They are identified with the LZ transitions at crossings of Zeeman levels belonging to different M. The hysteresis curve becomes temperature independent at temperature below 0.4K, but it strongly narrows at comparatively low temperature about 1.5-3K. The application of our theory to the problem of the hysteresis curve and relaxation requires several additional steps. The first is establishing of

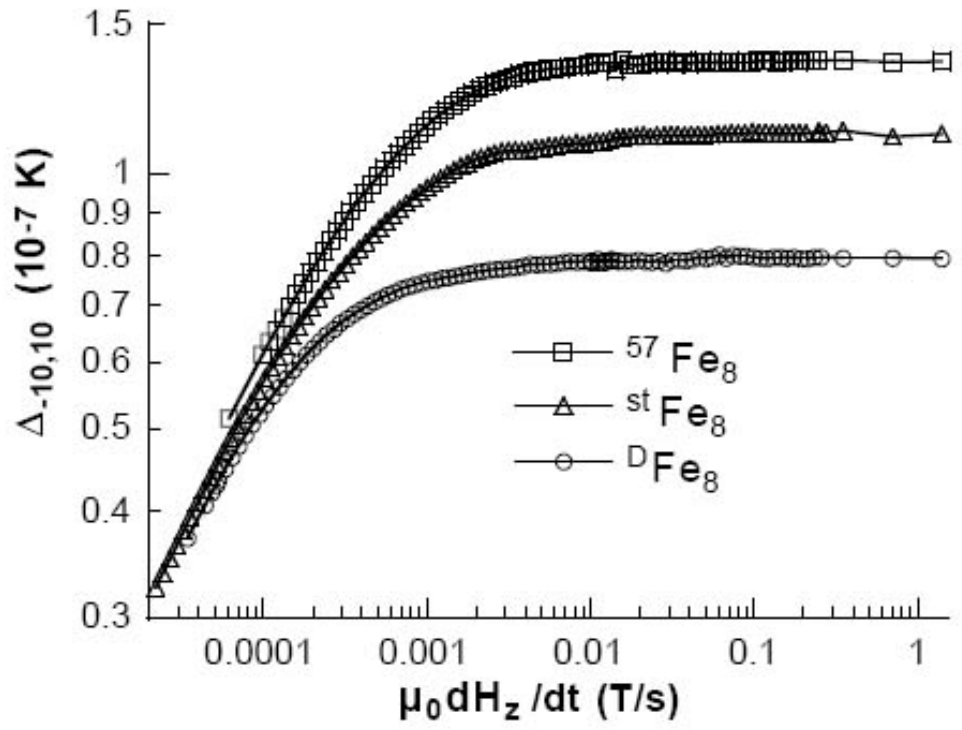

FIG. 14. Field sweeping rate dependence of the tunnel splitting$\Delta_{-10,10}$ measured by a Landau-Zener method for three Fe8 samples, for $H_x = 0$. The Landau-Zener method works in the region of high sweeping rates where $\Delta_{-10,10}$ is sweeping rate independent.

the spin-phonon Hamiltonian. Its simplest form is $H_{s-ph} = \Lambda_{\alpha\beta,\gamma\delta} u_{a\beta} S_\gamma S_\delta$ for interaction with acoustic phonons or $H_{s-ph} = \Lambda_{\alpha,\beta\gamma} u_\alpha S_\beta S_\gamma$ for interaction with optic phonons. The coefficients $\Lambda_{\alpha\beta,\gamma\delta}$ can be obtained from the measurements of magnetization curves under the pressure and shear deformation. To our knowledge, there is no such experimental data so far. We do not know how to extract the optic-phonon coupling constants $\Lambda_{\alpha,\beta\gamma}$ from experimental data. Both these sets can be found by numerical calculations for a single molecule. Keeping in mind a large number of atoms in it , it is not a simple computational problem. We plan to derive a kind of

effective media approach. But even if the spin-phonon coupling would be known, it is necessary to translate them into the language of the two-level (spin 1/2) system near each diabatic Zeeman level crossing. This procedure does not require additional knowledge of parameters, but it requires work and time. We will give here a rough estimate of the noise intensity. The transverse noise is very weak for transitions with a large change of the spin projection, for example, from +10 to -10, since the standard coupling of the deformations to spin can change the spin projection only by $\pm 1, \pm 2$. Therefore, the transverse noise linear in phonon operators appears only in combination with high-order perturbation caused by the biaxial anisotropy b. For transitions with the small change of the spin projection the transverse noise is of the same order of magnitude as longitudinal one. Assuming that the coefficients $\Lambda_{\alpha\beta,\gamma\delta}$ have the same order of magnitude as a and b, intensity can be estimated from the known value of magnetic anisotropy energy $a \simeq 0.06K$ (for Fe_8) and the statistical weight of phonons with frequency smaller than the anisotropy energy $\sim (a/E_D)^3$, where E_D is the Debye energy. An additional factor a/E_D comes from the square of coupling function $|g_{\mathbf{q}}|^2$, which is proportional to q at small wave vectors. Thus, $\left\langle u_{\parallel}^2 \right\rangle \sim a^2 (a/E_D)^4 \sqrt{\frac{m}{M}} \ll a = \hbar\omega_g$. This inequality shows that the condition of moderately strong noise is well satisfied for the acoustic noise. Numerical estimate of the value $\left\langle u_{\parallel}^2 \right\rangle / \hbar^2 \dot{\Omega}$ shows that it is small for the magnetic sweeping rate from 1 to 1000 Gs/s used in the experiment. Thus, the acoustic noise scarcely can explain the strong temperature dependence of the hysteresis curve. More plausibly low-frequency intramolecular oscillation are responsible for this phenomenon. However, there is no doubt, that the thermal noise becomes important at a temperature of few Kelvin and that the noise is fast and quantum. Though the longitudinal noise does not produce transitions between diabatic levels, it is effective for transitions between adiabatic levels [35].

CHAPTER III

LANDAU-ZENER THEORY AND ULTRACOLD DILUTE FERMI GAS

A. Introduction

In recent years there have been numerous achievements in experimental studies of ultra-cold gas of Fermi atoms. In this many-body system, the LZ transitions play an important role. In this chapter we limit the discussion to the system through a broad Feshbach resonance. The static and dynamics of the narrow resonance was thoroughly analyzed theoretically in the review by Gurarie and Radzihovsky [59]. The case of the broad resonance was not fully understood since it is a strong interaction problem. In this chapter we show that rather crude but qualitatively reasonable approximations naturally stemming from the condition of the broad resonance allow solving the static and dynamic problem exactly.

Bosonic superfluidity and fermionic superfluidity have long been the rich and fruitful subjects of research frontier over the past century since Kamerlingh Onnes liquefied helium-4 in 1908, and lowered its temperature below the λ-point $T_\lambda = 2.2K$ and noticed a maximal density at that point [60]. Onnes's laboratory in 1923 also noted again the possible discontinuity in the latent heart near the same temperature. However the significance of these discoveries was not realized until later in 1938. Onnes was then focusing on the electrical conductivity of metals at low temperature and he then found in 1911 that mercury below $T_C = 4.2K$ showed zero resistance and this phenomenon is called superconductivity, which is now also known as charged superfluidity. In 1938 two groups, one by Kapitza and the other by Allen and Misener, independently discovered the vanishing viscosity of He^4. This phenomenon was then called superfluidity in direct analogy with superconductivity.

Bose and Einstein had predicted earlier the phenomenon of Bose Einstein condensation(BEC) in an ideal gas of non-interacting particles obeying Bose-Einstein statistics. Below some temperature a fraction of particles go to a single particle state with minimal energy(zero momentum). F. London noticed that the BEC would occur at $3.3K$ for noninteracting gas with same mass and density as He^4. Lev Landau then in 1941 approached the problem of superfluidity with a highly successful phenomenological two-fluid model. The microscopic mechanism was explained by N. Bogoliubov in 1946 by considering a weakly interacting Bose gas. He showed that the excitation spectrum of a weakly interacting Bose gas is linear in the momentum of the excitation and the critical velocity of superfluidity is finite. The weak interaction does not destroy the Bose-Einstein condensate but an ideal Bose gas in BEC state has a vanishing critical velocity and hence is not a superfluid. Generally a superfluid requires correlation (the interaction) between particles to ensure collective motions. Further investigation into liquid helium is still on-going [61].

Superconductivity was more difficult to understand, though it was discovered earlier. Nevertheless these two kinds of superfluid turned out to be connected. A breakthrough came in 1956 when Cooper realized that two fermions with opposite spin and momentum on top of a filled Fermi sea would form bound pairs via an arbitrarily weak attractive interaction. The electron pairs, also known as Cooper pairs, occur not in real space but in momentum space. The attraction of these pairs are via electron phonon interactions, which overcomes the Coulomb repulsion. Bardeen-Cooper-Schrieffer(BCS) theory was then developed to describe the collective and correlated state and was able to explain the isotope effect and metal superconductivity quantitatively. Although the BCS theory is successful in describing superconductivity and has applications in higher angular momentum paring and neutral superfluidity and other pairing such as that in nuclear matter and neutron

stars, it still describes a weak interaction. In 1986 high T_C cuprate superconductors were discovered and traditional BSC theory failed to explain. It then became important to consider strongly interacting fermions. Actually before the discovery of high T_C superconductivity, there was development trying to generalize BCS theory to include strong interactions.

Using a generic two-body potential, Leggett [62] showed in 1980 that the limits of tightly bound molecules and long-range Cooper pairs are connected in a smooth crossover. The size of the fermion pairs changes smoothly from being much larger than the interparticle spacing in the BCS-limit to the small size of a molecular bound state. Accordingly, the pair binding energy varies smoothly from its small BCS value (weak, fragile pairing) to the large binding energy of a molecule in the BEC limit (stable molecular pairing). The tool that modulates the binding energy is the Feshbach resonance. This technique was used by three groups on ultracold Fermi atoms in 2003. In 1993 following the result of Leggett, Sa De melo *et al.* [63] smoothly interpolated the BCS and BEC limits. The phase digram is qualitatively like Fig. 15. The BCS-BEC crossover phase diagram is still currently under development efforts from both experimentalists and theorists.

The first laboratory realization of BEC in ultracold dilute atomic gases in 1995 has led to a revolution in atomic physics. Beautiful experiments for example on interference, on solitons and on vortices have directly demonstrated coherence, the wave-like nature of the gas and supefluid flow [64, 65, 66]. From a condensed matter perspective, these weakly interacting condensates represent the most fundamental, basic many-body wave functions.

Comparing with conventional helium, superconductors, nuclear matter and neutron stars, ultracold dilute fermi gas, as a many-body system, is generally simpler and easier to be controled in laborotory. And hence it has has been extensively studied.

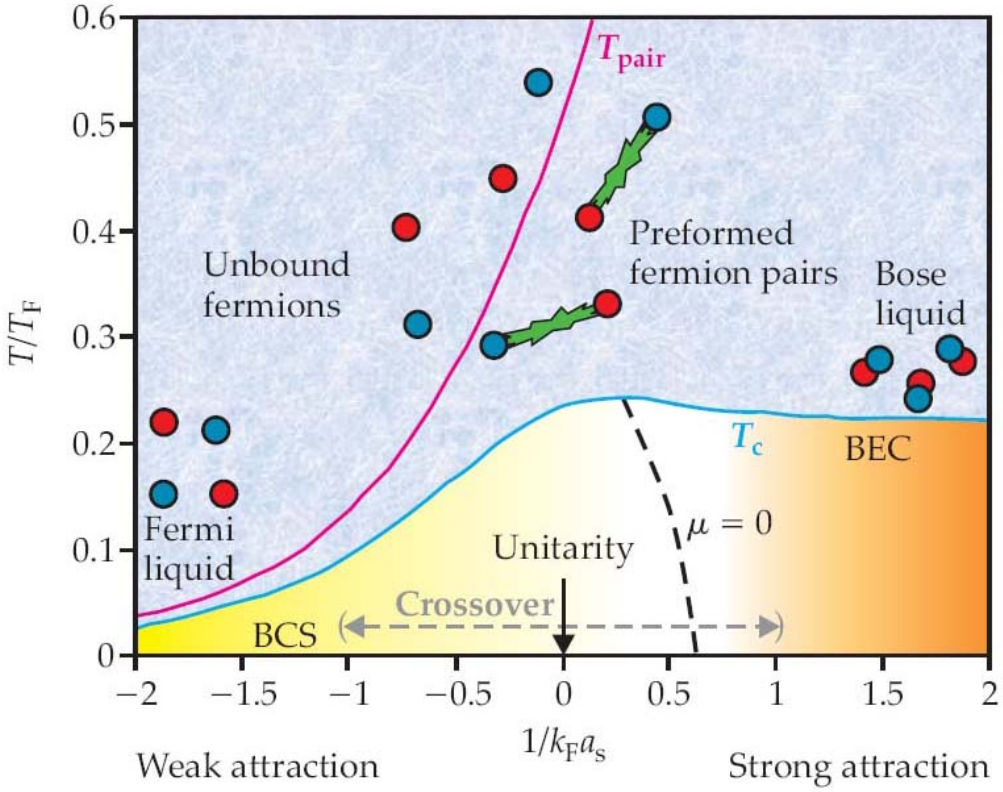

FIG. 15. Phase diagram for ultracold superfluid. Here a_S and k_F are scattering length and Fermi wavenumber. This diagram shows the Temperature T_{pair} when fermion pairs begin to form and T_c when fermion pairs become coherent and superfluid form. As the interaction strength increases, the Fermi liquid smoothly evolves into molecular Bose liquid. The line where $1/a_S k_F = 0$ is the so called unitary limit. At this limit the chemical potential is zero.

One of the few ways to tune the interactions is to directly modify the inter-atomic scattering using the so-called Feshbach resonance. Alkali atoms Li, Na, K, Rb, form diatomic molecules similar to H_2, but with very small binding energy($10^{-2}K$). Applying an external magnetic field one can tune the electronic Zeeman energy of a pair of atoms with parallel spins to the molecule energy. At this value of magnetic field an intensive production of molecules from atoms starts. In 2003 [67] Jin group produced molecules from fermi atoms of K^{40} by sweeping the magnetic field through

Feshbach resonance. These molecules were found remarkably stable and were later condensated to BEC state by three groups [68, 69, 70]. The major tool for these experiments is the Feshbach resonance, which occurs when the energy of a quasi-bound molecular state becomes equal to the energy of two free alkali atoms. The magnetic-field dependence of the resonance allows precise tuning of the atom-atom interaction strength in an ultracold gas [71]. Moreover, time-dependent magnetic fields can be used to reversibly convert from atom pairs to weakly bound molecules or from bound molecules to atom pairs [67, 72, 73, 70, 74, 75, 76, 77]. This technique has proved to be extremely effective in converting degenerate atomic gases of fermions [67, 72, 73, 78, 68, 70, 69] and bosons [79, 76, 77] into bosonic dimer molecules.

Theoretical works on the molecular production can be roughly divided in two categories. The first is a phenomenology suggesting that pairs of molecules independently undergo Landau-Zener (LZ) transitions [18, 19]. Therefore the total number of molecules at the end of the process is the LZ transition probability multiplied by the number of pairs. The most problematic issue in this approach is what should be accepted for the LZ transition matrix element Δ (called the LZ gap again). Direct calculation of the transition probability from a microscopic Hamiltonian, to the 4-th order in the interaction constant [80], shows that in contrast to the assumption of phenomenological works the many-body effects are essential. Another category includes works based on a simplified model [81] in which molecules have only one available state mimicking the condensate [82, 83, 84]. Although numerical works in this category display a reasonable temperature dependence, they give no clear physical picture and detailed parameter dependence. The series of semi-analytical works by Pazy *et al.* [85, 82, 86, 87] will be discussed later.

In this chapter we consider the process of molecule production from a Fermi gas

of atoms after a broad FR is swept across the Fermi sea. Our theory is valid under the assumption of strong interaction, equivalent to the condition of a broad resonance [59]. We derive a closed equation for the process of molecule production. We show that in a single-mode approximation this problem reduces to the linear LZ problem for operators. However, the strong interaction leads to a significant renormalization of the LZ gap. Contrary to the assumption of the phenomenological theories, this LZ gap is independent of the Fermi gas density. Our results display a significant dependence of the molecular production on the initial state preparation. For the inverse process of transformation of the BEC molecular gas into the atomic gas, immediately after magnetic field sweeping, the atomic gas appears in the state with a strongly developed BCS condensate. We also show the static limit of the conversion process. The condition of the broad resonance Eq. (3.4) allows simplification of the model despite of strong interaction between fermions. The key idea is a proper cutoff in the momentum space and neglection of the fermion dispersion. The resulting model is similar to the Dicke spin model for superradiance [88]. This model allows us to solve the static problem exactly. The complete spectrum and eigenstates are found. The solution displays a crossover from BCS to BEC in the range of detuning close to the FR. We find the density of the condensates and their correlation as function of the detuning.

B. Feshbach resonance

When fermi atoms are placed in magnetic field, they are subject to Zeeman splitting interaction in addition to the hyperfine splitting interaction. The Hamiltonian describing hyperfine and Zeeman interaction is $g_H \vec{I} \cdot \vec{S} + 2\mu_B B S_z$, where $\vec{I}$ and $\vec{S}$ are nuclear and electron angular momentum, μ_B is the magnetic momentum, B is the

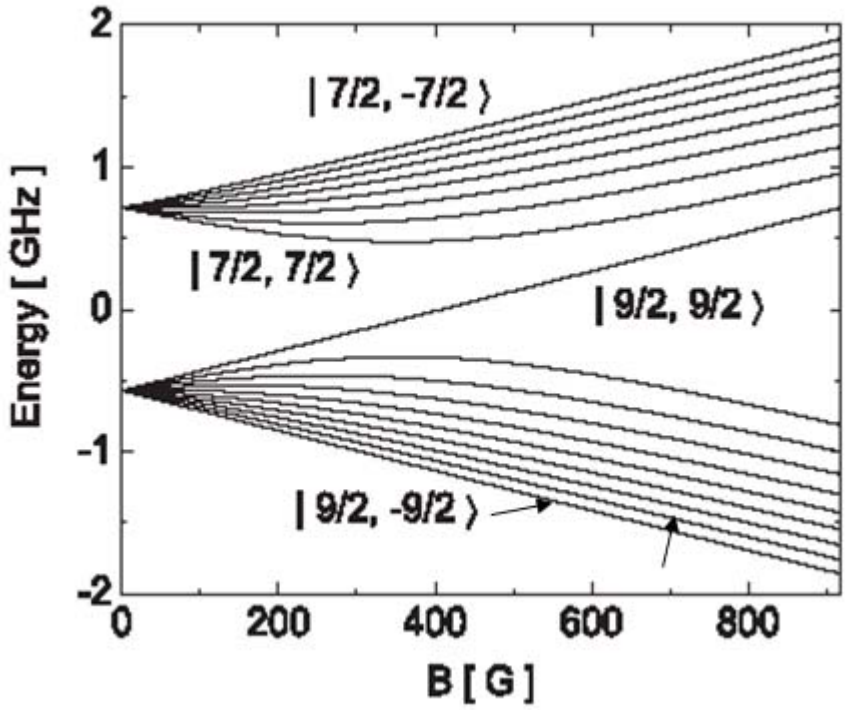

FIG. 16. ^{40}K atomic energy spectrum in presence of magnetic field. $I = 4$ for ^{40}K.

magnetic field and S_z is the spin projection on the direction of the field. Since the orbital momentum of fermi alkali atom is 0, the total angular momentum of electron is just 1/2. The total spin $\vec{F} \equiv \vec{I} + \vec{S}$ has value $I \pm 1/2$. The atomic state can be completely described by this quantum number and its z component m_f. The atomic energy spectrum for the example of ^{40}K is shown in Fig. 16. The degeneracy in total spin F is removed by hyperfine interaction and the degeneracy in m_f is removed by applying a magnetic field. Collisions of two fermi atoms in the s-wave channel is possible only if they have different hyperfine states. In a typical experiment [67, 68] an admixture of atoms of K^{40} with the same total atomic spin 9/2 but different spin projection quantum numbers $-7/2$ and $-9/2$ was used. Further we will describe

these two different states by a pseudospin σ, accepting two values $\uparrow, \downarrow$ respectively as shown by the two small arrows in Fig. 16. We can also see that the energy of these two states decrease as magnetic field increases.

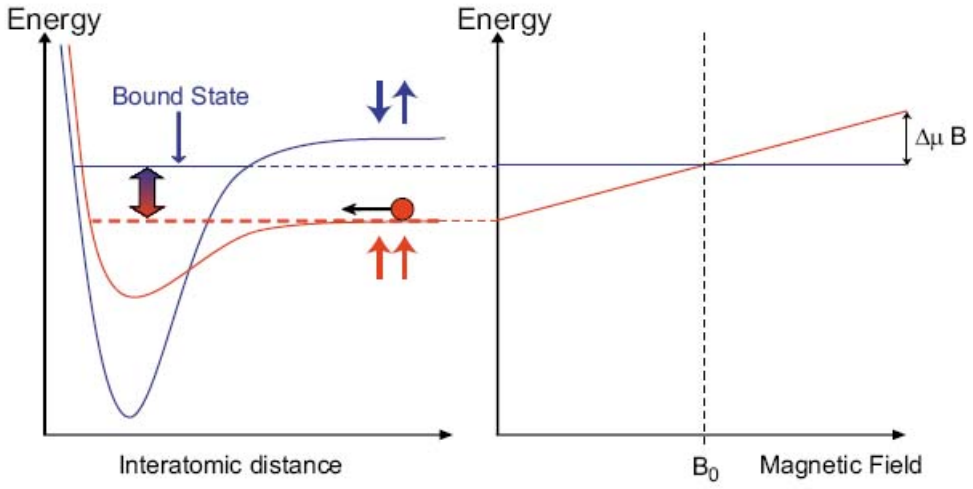

FIG. 17. Energies of states vs interatomic distance(left) and magnetic field(right). Alkali atoms entering in the triplet potential(red) are coupled to a singlet bound molecular state(blue). By tuning the external magnetic field, this bound state can be brought into resonance with the incoming state.

Feshbach resonance, first investigated in the context of nuclear physics [89], refers to the phenomenon of the change of scattering length in an open channel due to the coupling to a bound state in the nearby closed channels. There's no coupling to first order between open and closed channels, because there's no continuum state in closed channel. To the second order perturbation, two particles in an open channel can scatter to an intermediate state in a closed channel, which subsequently decays into two particles in one of the open channels. As one would expect from second-order perturbation theory for energy shifts, coupling between channels gives rise to a repulsive interaction if the energy of the incoming particles is greater than that of a bound state, and an attractive interaction if less. The closer the energy of the

incoming particles is to that of a bound state, the larger the effect on the scattering. Such second-order process would contribute a term proportional to $1/(E-E_0)$ to the scattering length, where E_0 is the bound state energy and is almost flat respecting to magnetic field changes, as seen in Fig. 17. In this figure, two atoms enter in spin triplet configuration. And if there was no coupling between the singlet potential(blue curve) and the triplet potential(red curve), the atoms would simply scatter off each other in triplet potential, acquiring some phase shift. However if there is a bound state in the singlet potential with energy E_0 close to the threshold energy E of the open channel, these two channels are coupled, due to spin-exchange and dipole-dipole interaction. The energy of the open channel depends on magnetic field and hence the energy difference between the two channels can be tuned by the magnetic field according to this formula

$$E - E_0 = (\mu_1 + \mu_2 - \mu_0)(B - B_0), \tag{3.1}$$

where μ is the magnetic moment of each particle with subscripts 1 and 2 for atoms and 0 for molecule, and B_0 is the point when the energies of these two channels become same. So the scattering length depends on the magnetic field,

$$a\,(B) = a_{nr}\left(1 - \frac{B_w}{B - B_0}\right). \tag{3.2}$$

where a_{nr} is the non-resonant scattering length far away from B_0, B_0 is the magnetic field at resonance point, and B_w is the magnetic-field width of resonance. The Feshbach resonance makes it possible to tune up the interaction strength between atoms via change of magnetic field. The Fig. 17 shows a sketch of the mechanism. As magnetic field B is swept down, the atomic state is energy favorable at first. But as the field B passes through the strongest resonant point B_0, the triplet potential moves above the the singlet potential. Then the bound molecule state is energy favorable.

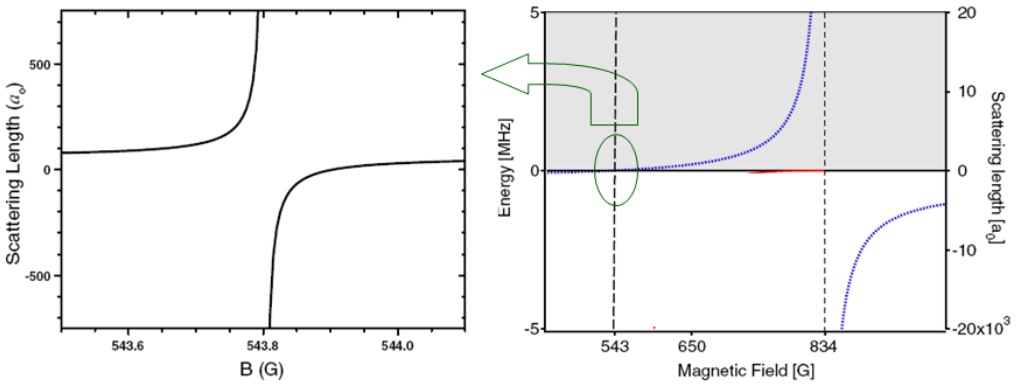

FIG. 18. The right side curve shows the broad resonance of ^6Li and the left side curve shows the narrow resonance, which is just a vertical line in the graph on the right side.

We can then consider a Landau-Zener transition happens during the energy curve crossing at B_0 as field is swept.

A Feshbach resonance might be very broad or very narrow. Take the ^6Li for example, its resonance at $B_0 = 834G$ is more wide than 100G but its resonance at $B_0 = 543G$ is less than 0.1G as shown in Fig. 18. The origination of and the difference between broad FR and narrow FR require complete derivation of resonance states. I will just present some results here partially according to the book [90] and review [59]. By considering a simple potential, the state close to resonance is $|\varphi\rangle = \alpha\,|m\rangle + \sum c_k\,|k\rangle$, where $|m\rangle$ represents the bound state close to resonance and $|k\rangle$ is the continuum state, and α and c_k are the amplitudes of each state. It is shown that $\alpha^2 \approx \sqrt{\frac{E_F}{\tilde{\Delta}}}\frac{1}{k_F a}$, where $\tilde{\Delta}$ is an intrinsic energy scale associated with the strength of the Feshbach coupling between the molecular state and the scattering continuum. This intrinsic energy scale $\tilde{\Delta}$ can be connected to experimental parameters as

$$\tilde{\Delta} = \frac{4\mu_B^2 B_w^2}{\hbar^2/m a_{nr}^2} \tag{3.3}$$

If $\alpha^2 \ll 1$, the molecular state is is dressed and dissolved in open continuum

throughout the crossover and the details of the original molecular state $|m\rangle$ do not play a role, which is the case of a broad Feshbach resonance. The crossover occurs for $-1 \ll \frac{1}{k_F a} \ll 1$. So the resonance is broad if

$$\Gamma \equiv \sqrt{\frac{\tilde{\Delta}}{E_F}} \gg 1, \tag{3.4}$$

and is narrow if $\Gamma \ll 1$,where E_F is the Fermi Energy

$$E_F = \frac{\hbar^2}{2m}(3\pi^2 N/V)^{2/3} = \frac{\hbar^2}{2m}(3\pi^2 n)^{2/3}. \tag{3.5}$$

We will show later that the value $\tilde{\Delta}$ characterizes the interaction in the Fermi-gas or the interaction of the BCS pairs with the BEC condensate.

C. Approximation of the Hamiltonian

We start with the Timmermans *et al.* Hamiltonian [91]:

$$\begin{aligned}\hat{H} = &\sum_{\mathbf{p},\sigma}(\epsilon + \varepsilon_{\mathbf{p}})\hat{a}^\dagger_{\mathbf{p}\sigma}\hat{a}_{\mathbf{p}\sigma} + \sum_q \omega_{\mathbf{q}}\hat{b}^\dagger_{\mathbf{q}}\hat{b}_{\mathbf{q}} \\ &+ \frac{g}{\sqrt{V}}\sum_{\mathbf{p},\mathbf{q}}\left(\hat{b}_{\mathbf{q}}\hat{a}^\dagger_{\mathbf{p}+\mathbf{q}\uparrow}\hat{a}^\dagger_{-\mathbf{p}\downarrow} + \hat{b}^\dagger_{\mathbf{q}}\hat{a}_{-\mathbf{p}\downarrow}\hat{a}_{\mathbf{p}+\mathbf{q}\uparrow}\right)\end{aligned} \tag{3.6}$$

Here $\hat{a}^\dagger_{p\sigma}$ are creation operators of fermionic atoms with momentum $\mathbf{p}$ and kinetic energy $\varepsilon_{\mathbf{p}} = \frac{\mathbf{p}^2}{2m}$, $\hat{b}^\dagger_{\mathbf{q}}$ are the creation operators of the bosonic diatomic with kinetic energy $\omega_{\mathbf{q}} = \frac{\mathbf{q}^2}{4m}$, the position of the FR is controlled by the experimentally tunable detuning energy ϵ, which becomes time-dependent in the dynamic problem, the coupling constant g relates to the reaction of molecule formation from two atoms and the inverse process of molecular dissociation. As it was explained earlier, the coupling constant g stems from the hyperfine interaction. Its value can be estimated as $g \sim \varepsilon_{hf}\sqrt{a_m^3}$, where ε_{hf} is a characteristic hyperfine energy (about 1mK) and a_m

is the size of the diatomic molecule. The Hamiltonian (3.6) neglects nonresonant atom-atom and molecule-molecule interactions that near a FR are subdominant to the resonant scattering. To some extent the direct atom-atom interaction is taken into account by the value a_0 in Eq. (3.2). From now on, we use the word "atoms" for both uncoupled atoms and atoms within molecules, and the word "fermions" for atoms that are not bound in molecules. Correspondingly, we denote the number of atoms as N and the number of fermions as $\hat{N}_F$.

To find the connection between the coupling constant g in the Hamiltonian (3.6) and the value $\tilde{\Delta}$ defined by equation (3.3) we eliminate $\hat{b}_{\mathbf{q}}$ and $\hat{b}^{\dagger}_{\mathbf{q}}$ from the static Hamiltonian (3.6) and obtain the Hamiltonian for fermions only with 4-fermion interaction. Assuming that $\varepsilon_{\mathbf{p}}$ and $\omega_{\mathbf{q}}$ can be neglected in comparison to ϵ (this assumption will be justified later), the interaction Hamiltonian reads:

$$H_{int} = \frac{g^2}{2V\epsilon} \sum_{\mathbf{p},\mathbf{p}',\mathbf{q}} \hat{a}^{\dagger}_{\mathbf{p}+\mathbf{q}\uparrow} \hat{a}^{\dagger}_{-\mathbf{p}\downarrow} \hat{a}_{-\mathbf{p}'\downarrow} \hat{a}_{\mathbf{p}'+\mathbf{q}\uparrow} \tag{3.7}$$

$g_F = g^2/2\epsilon$. It is negative (attraction) at negative ϵ. The s-scattering length a is related to the interaction constant g_F by a standard relation [92] $g_F = 4\pi\hbar^2 a/m$. Thus, the singular part of the scattering length is associated with the fermion-boson coupling constant g and the detuning energy ϵ as follows:

$$a(\epsilon) = \frac{mg^2}{8\pi\hbar^2\epsilon} \tag{3.8}$$

Comparing equation (3.8) with the resonance term in equation (3.2) and identifying $\epsilon = \mu_B (B - B_0)$, we arrive at a relation $2B_w a_{nr}\mu_B = mg^2/4\pi\hbar^2$. Using $\epsilon_F = \hbar^2(3\pi^2 n)^{2/3}/2m$, where n is the density of fermions, and substituting this into equations (3.3, 3.4) we express the intrinsic energy $\tilde{\Delta}$ and dimensionless parameter

Γ in terms of the coupling constant g:

$$\tilde{\Delta} = \frac{m^3 g^4}{16\pi^2\hbar^6} \tag{3.9}$$

$$\Gamma = \frac{m^2 g^2}{\hbar^4 n^{1/3}} \frac{1}{\pi^{5/3} 3^{1/3} 2^{3/2}} \tag{3.10}$$

The Hamiltonian (3.6) is still too complicated. However, we find out that the broad resonance condition results in two approximations. The first important approximation leading to the simplification of Hamiltonian is the single-boson-mode approximation. It means that all amplitudes $\hat{b}_{\mathbf{q}}$ will be neglected except that of $\hat{b}_{\mathbf{q}=\mathbf{0}}$. To justify this approximation we note that the characteristic energy scale in statics and dynamics is $\tilde{\Delta}$. The corresponding value of the scattering length following from equation (3.9) is $a \sim 1/\left(\Gamma n^{1/3}\right)$. It means that the characteristic value of the gas parameter $an^{1/3}$ is small: $an^{1/3} \sim 1/\Gamma \ll 1$. At this condition and zero temperature almost all particles of the Bose-gas fall into the coherent condensate with zero momentum. The approximation is not obvious at small $|\epsilon| \sim \tilde{\Delta}/\Gamma$. We will show later that they are not essential for the dynamic process. In the static state these values of ϵ correspond to the strong interaction regime in which the fermions are distributed in the broad range of momentum $\sim \sqrt{2m\tilde{\Delta}}$. The maximal modulus of the scattering length for such particles corresponding to the unitary limit is $a \sim \hbar/\sqrt{2m\tilde{\Delta}}$. The corresponding value of the gas parameter $an^{1/3}$ is again of the order $1/\Gamma$ and the single-mode approximation survives.

The Hamiltonian (3.6) conserves the total number of atoms:

$$\begin{aligned} N &= \hat{N}_F + 2w_0 \hat{b}_0^\dagger \hat{b}_0 \\ &= \hat{N}_F + 2w_0 \hat{b}^\dagger \hat{b}, \text{ if we omit the subscript 0.} \end{aligned} \tag{3.11}$$

Therefore, in the Hamiltonian (3.6) the detuning energy can be transformed to absorb the term of energy of the molecules, only at the cost of a constant term in Hamilto-

nian. So the bosonic term is absorbed by a newly defined detuning energy(we will still use the same symbol for the new detuning energy though),

$$\begin{aligned}\sum_{\mathbf{p},\sigma}\epsilon\hat{a}^{\dagger}_{\mathbf{p}\sigma}\hat{a}_{\mathbf{p}\sigma}+\sum_{q}\omega_{\mathbf{q}}\hat{b}^{\dagger}_{\mathbf{q}}\hat{b}_{\mathbf{q}} &= \sum_{\mathbf{p},\sigma}\epsilon\hat{a}^{\dagger}_{\mathbf{p}\sigma}\hat{a}_{\mathbf{p}\sigma}+w_0\hat{b}^{\dagger}_0\hat{b}_0 \\ &= w_0N/2+\sum_{\mathbf{p},\sigma}(\epsilon-w_0/2)\hat{a}^{\dagger}_{\mathbf{p}\sigma}\hat{a}_{\mathbf{p}\sigma} \\ &\to \sum_{\mathbf{p},\sigma}\epsilon\hat{a}^{\dagger}_{\mathbf{p}\sigma}\hat{a}_{\mathbf{p}\sigma}.\end{aligned} \tag{3.12}$$

The other approximation is neglecting the fermion dispersion $\varepsilon_{\mathbf{p}}$ which is small comparing to typical interaction energy. A typical value of b_0 is $\sqrt{N}$. In the broad resonance approximation $g\sqrt{N}/\sqrt{V}\equiv g\sqrt{n}$ is much larger than ε_F, because $(\frac{g\sqrt{n}}{\varepsilon_F})^2/\Gamma\approx 1.2$ and $\Gamma\gg 1$. Therefore, it seems reasonable to neglect the kinetic energy of fermions in comparison to ϵ. We will see that this approximation is well justified for the dynamic problem, though it may be not so good for statics of the model (3.17).

In the approximation of single mode and approximation of fermion dispersion neglection, the Hamiltonian (3.6) is strongly simplified:

$$H_{sm}=\sum_{\mathbf{p},\sigma}\epsilon\hat{a}^{\dagger}_{\mathbf{p}\sigma}\hat{a}_{\mathbf{p}\sigma}+\frac{g}{\sqrt{V}}\left[b_0\sum_{\mathbf{p}}a^{\dagger}_{\mathbf{p}\uparrow}a^{\dagger}_{-\mathbf{p}\downarrow}+b^{\dagger}_0\sum_{\mathbf{p}}a_{\mathbf{p}\downarrow}a_{-\mathbf{p}\uparrow}\right] \tag{3.13}$$

D. The global spin model and its Hilbert space

The Hamiltonian (3.13) acts separately in the subspace of single-occupied and in the subspace of double-occupied or empty fermionic states. Following Anderson

[93] we introduce spin operators:

$$s_{\mathbf{p}z} = \frac{1}{2}\left(a^{\dagger}_{\mathbf{p}\uparrow}a_{\mathbf{p}\uparrow} + a^{\dagger}_{-\mathbf{p}\downarrow}a_{-\mathbf{p}\downarrow} - 1\right) \tag{3.14}$$

$$s_{\mathbf{p}+} = a^{\dagger}_{-\mathbf{p}\downarrow}a^{\dagger}_{\mathbf{p}\uparrow};\ s_{\mathbf{p}-} = a_{\mathbf{p}\uparrow}a_{-\mathbf{p}\downarrow} \tag{3.15}$$

In the double-occupied or empty fermionic states subspace they obey the standard commutation relation:

$$[s_{\mathbf{p}z}, s_{\mathbf{p}'\pm}] = \pm\delta_{\mathbf{p}\mathbf{p}'}s_{\mathbf{p}\pm};\ \ [s_{\mathbf{p}+}, s_{\mathbf{p}'-}] = 2\delta_{\mathbf{p}\mathbf{p}'}s_{\mathbf{p}z} \tag{3.16}$$

so that the double occupied state corresponds to $s_{\mathbf{p}z} = +\frac{1}{2}$ and empty state corresponds to $s_{\mathbf{p}z} = -\frac{1}{2}$. Note that single-occupied fermionc state corresponds to a singlet spin state: all three spin operators (3.14, 3.15) turn such a state to zero. In terms of spin operators the Hamiltonian (3.13) reads:

$$H_{sm} = 2\sum_{\mathbf{p},\sigma}\epsilon s_{\mathbf{p}z} + \frac{g}{\sqrt{V}}\left[b_0\sum_{\mathbf{p}}s_{\mathbf{p}+} + b_0^{\dagger}\sum_{\mathbf{p}}s_{\mathbf{p}-}\right], \tag{3.17}$$

where we have omitted an infinite constant originated from the term -1 in equation (3.14).

By introducing the global spin S from summating the individual spins over momenta, the Hamiltonian (3.17) reduces to one containing only global spin operators:

$$H_S = 2\epsilon S_z + \frac{g}{\sqrt{V}}\left(b_0 S_+ + b_0^{\dagger}S_-\right) \tag{3.18}$$

where

$$S_z = \sum s_{\mathbf{p}z};\ S_{\pm} = \sum s_{\mathbf{p}\pm} \tag{3.19}$$

obeying the standard permutation relationships: $[S_z, S_{\pm}] = \pm S_{\pm};\ \ [S_{+,}S_{-}] = 2S_z$. A subtle assumption incorporated in the derivation of the Hamiltonian (3.18) and the permutation relations for the global spin components is that the summation in

the two definitions (3.19) runs over the same range of momenta. It is not obvious since the summation in the sum for S_z is limited by the condition $\varepsilon_{\mathbf{p}} \ll |\epsilon|$, whereas the summation in the second sum is naturally cut off by the range of interaction (it means that g is a function of momentum vanishing at sufficiently large values of the momentum modulus). In dynamical problem the Anderson spins rotate with the frequencies $(\epsilon + \varepsilon_{\mathbf{p}})/\hbar$. Therefore they can rotate coherently and enhance remarkably their effective field exerted to the molecular amplitude b_0 only if $\varepsilon_{\mathbf{p}} < |\epsilon|$. We will see that such a coherence indeed takes place in the dynamic problem. The contributions from larger values of momenta to $S_{\pm}$ are incoherent and mutually compensate their effect. Thus, for dynamic problem, the summation in the same momentum region in the two equations (3.19) is justified. It is not as clear for the static problem. We will see later that the static model has many qualitative features resembling those of the initial Timmermanns *et al.* model. In particular it displays a crossover from BCS to BEC condensate with a large gap due to strong interaction in a broad vicinity of the Feshbach resonance. However, in quantitative details they are different. Besides, the global spin model (3.18) has an additional symmetry and additional conserved value which the Timmermans Hamiltonian does not possess. Indeed the Hamiltonian (3.18) conserves not only the value

$$I = S_z + b^{\dagger} b \tag{3.20}$$

(this conservation law is equivalent to the conservation of the number of atoms (3.11), but it also conserves the total spin S, where:

$$S\left(S+1\right) = S_z^2 + \frac{1}{2}\left(S_+ S_- + S_- S_+\right) \tag{3.21}$$

Further we will see that in the thermodynamic limit of large system it is possible neglecting 1 in comparison to S and non-commutativity of S_+ and S_-. The conser-

vation law (3.21) together with the conservation law (3.20) will be shown to establish a simple relationship between the BCS and BEC condensates such that the quantity of one of them can be increased only at expense of the other.

The cut-off in the momentum space define a finite-dimensional Hilbert space of states. This Hilbert space and the Hamiltonian (3.18) acting in it form what we call the Global Spin Model (GSM). Let the number of single-particle states defined by the cut-off is N_s and the total number of atoms, both free and bound in molecules is N. Then the dimensionality of the Hilbert space of the GSM is:

$$\mathcal{N}(N, N_s) = \sum_{M=0}^{N/2} \frac{N_s!}{(M)!\,(N_s - M)!} \tag{3.22}$$

This formula follows directly from the Fermi-Bose-gas picture if each single-particle state can be either double occupied or empty. The expression which is summated in Eq. (3.22) is the number of possible distributions of M electron pairs among N_s single-particle states. Each state in this model is a vector of a direct product of N_s spin 1/2 representations corresponding to the Anderson spins $\mathbf{s_p}$. The combinatorial coefficient $N_s!/\,(M)!\,(N_s - M)!$ entering Eq. (3.22) is the number of possible distributions of M spins up and $N_s - M$ spins down, i.e. the number of different states with the spin projection:

$$S_z = (\frac{N}{2} - M) - \frac{N_s}{2} = \frac{N - N_s}{2} - M \tag{3.23}$$

Generally the direct product of N_s spin-1/2 states gives the maximal possible total spin $N_s/2$ and the minimal total spin zero (we assume that Ns is even). However, not any vector of the direct product is allowed by the conservation law (3.20). Indeed, the number of electron pairs or the spin-up projections M satisfies $0 \leq M \leq N/2$,

the projection S_z is limited by inequalities:

$$-N_s/2 \leq S_z \leq (N - N_s)/2. \tag{3.24}$$

According to (3.32), S_z is always negative and large in absolute value. The total spin S cannot be smaller than $|S_z|$, it also cannot be larger than $N_s/2$. Thus, the allowed values of the total spin S are

$$(N_s - N)/2 \leq S \leq N_s/2. \tag{3.25}$$

The number of different representations with the total spin

$$S = \frac{N_s}{2} - i, \text{where } \left(0 < i < \tfrac{N}{2}\right) \tag{3.26}$$

is [94]:

$$\begin{aligned} \mathcal{N}(S) &= \frac{N_s!}{\left(\frac{N_s}{2} - S + 1\right)!\left(\frac{N_s}{2} + S - 1\right)!} - \frac{N_s!}{\left(\frac{N_s}{2} - S\right)!\left(\frac{N_s}{2} + S\right)!} \\ &= \frac{N_s!\,(2S+1)}{\left(\frac{N_s}{2} - S + 1\right)!\left(\frac{N_s}{2} + S\right)!} \end{aligned} \tag{3.27}$$

Each of these representations contains generally $2S+1$ states, but only $S-(N_s-N)/2$ of them are allowed by the conservation law.

E. Number of available states

So far the number of available single-particle states N_s entered as a phenomenological parameter.

1. Definition from intrinsic energy scale

Below we calculate it employing a kind of self-consistency arguments. Let introduce the momentum cut-off p_s. The number of available states reads:

$$N_s = V\frac{p_s^3}{3\pi^2\hbar^3} \tag{3.28}$$

It is reasonable also to introduce the density of available states $n_s = N_s/V$. The requirement of our theory is that the fermionic dispersion can be neglected at the characteristic energy scale $\tilde{\Delta}$ defined by equation (3.3). Thus, a reasonable momentum cut-off is:

$$p_s = \sqrt{2m\tilde{\Delta}} \tag{3.29}$$

Plugging Eq. (3.9) into Eq. (3.29), we find:

$$p_s = \frac{m^2g^2}{2^{3/2}\pi\hbar^3} \tag{3.30}$$

The last equation and Eq. (3.28) implies the following result for n_s:

$$n_s = \frac{m^6g^6}{2^{9/2}\cdot 3\pi^5\hbar^{12}} \tag{3.31}$$

With precision of the coefficient 1.09 the value $\Delta = g\sqrt{n_s}$ coincides with $\tilde{\Delta}$, see IV. Because $n_s = n\Gamma^3$, the condition of the broad resonance is equivalent to the strong inequality:

$$N_s \gg N \tag{3.32}$$

Hence the determination of N_s is self-consistent.

2. Definition from LZ equation

While in the previous work we worked out N_s in the following different way. It follows from the first equation (3.15) that $S_z = (\hat{N}_F - N_s)/2$, where $\hat{N}_F$is the number of

fermions and $N_s$is the number of available fermionic states. $N_s$is determined below by the model self-consistency requirement (see Eq. (3.36)) and turns out to be much larger than the number of atoms N. Therefore, $S_z \approx -N_s/2$. The Heisenberg equations of motion are:

$$\hbar\dot{\hat{b}} = -i\tilde{g}\hat{S}_-; \qquad \hbar\dot{\hat{S}}_- = -2i\epsilon(t)\hat{S}_- + 2i\tilde{g}\hat{b}^\dagger\hat{S}_z \tag{3.33}$$

where $\tilde{g} = g/\sqrt{V}$ and dots denote the time derivatives. Generally these equations are non-linear. However, in the broad-resonance approximation $S_z = -N_s/2$, they become linear. Eliminating S_-, we arrive at an ordinary linear differential equation for the operator $\hat{b}$:

$$\hbar^2\ddot{\hat{b}} + 2i\hbar\epsilon(t)\dot{\hat{b}} + \Delta^2\hat{b} = 0 \tag{3.34}$$

where

$$\Delta = g\sqrt{n_s} \tag{3.35}$$

and $n_s = N_s/V$ is the density of available states. Equation (3.34) becomes the parabolic cylinder equation if $\epsilon(t)$ is a linear function of time. In the LZ theory it describes the evolution of the probability amplitude to find the system in one of its two states. The role of the LZ gap is played by Δ, which greatly exceeds $g\sqrt{n}$.

In the genuine LZ theory it is known that the transition proceeds during a characteristic time interval at which the absolute value of detuning is less then Δ. The formation of molecules starts when the detuning $|\epsilon|$ is of the order of Δ. Thus the cutoff on the available (relevant) states is $\epsilon_{p_s} = p_s^2/2m = \Delta \gg \epsilon_F$. The density of available states is then simply given by

$$n_s = \frac{(p_s/\hbar)^3}{3\pi^2} = \frac{(2mg/\hbar^2)^6}{(3\pi^2)^4} = 1.73n\Gamma^3, \tag{3.36}$$

where we have used equation (3.35). Note that both n_s and Δ are independent of

Table IV. The table for relevant quantities at different cutoff momentum. The left column takes value if cutoff is chosen such that $p_s^2/2m = \tilde{\Delta}$ while the right column is such that $p_s^2/2m = \Delta$. The middle column shows their differences by numerical value. The new choice of p_s would make the cutoff momentum(energy) smaller to 0.83(0.69) of the value previous momentum(energy), and would make the available states smaller to 0.58 of the previous value. Note that the definitions of $\tilde{\Delta}$, E_F and Γ are not affected by value of p_s.

Cutoff $\frac{p_s^2}{2m} \equiv \tilde{\Delta}$	$\frac{\times 1.20^2 \rightarrow}{\leftarrow 0.83^2 \div}$	Cutoff $\frac{p_s^2}{2m} \equiv g\sqrt{n_s}$
$p_s = \frac{m^2 g^2}{2^{3/2}\pi\hbar^3}$	$\frac{\times 1.20 \rightarrow}{\leftarrow 0.83 \div}$	$p_s = \frac{4m^2 g^2}{3\pi^2\hbar^3}$
$n_s = \frac{m^6 g^6}{2^{9/2}3\pi^5\hbar^{12}}$	$\frac{\times 1.73 \rightarrow}{\leftarrow 0.578 \div}$	$n_s = \frac{(2mg/\hbar)^6}{(3\pi^2)^4}$
$\Delta \equiv g\sqrt{n_s}$	$\frac{\times \sqrt{1.73} \rightarrow}{\leftarrow \sqrt{0.578} \div}$	$\Delta \equiv g\sqrt{n_s}$
$\tilde{\Delta} = 0.91 g\sqrt{n_s}$	same	$\tilde{\Delta} = 0.69 g\sqrt{n_s}$

the fermion density n.

3. Comparison of these two definitions and Importance of this cut-off

Note that the n_s in these two different definitions is different by a factor of 0.578, the current being smaller. Considering the Landau-Zener time is defined in a exponent and is hence actually not very accurate, we are still very satisfied because the conclusion does not really depend on the numerical factor. With the new definition, the transition occurs at 0.69 of the original Δ. And the comparison of all the quantities derived from two different choices of cutoff of momentum p_s is shown in Table IV.

The broad resonance condition (3.4) ensures that $N_s \gg N$, thus justifying this approximation. In a series of works by Pazy, Tikhonenkov *et al.* [86, 87], the authors neglected dispersion and set $N_s = N$. As demonstrated above, these two assumptions are physically incompatible, at least for a broad resonance, although mathematically

their model is consistent. The exact quantum solution of the same problem was recently found by Altland and Gurarie [95].

The value g can be extracted from the experimental data on the magnetic field dependence of the scattering length a near the FR [96] using the well-known relation: $g = \hbar\sqrt{4\pi(a - a_0)\varepsilon/m}$ (a_0 is the scattering length far from resonance). On the other hand g can be estimated theoretically as $g \sim \epsilon_{hf}\sqrt{a_0^3}$, where ϵ_{hf} is the hyperfine energy. Both these estimates give for ^{40}K $g \sim 10^{-28} erg \times cm^{3/2}$ and from eqs. (3.35) and (3.36) $\Delta \sim 3 \times 10^{-4} K$. However, Eq. (3.35) overestimates Δ by assuming that the limiting kinetic energy is Δ instead of it being much smaller. A more reliable estimate can be extracted from a comparison of Eq. (3.63) with experimental data by Regal *et al.* [67]. The fitting gives the value $\Delta \sim 10^{-5} K$ for the broad resonance at $B_0 = 224.21G$ in ^{40}K. The cited measurements were performed at the finite temperature $T \sim T_F/3$, and therefore the corresponding value of Δ is underestimated in comparison to its zero-temperature value. Thus, a reasonable estimate for Δ is between 10^{-5}K and 10^{-4}K. In the cited experiment the magnetic field sweep amplitude was about 12G. It corresponds to an energy scale of about $10^{-3} K$, larger than Δ.

An important conclusion is that a strong interaction renormalizes the LZ gap. The energy scale which appears in perturbation theory is $\Delta^{(0)} = g\sqrt{n}$ [80]. For a broad resonance $\Delta = g\sqrt{n_s}$ is much larger than $\Delta^{(0)}$ and does not depend on the atomic density.

F. Static properties, spectra and eigenstates of the GSM

1. For general states

At fixed values N_s,N and S, the stationary states $|\Psi\rangle$ of the Hamiltonian (3.18) can be represented by a superposition of the states with fixed values of number of molecules M:

$$|\Psi\rangle = \sum_{M=0}^{M=N/2} \Psi_M |M\rangle , \tag{3.37}$$

with the amplitudes Ψ_M obeying the stationary Schrödinger equation:

$$\begin{aligned} E\Psi_M = -2\epsilon M\Psi_M + \frac{g}{\sqrt{V}}\sqrt{M\left(S-S_z\right)\left(S+S_z+1\right)}\Psi_{M-1} \\ + \frac{g}{\sqrt{V}}\sqrt{\left(M+1\right)\left(S+S_z\right)\left(S-S_z+1\right)}\Psi_{M+1} \end{aligned} \tag{3.38}$$

The solution of this system is still rather complicated, but it is strongly simplified by the broad resonance condition (3.32). Indeed, due to this inequality and stemming from it approximate relationships: $S \approx -S_z \approx N_s/2$, it is possible to replace $S - S_z$ and $S - S_z + 1$ in Eq. (3.38) by N_s. We should be more careful with the expression $S + S_z$ since the two terms almost completely cancel each other. By using the following formula

$$\hat{b}^\dagger \hat{S}_- |S, M\rangle = \sqrt{(S+S_z)(S-S_z+1)(M+1)}\,|S, M+1\rangle ,$$

and valuing it at $M = M_{max}$ when $M_{max} = \frac{N}{2}$, we may infer that

$$S + S_z = 0 \Rightarrow S = \frac{N_S - N}{2} + M_{max} = \frac{N_S}{2} \tag{3.39}$$

And hence $S + S_z = \frac{N}{2} - M$. We can also value the above equation when M_{max} is another value, and we have the correspondence such that if $M_{max} = \frac{N}{2} - i$, then $S = \frac{N_S}{2} - i$, where i is any integer in the range $[0, N/2]$.

Employing the notation defined earlier $\Delta = g\sqrt{n_s}$ and introducing new variables

$$m \equiv M - \frac{N}{4}; \quad s \equiv \frac{N}{4}, \tag{3.40}$$

we arrive at a simplified version of equations (3.38):

$$\begin{aligned}(E + 2s\epsilon)\,\Psi_m = &-2\epsilon m\Psi_m \\ &+ \Delta\left(\sqrt{(s-m)\,(s+m+1)}\Psi_{m+1} + \sqrt{(s+m)\,(s-m+1)}\Psi_{m+1}\right),\end{aligned} \tag{3.41}$$

in which m runs from $-s$ to s, or equivalently $[-\frac{N}{4}, \frac{N}{4}]$. The equation above is easily recognizable, as is generated by the following reduced spin Hamiltonian:

$$H_r = 2\epsilon s_z + 2\Delta s_x \tag{3.42}$$

where s_x, s_z are spin operators corresponding to the total spin s. This is a Hamiltonian of a spin s in the magnetic field $2\sqrt{\epsilon^2 + \Delta^2}$ tilted in the xz plane at the angle $\theta = -\tan^{-1}(\Delta/\epsilon)$ to the z axis.

The energy levels are labeled by two integers s and m as (s, m):

$$E_{sm}\,(\epsilon) = 2m\sqrt{\epsilon^2 + \Delta^2} - 2s\epsilon; \;\; -s \leq m \leq s; \; 0 \leq s \leq N/4 \tag{3.43}$$

and the average of number of molecules is

$$\langle M \rangle = s - m\frac{\epsilon}{\sqrt{\epsilon^2 + \Delta^2}}. \tag{3.44}$$

The spectrum (3.43) possesses a symmetry:

$$E_{sm}\,(\epsilon) = -E_{s,-m}\,(-\epsilon) \tag{3.45}$$

Levels with the same s and different m do not cross, but the levels with different s and m cross each other. The crossing of the levels (s, m) and (s', m') happens at the

point:

$$\epsilon = \Delta \frac{\operatorname{sign}\left(\frac{m-m'}{s-s'}\right)}{\sqrt{\left(\frac{m-m'}{s-s'}\right)^2 - 1}} \tag{3.46}$$

Besides of crossings each level (s, m) at any ϵ is $\mathcal{N}(S)-$fold degenerate as it is determined by Eq. (3.27).

2. For ground states

For each s the state with minimal energy is $(s, -s)$. The ground state corresponds to maximal possible value $s = N/4$ and $m = -s$. Its energy reads:

$$E_G = E_{N/4,N/4} = -\frac{N}{2}\left(\sqrt{\epsilon^2 + \Delta^2} + \epsilon\right) \tag{3.47}$$

The eigen-vectors are not so simple since they generally include the Jacobi polynomials. However, the ground state is easy to construct since it corresponds to the maximal total spin $s = N/4$. The spin $\mathbf{s}$ is oriented in the $xz-$plane at the angle $\theta = -\arctan\frac{\Delta}{\epsilon}$ to $z-$axis. Therefore the average value of $s_z = m$ in the ground state is equal to $\langle m\rangle_G = \frac{N}{4}\cos\theta = \frac{N\epsilon}{4\sqrt{\epsilon^2+\Delta^2}}$. Employing the second equation (3.40), we find the average number of molecules:

$$\langle M\rangle_G = \frac{N}{4}\left(1 + \frac{\epsilon}{\sqrt{\epsilon^2 + \Delta^2}}\right) \tag{3.48}$$

It smoothly varies from 0 at $\epsilon = -\infty$ to $N/2$ at $\epsilon = +\infty$. The value $\langle M\rangle_G - N/4$ is an odd function of the detuning energy. The average number of fermions $\langle N_F\rangle$ can be found from the conservation law $N_F + 2M = N$. For the ground state it is possible to find all amplitudes Ψ_M in the expansion (3.37). We start with the vector of the ground state $|\Psi_G\rangle$in terms of the spin $\mathbf{s}$. It can be represented as the direct product of $N/2$ spin-1/2 states all oriented at the angle $\theta = -\arctan\frac{\Delta}{\epsilon}$ to $z-$axis.

This direct product can be represented as a superposition:

$$|\Psi_G\rangle = \sum_{m=-N/4}^{N/4} \Phi_m |m\rangle\,;\ \Phi_m = \left[\frac{\left(\frac{N}{2}\right)!}{\left(\frac{N}{4}-m\right)!\left(\frac{N}{4}+m\right)!}\right]^{1/2} \left(\cos\frac{\theta}{2}\right)^{\frac{N}{4}+m} \left(\sin\frac{\theta}{2}\right)^{\frac{N}{4}-m} \tag{3.49}$$

According to the operator relationship (3.40), the amplitudes Φ_m coincide with Ψ_M at $M = N/4 + m$. Thus:

$$\Psi_M = \left[\frac{\left(\frac{N}{2}\right)!}{M!\left(\frac{N}{2}-M\right)!}\right]^{1/2} \left(\cos\frac{\theta}{2}\right)^{M} \left(\sin\frac{\theta}{2}\right)^{\frac{N}{2}-M} \tag{3.50}$$

As we explained earlier, the state $|M\rangle$ corresponds to the projection $S_z = \frac{N-N_2}{2} - M$ and the total spin $S = \frac{N_s}{2}$. There are $\frac{N}{2} - M$ spins up on sites. The vector of the ground state is symmetric with respect to any permutations of all N_s spins on sites. Ψ_M has a sharp maximum at $M = \frac{N}{2}\cos^2\frac{\theta}{2}$. The position of this peak corresponds to the most probable state and statistically the value of this position is called average, which gives $M = \frac{N}{4}(1 + cos\theta)$, as seen in Eq. (3.48). The value of Ψ_M in maximum is 1, the width of the peak is $\sqrt{N/2}\sin\theta/2\cos\theta/2$.

The knowledge of the vector of state $|\Psi_G\rangle$ allows calculation of other physically interesting values, like fluctuations of number of molecules. But an easier way is using the operator method. The square fluctuation reads:

$$\langle(\Delta N_m)^2\rangle_G = \langle\psi|(s_z)^2|\psi\rangle - \langle\psi|s_z|\psi\rangle^2, \tag{3.51}$$

where the wave function $|\psi\rangle \equiv \prod_{i=1}^{N/2} \otimes |\psi_i\rangle$ is a direct product of each individual spin wave function $|\psi_i\rangle = (\cos\theta/2, \sin\theta/2)_i^T$, and the operator s_z is accordingly $s_z = \sum_{i=1}^{N/2} s_z^i$. Since $\langle m\rangle_G = \langle\psi|s_z|\psi\rangle = \sum_{i=1}^{N/2}\langle\psi_i|s_z^i|\psi_i\rangle = \frac{N}{4}\cos\theta$, and $\langle\psi|(s_z)^2|\psi\rangle = N/8 + \sum_{i\neq j}^{N/2}\langle\psi_i|s_z^i|\psi_i\rangle\langle\psi_j|s_z^j|\psi_j\rangle = N/8 + \cos^2(\theta)N(N-2)/16$, we have the quadratic

fluctuation of the number of molecules as

$$\langle(\Delta N_m)^2\rangle_G = \frac{N}{8} sin^2\theta = \frac{N}{8}\frac{\Delta^2}{\epsilon^2+\Delta^2} \tag{3.52}$$

The fluctuation $\langle(\Delta N_m)^2\rangle$ is maximal at $\epsilon = 0$ where is the Feshbach Resonance, and is an even function of the detuning ϵ.

An important value is the BCS condensate amplitude $\langle S_+\rangle_G$ in the ground state. Using the equation (3.23) $\hat{S}_z = \frac{N-N_s}{2} - \hat{M} = -\frac{N_s}{2} + \frac{N}{4} - \hat{m}$ and (3.21), we find that $|\langle S_+\rangle_G|^2 \approx S^2 - \langle S_z^2\rangle_G \approx (N_s/2)^2 - (N_s/2 - N/4)^2 - N_s\langle s_z\rangle_G \approx \frac{1}{4}NN_s(1-\cos\theta)$ and thus

$$|\langle S_+\rangle_G| = \sqrt{\frac{NN_s}{2}}|\sin\theta/2| \tag{3.53}$$

Finally, we find the BEC-BCS correlation function $\langle b_0 S_+\rangle$. We demonstrated earlier (see the derivation of Eq. (3.41) from Eq. (3.38)) that in the broad resonance approximation $N_s \gg N$ the product of operators $b_0 S_+$ can be replaced by $\sqrt{N_s}s_+$. Thus,

$$\langle b_0 S_+\rangle = \sqrt{N_s}\,\langle s_+\rangle = \frac{\sqrt{N_s}N}{4}\sin\theta = \frac{\sqrt{N_s}N}{4}\frac{\Delta}{\sqrt{\epsilon^2+\Delta^2}} \tag{3.54}$$

This correlator vanishes at $\epsilon = \pm\infty$ and has maximum at $\epsilon = 0$.

The GSM displays BCS-BEC crossover in the range $|\epsilon| \sim \Delta$ near the Feshbach resonance. In this range the BCS condensate amplitude grows to the value $\sim \sqrt{\frac{N_s N}{2}} \gg \frac{N}{2}$. This enhancement of the condensate is due to a distribution of the Cooper pairs over a wide range of momenta strongly exceeding the Fermi sphere. It indicates that the famous BCS exponentially small condensate does not appear even at very large detuning exceeding Δ. The reason for its appearance in the BCS theory is not only the weakness of interaction, but also the narrowness of the attraction range in the momentum space. This condition is violated not only in the GSM, but also in the initial Timmermanns *et al.*model.

G. Dynamics processes, production and dissociation

Employing equations (3.33), the general solution of the ordinary differential equation (3.34) reads (further we put $\hbar = 1$):

$$\hat{b}\,(t) = u\,(t,t_0)\,\hat{b}\,(t_0) - i\tilde{g}v\,(t,t_0)\,\hat{S}_-\,(t_0)\,, \tag{3.55}$$

$$i\tilde{g}\hat{S}_-(t) = -\dot{u}\,(t,t_0)\,\hat{b}\,(t_0) + i\tilde{g}\dot{v}\,(t,t_0)\,\hat{S}_-\,(t_0)\,, \tag{3.56}$$

where $u\,(t,t_0)$ and $v\,(t,t_0)$ are standard solutions of the same equation satisfying the initial conditions $u\,(t_0,t_0) = 1$, $\dot{u}\,(t_0,t_0) = 0$ and $v\,(t_0,t_0) = 0$, $\dot{v}\,(t_0,t_0) = 1$. These solutions have the following properties:

$$|u|^2 + \Delta^{-2}\left|\dot{u}^2\right| = \Delta^2\left|v^2\right| + \left|\dot{v}^2\right| = 1; \dot{u}^*\dot{v} + \Delta^2 u^* v = 0. \tag{3.57}$$

The solution (3.55, 3.56) allows finding the evolution of the number of molecules $N_m(t) = \langle\hat{b}^\dagger\hat{b}\rangle(t)$, the BCS condensate amplitude $F(t)$ defined by equation $F^2(t) \equiv \langle\hat{S}_+\hat{S}_-\rangle(t)$, and the BCS-BEC coherence factor $C(t) \equiv \langle\hat{b}^\dagger\hat{S}_-\rangle(t)$. If the initial coherence factor $C(t_0)$ is zero, the evolution is given by:

$$N_m(t) = |u|^2 N_m(t_0) + \tilde{g}^2|v|^2 F^2(t_0) \tag{3.58}$$

$$\tilde{g}^2 F^2(t) = |\dot{u}|^2 N_m(t_0) + \tilde{g}^2|\dot{v}|^2 F^2(t_0) \tag{3.59}$$

$$C(t) = i\tilde{g}^{-1}\dot{u}u^* N_m(t_0) + i\tilde{g}\dot{v}v^* F^2(t_0), \tag{3.60}$$

Using (3.57) and summing eqs. (3.58) and (3.59), we find:

$$N_s N_m(t) + F^2(t) = \text{const}, \tag{3.61}$$

which is a consequence of the conservation laws. Since for any state $F^2(t) > 0$, if there are no molecules in the initial state, their number $N_m(t)$ can not exceed the value $F^2(t_0)/N_s$ at any time.

Below we consider two experimentally most relevant situations: only fermions and no molecules; and only molecules and no fermions in the initial state. In both these cases the initial value $C = \langle \hat{b}^\dagger \hat{S}_- \rangle (t_0) = 0$. In the case of no molecules in the initial state, so $N_m(t_0) = 0$, the general equations (3.58, 3.60) simplify to

$$N_m(t) = \tilde{g}^2 |v|^2 F^2(t_0); \qquad i\tilde{g}C(t) = -\tilde{g}^2 \dot{v} v^* F^2(t_0) \tag{3.62}$$

The evolution of $F(t)$ in this case is determined by (3.61) and (3.62). Note that the coherence factor $C(t)$ does not remain zero.

Far from the FR the relaxation is provided by collisions. The collision time τ_{coll} is no shorter than $(n\sigma v_F)^{-1}$, where $\sigma = \pi a_0^2$ is the collision cross-section and v_F is the Fermi velocity. For ^{40}K at $n \sim 10^{13} cm^{-3}$, we find $\tau_{coll} \sim 1ms$. In this Letter we assume that the sweeping time is much less than τ_{coll}.

To produce a reasonable fraction of molecules it is necessary to have a large condensate amplitude in the initial state. A natural way to generate such an initial state is to start with a sufficiently small negative detuning energy ϵ. The effective dimensionless BCS coupling constant is $\lambda_{BCS} = -\nu_F g^2/\epsilon$, where ν_F is the density of state at the Fermi-energy [59]. It becomes of the order of 1 at $\mid \epsilon \mid \sim \Gamma \epsilon_F$, a value of detuning between Fermi-energy and the gap Δ. When detuning becomes less than this value the condensate spreads from the exponentially narrow spherical layer near the Fermi sphere to a sphere of much larger radius.

Such a strong dependence of the final molecular production on the initial state (in particular on the value of the initial magnetic field) explains why different experimenters obtain different fractions of molecules in the final state even in the adiabatic regime [72, 69, 68, 67]. Note that in experiments where a significant molecular production was achieved the initial state was indeed close to the FR, whereas the final state was rather far from the FR. Thus, in a realistic experimental setup the ini-

tial value of ϵ is small $|\epsilon_0| \leq \Gamma\epsilon_F \ll \Delta$ and then ϵ increases linearly with time. In this case one can put $t_0 = 0$, and $\epsilon(t) = \dot{\epsilon}t$. Equation (3.34) turns into the parabolic cylinder equation. Its standard solution $u(t, 0)$ has the asymptotic behavior: $|u(\infty, 0)|^2 = \exp(-\pi\Delta^2/2\hbar\dot{\epsilon})$. Employing it together with Eq. (3.57) and Eq. (3.62), we arrive at the following number of molecules in the final state:

$$N_m(+\infty) = F_0^2 N_s^{-1} \left[1 - \exp\left(-\pi\Delta^2/2\hbar\dot{\epsilon}\right)\right] \tag{3.63}$$

It can be proven from Eq. (3.53) that the maximal possible value of F^2 is $N_s N/2$. This corresponds to the complete transformation of atoms into molecules in the adiabatic regime $\dot{\epsilon} \to 0$. Equation (3.63) looks exactly like the LZ transition probability multiplied by an effective number of pairs. However, in contrast to phenomenological theories [18, 19] and the perturbation theory result [80], the coefficient in front of $1/\dot{\epsilon}$ in the exponent does not depend on the initial atom density. This theoretical prediction can be checked experimentally. The effective number of pairs (pre-exponent) depends on the initial BCS condensate amplitude $F(t_0)$. Finite temperature destroys a fraction of the initial Cooper pairs and decreases the molecular production.

Finally, we consider an inverse process with no fermions, no BCS condensate and only the molecular condensate in the initial state: $\langle\hat{b}\rangle(-\infty) = \sqrt{N/2}$ and sweeping of the magnetic field in the opposite direction. Then at the end of the sweeping the condensate density is determined by the LZ value: $\langle\hat{b}\rangle(+\infty) = \sqrt{N/2}\exp(-\pi\Delta^2/2\hbar\dot{\epsilon})$, whereas the absolute value of the BCS condensate amplitude $\langle\hat{S}_-\rangle$ can be found from the conservation law (3.61) for macroscopic condensate amplitude we can neglect the non-commutativity of S_+ and S_-:

$$|\langle\hat{S}_-\rangle|^2 = \frac{N_s N}{2}\left[1 - \exp\left(-\frac{\pi\Delta^2}{\hbar\dot{\epsilon}}\right)\right] \tag{3.64}$$

Notice factor of 2 difference in the exponents of (3.63) and (3.64). The result (3.64)

has a clear physical interpretation. It corresponds to $N/2 \times [1 - \exp(-\pi\Delta^2/\hbar\dot{\epsilon})]$ Cooper pairs distributed with equal probability $w = \frac{N}{2N_s}[1 - \exp(-\pi\Delta^2/\hbar\dot{\epsilon})]$ between N_s available states. Then the modulus of the pair amplitude at a fixed state is $|\langle \hat{a}_{\mathbf{p}\uparrow}\hat{a}_{-\mathbf{p}\downarrow}\rangle| = \sqrt{w}$. If all these amplitudes have the same phase, the total condensate amplitude is equal to $\langle \hat{S}_-\rangle = N_s\sqrt{w}$, which is equivalent to equation (3.64). This result has experimentally verifiable consequences. Indeed, estimating the size of the pair created after the sweeping of magnetic field from the Heisenberg uncertainty principle, we find $r_{\text{pair}} = \hbar/p_s \ll n^{-1/3}$. It means that the pair is a compact object well separated from other pairs, and therefore can be called quasimolecule in contrast to the real molecules in the initial state before the magnetic field sweep.

The quasimolecules have two peculiarities. First, in contrast to the real molecules the quasimolecules have parallel electron spins. Second, they are unstable: after magnetic field sweep ends whereas the trap remains, the quasimolecules decay. The relaxation time is rather long since fermion pair collisions do not produce energy relaxation. The experimental estimate for the relaxation time is in the range from milliseconds to seconds. Therefore, it seems quite feasible to switch off the trap before the quasimolecules relax and observe the correlations of momenta and spins in runaway particles. The prediction of our theory is that the correlation prefers opposite velocities and parallel spins in the range of energy up to Δ. The remaining molecules give rise to correlated atoms with opposite momenta and spins, providing an alternative opportunity to find their number.

CHAPTER IV

SUMMARY AND CONCLUSION

We have discussed the Landau-Zener transitions in the noisy environment and many-body system.

At first we gave an introduction to Landau-Zener theory. We discussed the general two level time-dependent system, and different solvable models especially the LZ model. We gave a thorough review on different limit situations of LZ model, especially the static limit. The asymptotic solution to the LZ transition problem was presented by solving the Weber Equation directly or using a semiclassical approach.

Employing this LZ theory as a useful tool, we invested two research projects that are closely related to LZ theory.

For the first project of fast quantum noise in LZ transitions, we obtained the transition probability of the two-state system and discussed application to the single molecular magnet.

We reviewed the research history for noise interacting with LZ transitions. Motivated by the current progress and experimental puzzles, we focus on the fast and quantum noise. We presented the problem, by proposing the Hamiltonian and analyzing the properties of noise including strength and characteristic time scales. For strong noise, it becomes the classical situation. Our result is good for weak and moderately strong noise, though for moderately strong noise the longitudinal-longitudinal correlation inside the LZ time interval is not completely studied. We demonstrated that the action of the regular LZ transition matrix element and the longitudinal-longitudinal noise correlation is limited by the LZ time scale τ_{LZ}, whereas the action of the transverse noise is accumulated during much longer accumulation time τ_{acc}. And hence the evolution of the two-state system is separated in time. Inside the

LZ time interval, it is the longitudinal noise and LZ gap dominating the evolution. Outside the LZ time interval, it is the transverse noise dominating the evolution. The separation of time scales allows us to derive exact transition probability with the LZ gap, longitudinal and transverse noise taken into account simultaneously. Outside the LZ time interval we first tried an heuristic approach and then started from the microscopic Hamiltonian to derive the master equation. The population of each state was derived from establishing a differential equation by using the Keldysh technique. We showed that the mixed longitudinal-transverse noise correlation leads to the renormalization of the LZ gap Δ inside the LZ time interval. We also studied the correlation between purely longitudinal noises inside the interval. This part is not complete but this correlation was shown to be negligible if the noise is weak. The solution in each interval was studied and then matched at boundaries to give a complete picture of the evolution. Our theory successfully reproduced previous results. The transition probabilities depend explicitly on the noise commutator reflecting the quantum nature of the noise. It reproduces the result for fast classical noise if this commutator is zero. In the limiting case of adiabatic transverse noise, which means strong transverse noise or slow sweeping, the two-state system adiabatically follows its stationary state at an instantaneous value of frequency independently on the value of LZ parameter. In the limiting case of weak transverse noise or fast sweeping, the transition probability is reduced to the genuine LZ probability. In the extreme quantum regime at zero temperature our result coincides with exact result by Wubs *et al.* [37]. We argued that the strong-noise effects such as multiphonon processes and change of frequency appear only in the adiabatic regime for the fast noise and do not change substantially the transition probability. Our theory on the LZ transitions in a noisy environment is related single molecular magnet. We discussed the application of our theory to the explanation of the isotope effect and the quantized hysteresis

curve by introducing the phonon spin interaction. The pure longitudinal noise may require additional work to make it clearly understood. Immediate efforts would be the explanation of isotope effect and quantized hysteresis curve of single molecular magnet. Both are covered in concluding section of Chapter II.

For the ultracold dilute Fermi gas in magnetic field, we have considered the static limit and the dynamic molecule formation and dissociation when the magnetic field is swept across the broad Feshbach resonance.

We have briefly reviewed the history of experimental and theoretical discoveries on bosonic and fermionic superfluidity, including the recent experiments. We introduced the effect of magnetic field on alkali atoms, and hence the Feshbach resonance. We focused on the broad Feshbach resonance which belongs to a strong coupling regime. The broad resonance condition allowed us to use the single mode approximation and to neglect the fermion dispersion. After the approximation the Hamiltonian is greatly simplified but still reflects the physical essentials. For the static problem, by a spin transformation, the Hamiltonian is simplified to the Global Spin Model Hamiltonian, which allows us to completely solve the static problem at least for ground state. We obtained the energy spectrum, eigenvector, average number of molecules and its fluctuation, the amplitude of the BCS condensate, and the correlation between BCS and BEC amplitudes, as a function of experiment parameters. From these quantities, we got the knowledge of the static limit properties of the BEC-BCS crossover. And the dynamic problem, in the Global Spin Model, is converted to a Landau-Zener problem. We derived the differential equation and compared it with LZ equation. We gave general solution to the dynamic equation and give exact expression for asymptotic solution. The resulting molecular production from initial fermions is described by LZ-like formula with a strongly renormalized LZ gap independent of the initial fermion density. The molecular dissociation pro-

cess also shows LZ characteristics for the end values of condensates. The correlation between BEC condensates and BCS condensates, which is actually a conservation law. This conservation law may explain why there's a molecular conversion ratio limit. In both static and limit situations, we estimated the cutoff momentum and improved our previous estimate to the current one. One of our predictions is that the molecular production strongly depends on the initial value of magnetic field. This effect may explain why different experiments have different molecular conversion ratio limits. In the inverse process of molecular dissociation, immediately after the sweeping stops, there appear Cooper pairs with parallel electronic spins and opposite momenta, homogeneously distributed within a sphere of radius $p_s \gg p_F$ in the momentum space. Another experimentally verifiable prediction is the independence of the coefficient in front of $1/\dot{\epsilon}$ in the LZ exponents for the molecular production (3.63) and the BCS condensate (3.64) productions of the initial density of atoms (molecules). The more improvement on current work could be trying to solve the problem with less approximations. Also the subject of ultracold Fermi gas is a rich subject and there are many practical or fundamental questions.

REFERENCES

[1] A. Bambini and P. R. Berman, Phys. Rev. A **23**, 2496 (1981).

[2] G. F. Thomas, Phys. Rev. A **27**, 2744 (1983).

[3] R. T. Robiscoe, Phys. Rev. A **27**, 1365 (1983).

[4] C. E. Carroll and F. T. Hioe, J. Phys. A: Math. **19**, 3579 (1986).

[5] H.-W. Lee and T. F. George, Phys. Rev. A. **29**, 2509 (1984).

[6] L. Landau, Phys. Z. Sowietunion **2**, 46 (1932).

[7] C. Zener, Proc. R. Soc. A **137**, 696 (1932).

[8] E. E. Nikitin, Opt. Spectrosc. **6**, 431 (1962).

[9] Y. N. Demkov, Sov. Phys. JETP **18**, 138 (1964).

[10] N. Rosen and C. Zener, Phys. Rev. **40**, 502 (1932).

[11] E. Stückelberg, Helv. Phys. Acta **5**, 369 (1932).

[12] W. Wernsdorfer and R. Sessoli, Science **284**, 133 (1999).

[13] W. Wernsdorfer, M. Murugesu, and G. Christou, Science **96**, 057208 (2006).

[14] W. Wernsdorfer, R. Sessoli, A. Ganeschi, D. Gatteschi, and A. Cornia, Europhys. Lett. **50**, 552 (2000).

[15] D. V. Averin, Phys. Rev. Lett. **82**, 18 (1999).

[16] J. Ankerhold and H. Grabert, Phys. Rev. Lett. **91**, 016803 (2003).

[17] G. E. Murgida, D. A. Wisniacki, and P. I. Tamborenea, Phys. Rev. Lett. **99**, 036806 (2007).

[18] F. H. Mies, E. Tiesinga, and P. S. Julienne, Phys. Rev. A **61**, 022721 (2000).

[19] J. Chwedenczuk, K. Goral, T. Kohler, and P. S. Julienne, Phys. Rev. Lett. **93**, 260403 (2004).

[20] M. Wubs, K. Saito, S. Kohler, Y. Kayanuma, and P. Hanggi, New J. Phys. **7**, 218 (2005).

[21] M. Sillanpaa, T. Lehtinen, A. Paila, Y. Makhlin, and P. Hakonen, Phys. Rev. Lett. **96**, 187002 (2006).

[22] J. von Neumann and E. Wigner, Z. Physik **30**, 467 (1929).

[23] F. Hund, Z. Physik **40**, 742 (1927).

[24] E. Ohrendorf, L. S. Cederbaum, and H. Kuppel, Chem. Phys. Lett. **151**, 273 (1988).

[25] C. M. M. Benthem, A. H. Huizer, and J. J. C. Mulder, Chem. Phys. Lett. **51**, 93 (1977).

[26] G. J. Hatton, W. L. Lichten, and N. Ostrove, Chem. Phys. Lett. **40**, 437 (1976).

[27] V. Pokrovsky, *Semiclassical and Adiabatic Approximation in Quantum Mechanics* (Class Notes, http://faculty.physics.tamu.edu/valery/quantum2.pdf, 2008), unpublished.

[28] A. Izmalkov, M. Grajcar, E. Ilichev, N. Oukhanski, Th. Wagner, *et al.*, Europhys. Lett. **65**, 844 (2004).

[29] M. Kusunoki, Phys. Rev. B **20**, 2512 (1979).

[30] Y. Kayanuma, J. Phys. Soc. Jpn. **54**, 2037 (1985).

[31] V. Pokrovsky and N. Sinitsyn, Phys. Rev. B **67**, 144303 (2003).

[32] V. Pokrovsky and S. Scheidl, Phys. Rev. B **70**, 014416 (2004).

[33] Y. Kayanuma, J. Phys. Soc. Jpn. **53**, 108 (1984).

[34] Y. Gefen, E. Ben-Jacob, and A. O. Caldeira, Phys. Rev. B **36**, 2770 (1987).

[35] P. Ao and J. Rammer, Phys. Rev. B **43**, 5397 (1991).

[36] Y. Kayanuma and H. Nakayama, Phys. Rev. B **57**, 13099 (1998).

[37] M. Wubs, K. Saito, S. Kohler, P. Hänggi, and Y. Kayanuma, Phys. Rev. Lett. **97**, 200404 (2006).

[38] S. Brandobler and V. Elser, J. Phys. A: Math. Gen. **26**, 1211 (1993).

[39] B. Dobrescu and N. Sinitsyn, J. Phys. B: At. Mol. Phys. **39**, 1253 (2006).

[40] A. Shytov, Phys. Rev. A **71**, 085301 (2005).

[41] N. Synitsyn, J. Phys. A **37**, 10691 (2004).

[42] M. Volkov and V. Ostrovsky, J. Phys. B **37**, 4069 (2004).

[43] M. Volkov and V. Ostrovsky, J. Phys. B **38**, 907 (2005).

[44] A. Migdal, Soviet Physics JETP **7**, 996 (1958).

[45] L. Keldysh, Zh. Exp. Teor. Fiz. **47**, 1515 (1964).

[46] J. Schwinger, J. Math. Phys. **2**, 407 (1961).

[47] J. R. Friedman, M. P. Sarachik, J. Tejada, and R. Ziolo, Phys. Rev. Lett. **76**, 3830 (1996).

[48] T. Lis, Acta Chrytallogr. B **36**, 2042 (1980).

[49] C. D. Delfs, D. Gatteschi, L. Pardi, R. Sessoli, K. Wieghardt, *et al.*, Inorg.Chem. **32**, 3099 (1993).

[50] O. Waldmann, R. Koch, S. Schromm, J. Schlulein, P. Mululler, *et al.*, Inorg. Chem. **40**, 2986 (2001).

[51] F. Meier and D. Loss, Phys. Rev. Lett. **86**, 5373 (2001).

[52] A. Muller, M. Luban, C. Schroder, R. Modler, P. Kogerler, *et al.*, Chem. Phys. Chem. **2**, 517 (2001).

[53] M. Axenovich and M. Luban, Phys. Rev. B **63**, 100407 (2001).

[54] A. Muller, E. Krickemeyer, S. K. Das, P. Kogerler, S. Sarkar, *et al.*, Angew. Chem., Int. Ed. **39**, 1612 (2000).

[55] A. Muller, S. K. Das, M. O. Talismanova, H. Bogge, P. Kogerler, *et al.*, Solid State Sciences **2**, 847 (2000).

[56] A. Muller, S. K. Das, E. Krickemeyer, P. Kogerler, H. Bogge, *et al.*, Angew. Chem., Int. Ed. **41**, 579 (2000).

[57] Y. Furukawa, K. Watanabe, K. Kumagai, F. Borsa, and D. Gatteschi, Phys. Rev. B **64**, 104401 (2001).

[58] D. Gatteschi, R. Sessoli, and J. Villain, *Molecular Nanomagnets*, 1st ed. (Oxford University Press, NY, 2006).

[59] V. Gurarie and L. Radzihovsky, Annals of Physics **322**, 2 (2007).

[60] K. Onnes, in *Nobel lecture, Physics 1901-1921* (Elsevier Publishing Company, Amsterdam, 1967), p. 306.

[61] A. J. Leggett, Rev. Mod. Phys. **71**, S318 (1999).

[62] A. J. Leggett, in *Modern Trends in the Theory of Condensed Matter, Lecture Notes in Physics* (Springer, Verlag, 1980), Vol. 115, pp. 13–27.

[63] C. A. R. Sa De melo, M. Randeria, and J. R. Engelbrecht, Phys. Rev. Lett. **71**, 3202 (1993).

[64] M. A. Kasevich, Science **298**, 1363 (2002).

[65] S. L. Rolston and W. D. Phillips, Nature **416**, 219 (2002).

[66] J. R. Anglin and W. Ketterle, Nature **416**, 211 (2002).

[67] C. Regal, C. Ticknor, J. L. Bohn, and D. S. Jin, Nature **424**, 47 (2003).

[68] M. Greiner, C. A. Regal, and D. S. Jin, Nature **426**, 537 (2003).

[69] M. W. Zwierlein, C. H. Schunck, S. M. F. Raupach, S. Gupta, Z. Hadzibabic, *et al.*, Phys. Rev. Lett. **91**, 250401 (2003).

[70] S. Jochim, M. Bartenstein, A. Altmeyer, G. Hendl, S. Riedl, *et al.*, Science **302**, 2101 (2003).

[71] W. C. Stwalley, Phys. Rev. Lett. **37**, 1628 (1976).

[72] K. E. Strecker, G. B. Partridge, and R. G. Hulet, Phys. Rev. Lett. **91**, 080406 (2003).

[73] J. Cubizolles, T. Bourdel, S. J. J. M. F. Kokkelmans, G. V. Shlyapnikov, and C. Salomon, Phys. Rev. Lett. **91**, 240401 (2003).

[74] E. A. Donley, N. R. Claussen, S. T. Thompson, and C. E. Wieman, Nature **417**, 529 (2002).

[75] C. Chin, A. J. Kerman, V. Vuletic, and S. Chu, Phys. Rev. Lett. **90**, 033201 (2003).

[76] J. Herbig, T. Kraemer, M. Mark, T. Weber, C. Chin, *et al.*, Science **301**, 1510 (2003).

[77] S. Durr, T. Volz, A. Marte, and G. Rempe, Phys. Rev. Lett. **92**, 020406 (2004).

[78] E. Hodby, S. T. Thompson, C. A. Regal, M. Greiner, A. C. Wilson, *et al.*, Phys. Rev. Lett. **94**, 120402 (2005).

[79] N. R. Claussen, E. A. Donley, S. T. Thompson, and C. E. Wieman, Phys. Rev. Lett. **89**, 010401 (2002).

[80] B. E. Dobrescu and V. L. Pokrovsky, Phys. Lett. **A350**, 154 (2006).

[81] E. Timmermans, K. Furuya, P. W. Milloni, and A. K. Kerman, Phys. Lett. A **285**, 228 (2001).

[82] I. Tikhonenkov, E. Pazy, and A. Vardi, Optics Communications **264**, 321 (2006).

[83] J. Javanainen, M. Kostrun, Y, Zheng, A. Carmichael, U. Shrestha, *et al.*, Phys. Rev. Lett. **92**, 200402 (2004).

[84] J. E. Williams, T. Nikuni, N. Nygaard, and C. W. Clark, J. Phys. B **37**, L351 (2004).

[85] Y. Band, I. Tikhonenkov, E. Pazyy, M. Fleischhauer, and A. Vardi, Journal of Modern Optics **54**, 697 (2007).

[86] E. Pazy, I. Tikhonenkov, Y. Band, M. Fleischhauer, and A. Vardi, Phys. Rev. Lett. **95**, 170403 (2005).

[87] I. Tikhonenkov, E. Pazy, Y. B. Band, M. Fleischhauer, and A. Vardi, Phys. Rev. A **73**, 043605 (2006).

[88] R. H. Dicke, Phys. Rev. **93**, 99 (1954).

[89] H. Feshbach, Ann. Phys. **19**, 287 (1962).

[90] C. J. Pethick and H. Smith, *Bose-Einstein Condensation in Dilute Gases*, 1st ed. (Cambridge University Press, Cambridge, 2002).

[91] E. Timmermans, P. Tommasini, M. Hussein, and A. Kerman, Physics Reports **315**, 199 (1999).

[92] E. M. Lifshitz and L. P. Pitaevskii, *Course of Theoretical Physics, Statistical Physics, Part 2, vol. 9*, 1st ed. (Butterworth-Heinenann, Oxford, 2002).

[93] P. W. Anderson, Phys. Rev. **112**, 1900 (1958).

[94] L. D. Landau and E. M. Lifshitz, *Course of Theoretical Physics, Quantum Mechanics, vol. 3*, 1st ed. (Butterworth-Heinenann, Oxford, 2002).

[95] A. Altland and V. Gurarie, Physical Review Letters **100**, 063602 (2008).

[96] C. A. Regal, M. Greiner, and D. S. Jin, Phys. Rev. Lett. **92**, 040403 (2004).

APPENDIX A

APPLICATION OF THE KELDYSH TECHNIQUE IN DERIVING MASTER EQUATION

In this part we explain the derivation of the master equation in more details than Section D in Chapter II.

The occupation number equation is expanded from Eq. (2.18) as

$$N_{\alpha}\left(t\right)=\mathrm{Tr}\left[\rho_{0}\tilde{T}[e^{-i\int_{t_{0}}^{t}V_{I}(\tau)d\tau}]P_{\alpha}T[e^{-i\int_{t_{0}}^{t}V_{I}(\tau)d\tau}]\right], \tag{A.1}$$

where $\tilde{T}$ is the anti-chronological ordering operator and $V_I(\tau)$ is Eq. (2.18)

$$V_{I}\left(t\right)=e^{iH_{0}t}Ve^{-iH_{0}t}=u_{\perp}\left(t\right)\left(\left|1\right\rangle\left\langle 2\right|e^{-i\int_{t_{0}}^{t}\Omega(\tau)d\tau}+\left|2\right\rangle\left\langle 1\right|e^{i\int_{t_{0}}^{t}\Omega(\tau)d\tau}\right).$$

Now let us calculate the Green functions of fermions (here fermions correspond to state 1(thin red line) or state 2(thick green line)):

$$G_{\alpha}^{\pm,\pm}(t,t')\equiv\left\langle T_{c}[\left|\alpha\right\rangle_{t}\left\langle \alpha\right|_{t'}]\right\rangle, \tag{A.2}$$

where α index represents the state (1 or 2), the superscript $\pm,\pm$ represents the four components of the $2x2$ matrix of the Keldysh Green function, T_c means the time ordering along the Keldysh contour as shown in Fig. 5, the $+$ branch is the branch in the chronological ordering and the $-$ branch is the branch in the anti-chronological ordering, and $\left|\alpha\right\rangle_{t}=\left|\alpha\right\rangle e^{iE_{\alpha}t}$ is time dependent state vector. According to the Hamiltonian (2.2) and the negligible LZ effect outside the interval $(-\tau_{LZ},\tau_{LZ})$, $\left|1\right\rangle_{t}=\left|1\right\rangle e^{i(-\Omega(t)/2)t}$ and $\left|2\right\rangle_{t}=\left|2\right\rangle e^{i(+\Omega(t)/2)t}$.

Take state $|1\rangle$ for example, the four components of Keldysh Green function are

$$\begin{aligned} G_1^{-+}(t,t') &= \langle |\alpha\rangle_t \langle \alpha|_{t'} \rangle , \\ G_1^{+-}(t,t') &= \langle \langle \alpha|_{t'} |\alpha\rangle_t \rangle , \\ G_1^{--}(t,t') &= \left\langle \tilde{T} |\alpha\rangle_t \langle \alpha|_{t'} \right\rangle , \\ G_1^{++}(t,t') &= \langle T |\alpha\rangle_t \langle \alpha|_{t'} \rangle . \end{aligned} \tag{A.3}$$

Here follows the calculation of each component of $G_\alpha(t,t')$.

$$G_\alpha^{-+}(t,t') = \left\langle |\alpha\rangle e^{iE_\alpha t} \langle \alpha| (e^{iE_\alpha t'})^\dagger \right\rangle = \langle |\alpha\rangle \langle \alpha| \rangle e^{iE_\alpha (t-t')}. \tag{A.4}$$

In the second quantized form, we have

$$|\alpha\rangle = a_\alpha^\dagger |0\rangle , \tag{A.5}$$

or

$$\begin{aligned} |1\rangle &= a_1^\dagger |0\rangle , \\ |2\rangle &= a_2^\dagger |0\rangle . \end{aligned} \tag{A.6}$$

where $a_\alpha^\dagger$ is the creation operator for the state α from an empty state. Note that here the $|1\rangle$ and $|2\rangle$ do not include the usual meaning of the number of particles in that state, but just mean the state 1 and state 2. Due to this reason, there are two creation operators for two states, and there's no direct relation between these two operators. And for the same reason,

$$\begin{aligned} \langle |\alpha\rangle \langle \alpha| \rangle &= \langle 0| a_\alpha a_\alpha^\dagger |0\rangle = 1, \\ \langle \langle \alpha| |\alpha\rangle \rangle &= \langle 0| a_\alpha^\dagger a_\alpha |0\rangle = 0. \end{aligned} \tag{A.7}$$

So the ($-+$ and $+-$) components of propagators for state 1 and state 2 are

$$\begin{aligned} G_1^{-+}(t,t') &= e^{-\frac{i}{2}\int_{t'}^{t} \Omega(t) dt}, G_1^{+-} = 0, \\ G_2^{-+}(t,t') &= e^{+\frac{i}{2}\int_{t'}^{t} \Omega(t) dt}, G_2^{+-} = 0. \end{aligned} \tag{A.8}$$

By the fact that Green functions on the same branch are connected with those on different branches

$$\begin{aligned} G_\alpha^{++}(t,t') &= \theta(t-t')G_\alpha^{-+} + \theta(t'-t)G_\alpha^{+-}, \\ G_\alpha^{--}(t,t') &= \theta(t'-t)G_\alpha^{-+} + \theta(t-t')G_\alpha^{+-}, \end{aligned} \tag{A.9}$$

the remaining two components can also be found, if not calculated directly,

$$\begin{aligned} G_1^{++}(t,t') &= \theta(t-t')e^{-\frac{i}{2}\int_{t'}^{t}\Omega(t)dt}, \\ G_1^{--}(t,t') &= \theta(t'-t)e^{-\frac{i}{2}\int_{t'}^{t}\Omega(t)dt}, \\ G_2^{++}(t,t') &= \theta(t-t')e^{+\frac{i}{2}\int_{t'}^{t}\Omega(t)dt}, \\ G_2^{--}(t,t') &= \theta(t'-t)e^{+\frac{i}{2}\int_{t'}^{t}\Omega(t)dt}. \end{aligned} \tag{A.10}$$

Now let us calculate the propagator of Bose phonon

$$D(t,t') = \langle T_c[u_\perp(t)u_\perp(t')]\rangle = \left\langle T_c[\eta(t)\eta^\dagger(t')]\right\rangle + \left\langle T_c[\eta(t)\eta^\dagger(t')]\right\rangle. \tag{A.11}$$

Similar calculation as fermion propagator follows.

$$D^{-+}(t,t') = \left\langle \eta(t)\eta^\dagger(t')\right\rangle + \left\langle \eta(t)\eta^\dagger(t')\right\rangle, D^{+-}(t,t') = D^{-+}(t,t'), \tag{A.12}$$

where

$$\left\langle \eta(t)\eta^\dagger(t')\right\rangle = \tfrac{1}{V}\textstyle\sum_q |g_q|^2(n_q+1)e^{-i\omega_q(t'-t)}, \left\langle \eta^\dagger(t)\eta(t')\right\rangle = \tfrac{1}{V}\textstyle\sum_q |g_q|^2 n_q e^{-i\omega_q(t'-t)}. \tag{A.13}$$

Note that the coupling g_q between noise and system is absorbed in the noise operator. So the vertex in the Keldysh formalism is reduced to $-i\sigma_z$. As of now, we have the complete rules for each component in our Keldysh diagram. For each line or vertex in the diagram, we just multiply all the elements. Let us see a detailed example on the application of the Keldysh rules onto the diagrams. Take the the calculation of

Γ_1 in Fig. 9 for example, the state 1 element from t_1 to t' reads

$$\begin{aligned} G_1(t',t_1) &= \begin{pmatrix} G_1^{++}(t',t_1) & G_1^{+-}(t',t_1) \\ G_1^{-+}(t',t_1) & G_1^{--}(t',t_1) \end{pmatrix} \\ &= \begin{pmatrix} \theta(t'-t_1)e^{-\frac{i}{2}\int_{t_1}^{t'}\Omega(t)dt} & 0 \\ e^{-\frac{i}{2}\int_{t_1}^{t'}\Omega(t)dt} & \theta(t_1-t')e^{-\frac{i}{2}\int_{t_1}^{t'}\Omega(t)dt} \end{pmatrix} \\ &= e^{-\frac{i}{2}\int_{t_1}^{t'}\Omega(t)dt}\begin{pmatrix} 1 & 0 \\ 1 & 0 \end{pmatrix}, \end{aligned} \tag{A.14}$$

and there are similar expressions for state 2 and phonon line. Let $t+\Delta t \equiv t'$ in the calculation for abbreviation. We have

$$\begin{aligned} \Gamma_1 &= G_2(t_1,t)(-i\sigma_z)G_1(t',t_1)D(t_1,t_2)G_1(t_2,t')(-i\sigma_z)G_2(t,t_2), \\ &= \begin{pmatrix} G_2^{++}(t_1,t) & G_2^{+-}(t_1,t) \\ G_2^{-+}(t_1,t) & G_2^{--}(t_1,t) \end{pmatrix}(-i\sigma_z)\begin{pmatrix} G_1^{++}(t',t_1) & G_1^{+-}(t',t_1) \\ G_1^{-+}(t',t_1) & G_1^{--}(t',t_1) \end{pmatrix} D(t_1,t_2) \\ &\times \begin{pmatrix} G_1^{++}(t_2,t') & G_1^{+-}(t_2,t') \\ G_1^{-+}(t_2,t') & G_1^{--}(t_2,t') \end{pmatrix}(-i\sigma_z)\begin{pmatrix} G_2^{++}(t,t_2) & G_2^{+-}(t,t_2) \\ G_2^{-+}(t,t_2) & G_2^{--}(t,t_2) \end{pmatrix} \end{aligned} \tag{A.15}$$

It looks lengthy but the matrices for propagator of states are actually only half filled with nonzero values. Through a careful multiplication of these matrices, the final result is as simple as

$$\Gamma_1 = e^{-i\int_{t_2}^{t_1}\Omega(t)dt}D^{+-}(t_2,t_1) = e^{-i\int_{t_2}^{t_1}\Omega(t)dt}u_\perp(t_2)u_\perp(t_1). \tag{A.16}$$

If the two times t_1 and t_2 are integrated over and the operators are averaged, we just give the result in Eq. (2.24)

The formalism here is based on the Keldysh rules on different elements in dia-

grams. But if we actually go through the derivation of those rules by expanding the equation (A.1), or even the calculation of the matrices multiplication (A.15) above, we can get simpler rules.

The rules are, for each vertex there is a vertex function V(t), and the vertex functions are wrote in Keldysh contour order, and that is all. The vertex function is either $V_{2\to1}(t) \equiv \pm iu_{\perp}(t)\left|1\right\rangle\left\langle 2\right| e^{-i\int^{t}\Omega(\tau)d\tau}$ or $V_{1\to2}(t) \equiv \pm iu_{\perp}(t)\left|2\right\rangle\left\langle 1\right| e^{+i\int^{t}\Omega(\tau)d\tau}$, where $V_{2\to1}$ means through a phonon integration the state transits from state 2 to state 1, $V_{2\to1}$ means the transition from state 1 to state 2, and the sign $\pm$ depends on whether this vertex is located on chronological ordering branch $(+)$ or anti-chronological ordering branch $(-)$.

Use this new rule to calculate Π_1 for example. For the vertex at t_1, we write

$$V_{1\to2}(t_1) = +iu_{\perp}(t_1)\left|2\right\rangle\left\langle 1\right| e^{+i\int^{t_1}\Omega(\tau)d\tau} \tag{A.17}$$

And for the vertex at t_2, we write

$$V_{2\to1}(t_2) = +iu_{\perp}(t_2)\left|1\right\rangle\left\langle 2\right| e^{-i\int^{t_2}\Omega(\tau)d\tau} \tag{A.18}$$

So this diagram is equivalent to

$$V_{1\to2}(t_1)V_{2\to1}(t_2) = -\left|2\right\rangle\left\langle 2\right| u_{\perp}(t_1)\, u_{\perp}(t_2)\, e^{+i\int_{t_2}^{t_1}\Omega(\tau)d\tau}, \tag{A.19}$$

which can be seen as same as equation (2.25) if integrations and averages are performed.

APPENDIX B

EQUATIONS FOR FAST LONGITUDINAL NOISE

Here we derive a system of differential equations for the longitudinal noise acting together. The characteristic interval in which both these factors are effective is the LZ time τ_{LZ}. The action of transverse noise during this time can be neglected. First, we prove that the contribution of the irreducible graphs *, which do not connect different branches of the Keldysh contour, is zero. Indeed the remote ends of such graphs are separated by the time interval of the order of $\tau_n \ll \tau_{LZ}$. Therefore, it is possible to integrate over the time difference at a fixed "center of time" or "slow time" as we did in the case of the transverse noise. In contrast to the latter case, for longitudinal noise, the integral does not depend on slow time, since the longitudinal noise vertex in the interaction representation does not contain time-dependent phase factor(it connects identical states of the two-state system). By the same reason, it is the same for states 1 and 2. Therefore, in a slow time scale much longer than τ_n (but much less than τ_{LZ}) the contribution of such graphs is proportional to unit operator for the two-state system and can be completely ignored. The irreducible noise graphs connecting different branches of Keldysh contour form a four-pole vertex (see Fig. 19), which, by the same reason, does not depend on slow time and connects identical states at each branch of the Keldysh contour. We denote this vertex by Γ.

Since the number of $\Delta-$vertexes between vertexes Γ is arbitrary we need to extend the number of amplitudes in consideration. Namely, we define transition amplitudes $P_{\alpha\beta,\alpha_0\beta_0}(t,t_0)$ as the average value of the operator $|\alpha\rangle\langle\beta|$ at the moment

*Following the quantum field tradition, we call a graph irreducible if it can not be separated into too disconnected parts (which are not connected by a noise line).

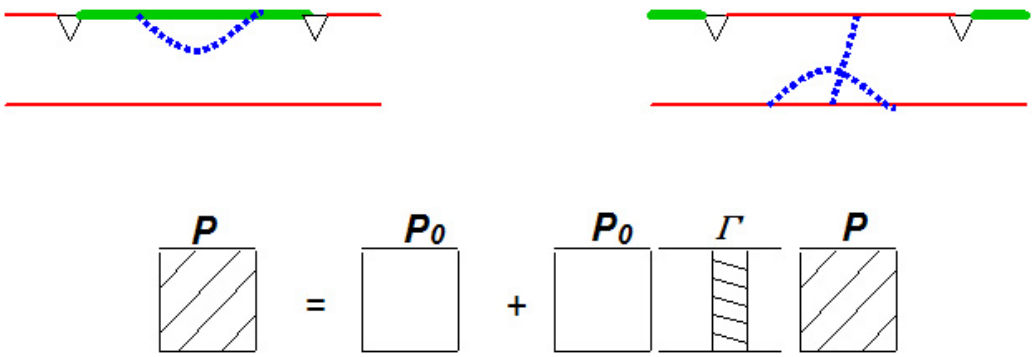

FIG. 19. Graphs containing the longitudinal noise only. Triangles correspond to the LZ gap Δ. The first graph shows one noise loop. In the slow time scale they are equivalent to addition of a constant energy. The second graph shows a noise line connecting Keldysh branches. The third graph shows the general graphic equation for P. See explanation in the text.

t if the density matrix for two-state system at the moment t_0 was $|\alpha_0\rangle\langle\beta_0|$. In the accepted approximation these amplitudes obey a system of linear integral equations:

$$\begin{aligned} P_{\alpha\beta,\alpha_0\beta_0}(t,t_0) &= P^{(0)}_{\alpha\beta,\alpha_0\beta_0}(t,t_0) \\ &- \Gamma\int_{t_0}^{t} P_{\alpha\beta,\alpha'\beta'}(t,t')\,P^{(0)}_{\alpha'\beta',\alpha_0\beta_0}(t',t_0)\,dt' \end{aligned} \tag{B.1}$$

Here $P^{(0)}_{\alpha\beta,\alpha_0\beta_0}(t,t_0)$ denotes the transition amplitude in the absence of noise. The validity of equations (B.1) is limited by moderately strong noise. Otherwise the amplitudes $P_{\alpha\beta,\alpha_0\beta_0}(t,t_0)$ vary significantly at a time scale τ_n. In this case more complicated equations with a non-local in time kernel Γ and amplitudes depending on 4 time arguments must be used.

VITA

Name: Deqiang Sun

Address: Department of Physics, Texas A&M University,
College Station, Texas 77843-4242

E-mail: dsun@physics.tamu.edu

Education: Ph.D., Physics, Texas A&M University, 2009
M.S., Physics, Texas A&M University, 2006
B.S., Physics, Nanjing University, 2003

Experience: Teaching Assistant and Research Assistant,
Department of Physics, Texas A&M University, 2003-2009